PB87-227104

EPA/600/2-87/049
July 1987

VERIFICATION OF THE LATERAL DRAINAGE COMPONENT OF THE HELP MODEL USING PHYSICAL MODELS

by

P. R. Schroeder and R. L. Peyton
U.S. Army Engineer Waterways Experiment Station
Vicksburg, MS 39180-0631

Interagency Agreement Number DW96930236-01-0

Project Officer

D. C. Ammon
Landfill Pollution Control Division
Hazardous Waste Engineering Research Laboratory
Cincinnati, OH 45268

APPROVED for Release for
Unlimited (Release to Public)

HAZARDOUS WASTE ENGINEERING RESEARCH LABORATORY
OFFICE OF RESEARCH AND DEVELOPMENT
U.S. ENVIRONMENTAL PROTECTION AGENCY
CINCINNATI, OH 45268

TECHNICAL REPORT DATA (Please read Instructions on the reverse before completing)		
1. REPORT NO. EPA/600/2-87/049	2.	3. RECIPIENT'S ACCESSION NO. PB87-227104
4. TITLE AND SUBTITLE Verification of the Lateral Drainage Component of the HELP Model Using Physical Models		5. REPORT DATE July 1987 6. PERFORMING ORGANIZATION CODE
7. AUTHOR(S) P.R. Schroeder and R. L. Peyton		8. PERFORMING ORGANIZATION REPORT NO.
9. PERFORMING ORGANIZATION NAME AND ADDRESS U.S. Army Engineer Waterways Experiment Station Vicksburg, Mississippi 39180		10. PROGRAM ELEMENT NO. 11. CONTRACT/GRANT NO. DW-96930236
12. SPONSORING AGENCY NAME AND ADDRESS Hazardous Waste Engineering Research Laboratory Office of Research and Development U.S. Environmental Protection Agency Cincinnati, Ohio 45268		13. TYPE OF REPORT AND PERIOD COVERED 14. SPONSORING AGENCY CODE EPA/600/12
15. SUPPLEMENTARY NOTES Project Officer: Douglas C. Ammon		

16. ABSTRACT

This report describes a study conducted to verify the lateral drainage component of the Hydrologic Evaluation of Landfill Performance (HELP) computer model using laboratory drainage data from two large-scale physical models of landfill liner/drainage systems. Drainage tests were run to examine the effects that drainage length, slope, hydraulic conductivity and depth of saturation have on the lateral drainage rate. The drainage results were compared with HELP model predictions and numerical solutions of the Boussinesq equation for unsteady, unconfined flow through porous media.

17. KEY WORDS AND DOCUMENT ANALYSIS		
a. DESCRIPTORS	b. IDENTIFIERS/OPEN ENDED TERMS	c. COSATI Field/Group
18. DISTRIBUTION STATEMENT Release to Public	19. SECURITY CLASS (This Report) Unclassified	21. NO. OF PAGES 132
	20. SECURITY CLASS (This page) Unclassified	22. PRICE

EPA Form 2220-1 (Rev. 4-77) PREVIOUS EDITION IS OBSOLETE

NOTICE

This document has been reviewed in accordance with U.S. Environmental Protection Agency policy and approved for publication. Mention of trade names or commercial products does not constitute endorsement or recommendation for use.

FOREWORD

Today's rapidly developing and changing technologies and industrial products and practices frequently carry with them the increased generation of solid and hazardous wastes. These materials, if improperly dealt with, can threaten both public health and the environment. Abandoned waste sites and accidental releases of toxic and hazardous substances to the environment also have important environmental and public health implications. The Hazardous Waste Engineering Research Laboratory assists in providing an authoritative and defensible engineering basis for assessing and solving these problems. Its products support the policies, programs and regulations of the Environmental Protection Agency, the permitting and other responsibilities of State and local governments and the needs of both large and small businesses in handling their wastes responsibly and economically.

This report describes a study conducted to verify the lateral drainage component of the Hydrologic Evaluation of Landfill Performance (HELP) computer model using laboratory drainage data from two large-scale physical models of landfill liner/drain systems. Drainage tests were run to examine the effects that drainage length, slope, hydraulic conductivity and depth of saturation have on the lateral drainage rate. The drainage results were compared with HELP model predictions and numerical solutions of the Boussinesq equation for unsteady, unconfined flow through porous media. Detailed water budgets, test summaries, and tables of the test data collected are published in appendices under a separate report cover.

Thomas R. Hauser, Director

Hazardous Waste Engineering Research Laboratory

ABSTRACT

Two large-scale physical models of landfill liner/drain systems were constructed to examine the effects that the length, slope and saturated hydraulic conductivity of the drain layer, and the depth of saturation above the liner have on the subsurface lateral drainage rate. The models have different lengths, 25.4 ft and 52.4 ft, and adjustable slope ranging from 2 to 10 percent. The models were filled with a 3-ft sand drain layer overlying a 1-ft clay liner. A 2-in. layer of gravel was placed under the liner to collect seepage from the clay liner.

Several drainage tests were run on each configuration of the models by applying water as rainfall to the surface of the sand layer, and then measuring the water table along the length of the models and the lateral drainage rate as a function of time. Lateral drainage rates and water table profiles were measured during periods of increasing, decreasing and steady-state drainage rates.

The drainage rates were used to verify the lateral drainage component of the Hydrologic Evaluation of Landfill Performance (HELP) model. Drainage results were compared with HELP model predictions and numerical solutions of the Boussinesq equation, which applies Darcy's law to unsteady, unconfined flow through porous media. Neither the HELP model nor the Boussinesq solution agreed completely with the drainage results. The HELP model predicted the effect of increases in depth of saturation and hydraulic conductivity very well, overestimated the drainage rate resulting from increases of slope, and underestimated the drainage rate resulting from increases of drainage length.

This report was submitted in partial fulfillment of Interagency Agreement DW96930236-01-0 between the U.S. Environmental Protection Agency and the U.S. Army Engineer Waterways Experiment Station. This report covers a period from June 1983 to September 1986, and work was completed as of September 1986.

CONTENTS

FIGURES

TABLES

ACKNOWLEDGMENTS

The authors would like to express their sincere appreciation to Mr. Sidney Ragsdale of the Environmental Engineering Division (EED), Environmental Laboratory (EL), U.S. Army Engineer Waterways Experiment Station (WES) and Mr. Roy Leach of the Geotechnical Laboratory (GL), WES, for their help in designing, constructing, and operating the physical models. The authors wish to acknowledge Mr. Stafford Cooper, GL, for designing the jacks for the model; the Engineering and Construction Services Division, WES, for constructing and preparing the physical models for testing; and the Instrumentation Services Division, WES, in particular Mr. Thomas McEwen, for instrumenting the physical models. The authors also wish to acknowledge Mr. Thomas E. Schaefer, Jr., and Mr. Roy Wade of the EED, WES, for running the drainage tests. The authors would like to thank Mr. Anthony Gibson and Mses. Charlotte Harness, Anita Zitta and Kathy Smart of the EED, WES, for their many contributions of technical support leading to the completion of this study. In addition, the authors would like to acknowledge the support and general supervision of Mr. F. Douglas Shields and Dr. Raymond L. Montgomery of the EED, WES. The authors would also like to thank Dr. Robert Havis and Dr. Bruce McEnroe of the EED, WES, for their technical review and the Information Products Division, WES, for preparation of the final figures and editorial review.

SECTION 1

EXECUTIVE SUMMARY

PURPOSE AND SCOPE

This study was conducted to test and verify the liquid management technology for lateral subsurface drainage in covers and leachate collection systems. The specific objective was to verify the lateral drainage component of the Hydrologic Evaluation of Landfill Performance (HELP) Model (1,2) and other regulatory and technical guidance, provisions and procedures developed by the U.S. Environmental Protection Agency (USEPA) (3).

The HELP model is a computer model that generates water budgets for a landfill by performing a daily sequential simulation of water movement into, through and out of the landfill. The model produces estimates of depths of saturation and volumes of runoff, evapotranspiration, lateral drainage, and percolation. Lateral drainage is computed in the model as a function of the average depth of saturation above the liner, the slope of the surface of the liner, the length to the drainage collector, and the hydraulic conductivity of the lateral drainage layer (1). Therefore, to accomplish the objective of this study, the lateral drainage rate was measured as a function of the hydraulic conductivity, slope, length and depth of saturation of the lateral drainage layer in large-scale physical models. The measured average depths of saturation, drainage rates and drainage times in the physical models were then compared with HELP model predictions and numerical solutions of the Boussinesq equation, which applies Darcy's law to unsteady, unconfined flow through porous media.

Two large-scale physical models of landfill liner/drain systems were constructed and filled with a 3-foot (ft) sand drain layer overlying a 1-ft clay liner. A 2-inch (in.) layer of gravel was placed under the liner to collect seepage from the clay. The models were instrumented to measure the water table profile, subsurface lateral drainage rate, water application, runoff and percolation through the liner. Evapotranspiration and other water losses were estimated from the water budget for each test. The models have adjustable slope, ranging from 2 to 10 percent in this study; and different lengths, one being 26.5 ft and the other being 53.5 ft.

Several drainage tests were run on each configuration of the models by applying water as rainfall to the surface of the sand layer, and then measuring the water table along the length of the models and the lateral drainage rate as a function of time. Lateral drainage rates and water table profiles were measured during periods of increasing, decreasing and steady-state drainage rates. In these drainage tests, two drainage lengths were

compared--25.4 ft and 52.4 ft. Three slopes were examined--approximately 2, 5 and 10 percent. Sands of two hydraulic conductivities were used--4 x 10^{-3} centimeter/second (cm/sec) (fine sand) and 2.2 x 10^{-1} cm/sec (coarse sand) as measured in soil testing permeameters. Four rainfall events were examined--a 1-hour (hr) rainfall at 0.50 inches/hour (in./hr), a 2-hr rainfall at 1.50 in./hr, a 6-hr rainfall at 0.50 in./hr and a 24-hr rainfall at 0.125 in./hr. Also, water was applied to the sand for a long period of time (generally more than 36 hr) at a rainfall intensity which would maintain the average depth of saturation in the sand at 12 in. In addition to these drainage tests, the sand was saturated, predominantly from the bottom up for several test conditions, and then allowed to drain. In total, more than sixty tests were performed.

A complete block experimental design was used to examine the effects of drainage length, slope, hydraulic conductivity, depth of saturation, rainfall intensity and rainfall duration on the lateral subsurface drainage rates. The block design was selected because it provided the most data with the least time and expense for construction and model preparation. Several slopes and rainfall events could be examined quickly since very little time was required for changing these test conditions. Also, the time requirements and costs for running an additional test with a different slope or rainfall were less than 10 percent of the requirements for preparing the model for a different sand. Additional rainfall events were examined in lieu of replicates since the lateral drainage rate as computed by the HELP model does not directly consider the effects of rainfall intensity or duration. Also, since a complete block design was used, the effect of a change in a variable is directly examined under multiple test conditions, reducing the need for replicates.

RESULTS OF DRAINAGE TESTS

A comparison of profile shapes for the depth of saturation along the length of the drainage layer indicates significant differences between the rising saturated-depth profile (during filling) and the falling saturated-depth profile (during draining) for the same average depth of saturation ($\bar{y}$). The profiles are steeper near the drain when filling than when draining. The difference is greater for higher infiltration rates. Steady-state profiles are very similar to the profiles for draining.

The drainage rate for a given average depth of saturation was greater during the filling portion of each experiment than during the draining portion. This is consistent with the saturated-depth profiles which show steeper hydraulic gradients near the drain for filling conditions. Plots of drainage rates as a function of average depth of saturation also show that drainage continues after $\bar{y}$ has essentially reached zero. This is presumed to be drainage of capillary water, commonly called delayed yield. An estimate of this capillary water volume when $\bar{y}$ had just drained to 0 in. based on an analysis of the experimental data is about 0.1 in. (cubic inches per square inch) for the fine sand and 0.3 in. for the coarse sand.

The drainage results indicated that the drainable porosity of the sands decreased with increasing depths of saturation above the clay liner. In addition, the drainable porosity at all depths was considerably smaller than

the value estimated from soil moisture data and other soil properties collected on the sands. Low drainable porosity values were obtained in part due to the delayed yield and capillary effects that results from the high drainage rate. However, the the presence and vertical distribution of entrapped air appear to be primarily responsible for the low drainable porosities and the change in drainable porosity with height, although no measurements of entrapped air were collected.

All parameters required to compute the drainage rate by the HELP equation except the hydraulic conductivity were measured for each drainage test. Due to variable air entrapment and differences in placement, compaction and preparation of the sand drainage media, the hydraulic conductivity measured in a permeameter in the soils testing laboratory differed significantly from the actual test values calculated from data on drainage rates and depths of saturation from the physical models. As described in the documentation report for the HELP model (1), the lateral drainage equation was developed to approximate numerical solutions of the Boussinesq equation for one-dimensional, unsteady, unconfined flow through porous media. Therefore, the actual hydraulic conductivity for the drainage tests was estimated by adjusting its value while solving the Boussinesq equation until the results matched the measured drainage rates and saturated depths. The hydraulic conductivity estimates are summarized in Appendix A. Determining the hydraulic conductivity in this manner provided the best estimate obtainable for each test since the Boussinesq solution is the commonly accepted representation of the actual drainage process. Comparisons were made for both steady-state drainage during rainfall and unsteady drainage following cessation of rainfall.

The computed hydraulic conductivity values differed significantly from the measured values. For steady-state drainage from the fine sand, the average computed value was only 8 percent greater than the measured value, while for unsteady drainage the average computed value was about 150 percent greater. For steady-state and unsteady drainage from the coarse sand, the average computed value was respectively 92 and 84 percent less than the measured value. For both sands, the average computed hydraulic conductivity for unsteady drainage was twice as large as the computed hydraulic conductivity for steady-state drainage.

In analyzing the computed hydraulic conductivity values, it was apparent that hydraulic conductivity decreased with increasing $\bar{y}$. This is consistent with the earlier hypothesis that the volume of entrapped air increased with increasing distance above the clay liner. A larger volume of entrapped air decreases drainable porosity and cross-sectional flow-through area, thereby decreasing hydraulic conductivity.

The computed hydraulic conductivity values varied considerably between tests on the same sand, even in the same model without disturbing the placement of the sand between tests. Considerable variability occurred between tests having exactly the same configuration of sand, slope, length, and depth of saturation, where only the rainfall intensity and duration differed. This variance was examined using an unequal three-way analysis of

variance (ANOVA) test to determine whether the computed hydraulic conductivity was a function of another variable besides average saturated depth.

The test variables used in the ANOVAs included type of sand, average saturated depth, slope, drainage length, rainfall duration and rainfall intensity. No effects of rainfall duration and intensity could be discerned by inspection; therefore, the initial ANOVAs were run using depth, slope and length as the variables for data sets containing hydraulic conductivity estimates for one type of sand. These ANOVAs indicated that the computed hydraulic conductivity estimates for both sands varied as a function of average saturated depth and slope. Additional ANOVAs indicated that drainage length, rainfall intensity and duration did not significantly contribute to the variance in the computed hydraulic conductivity values. No physical reasons are apparent for the variability of the hydraulic conductivity as a function of slope. Therefore, the variability due to slope probably arises from inaccuracies in the manner in which the effects of slope are modeled by the Boussinesq equation.

VERIFICATION OF THE HELP MODEL

The drainage rates computed by the HELP model was compared with the results of the drainage tests in several manners. The hydraulic conductivity that was needed to yield the measured drainage rate for the same drainage length, slope, and average saturated depth existing in the drainage test was computed for several times during each test. This hydraulic conductivity value was compared with the value measured in the soils testing laboratory and the value estimated using the Boussinesq equation. If the HELP equation accurately predicted the results of the drainage tests, the hydraulic conductivity value would agree with the measured or estimated hydraulic conductivity value for the sand. If the hydraulic conductivity value was greater than the value obtained for the sand, the HELP equation underpredicted the lateral drainage rate. Another method of comparison was to examine the effects of changing a single variable on the lateral drainage rate measured in the drainage tests and predicted by the HELP equation. The effects of drainage length, slope, average depth of saturation, and the head contributed by the slope of the liner were compared in this manner.

The hydraulic conductivity of the sand at various depths of saturation was estimated for each test using the Boussinesq solution of Darcy's law for unsteady, unconfined flow through porous media and the HELP lateral drainage equation. These hydraulic conductivity values were compared to determine the agreement between the HELP model and the Boussinesq solution. For steady-state drainage, the HELP model estimates of the hydraulic conductivity were 44 percent greater than the Boussinesq solution estimates. This result means that the HELP model underestimated the steady-state lateral drainage rate predicted by the Boussinesq solution by 30 percent. The HELP estimates were 31 percent greater than the laboratory measurements for the fine sand and 88 percent less than the laboratory measurements for the coarse sand. For unsteady drainage, the HELP model estimates were only 13 percent greater than the Boussinesq solution estimates which would underpredict the lateral drainage rate by 11 percent. The closeness of the estimates was not unexpected since the HELP lateral drainage equation was developed from numerical

solutions of the Boussinesq equation for saturated unconfined lateral flow through porous media under unsteady drainage conditions. The underprediction of the cumulative lateral drainage volume would be expected to be very small since the removal rate of water from the drain layer by all other means is much smaller than the lateral drainage rate. Consequently, the effect of differences in the predicted and actual drainage times are small.

The differences between the laboratory measurement of the hydraulic conductivity and either of the two estimates computed from drainage data were much larger than the differences between the estimates. The HELP model and Boussinesq equation predicted very similar drainage rates at 2-percent slope but the HELP model predicted lower drainage rates at 10-percent slope. Unlike the laboratory measurements, the hydraulic conductivity in the drainage tests varied as a function of the depth of saturation apparently due to entrapment of air in the sand. This phenomenon makes it very difficult to model the lateral drainage process and produce good agreement between the predicted and actual results for drainage rate and depth of saturation as a function of time.

An analysis was performed to determine how well the lateral drainage equation in the HELP model accounts for the effects of drainage length, slope of the liner, average depth of saturation and head above the drain contributed by the liner in the estimation of the drainage rate. The drainage equation overestimates the decrease in drainage rate resulting from an increase in length given the same sand, slope, depth of saturation and head from the liner. Using the drainage rate for a drainage length of 25.4 ft to predict the rate for a length of 52.4 ft, the HELP model underpredicted the rate by 18 percent. The HELP equation overestimated the increase in drainage rate by 30 percent that resulted from an increase in slope from 2 percent to 10 percent. Similarly, the HELP equation overestimated the increase in drainage rate by 20 percent that resulted from increasing the height (head) of the crest of the liner from 15.3 to 30.5 in. above the drain. The effects of changes in the average saturated depth on the drainage rate predicted by the HELP equation agreed very well with the actual results.

Since the HELP lateral drainage equation was developed to approximate numerical solutions of the one-dimensional Boussinesq equation for unsteady, unconfined, saturated flow through porous media, it cannot be expected to perform any better than the Boussinesq equation. Therefore, it was necessary to compare the Boussinesq solutions to the laboratory measurements in order to form a basis for judging the significance of the differences between the HELP equation predictions and the laboratory measurements, and between the HELP equation and the Boussinesq solution.

To summarize, the Boussinesq solution after calibration still produced results significantly different from those measured in the drainage tests. The results obtained with the HELP model were generally as good or better than the Boussinesq solution. The HELP equation performed better on tests conducted with 2-percent slope and the Boussinesq solution performed somewhat better on tests conducted at 10-percent slope. The differences between predictions by the two methods for a given set of conditions were small in comparison to the range of actual results. Similarly, the differences between

the predictions and the actual results were much larger than the differences between the HELP equation and the Boussinesq equation.

CONCLUSIONS AND RECOMMENDATIONS

The following conclusions and recommendations are made. Lateral drainage in landfill liner/drain systems is quite variable, probably due to air entrapment. The hydraulic conductivity measurement made in the laboratory is quite different than the in-place value. Consequently, the estimation of the lateral drainage rate is prone to considerable error despite having a good equation or solution method for the estimation. Neither the HELP model nor the Boussinesq solution agreed completely with the drainage results. Nevertheless, the prediction of the cumulative volume of lateral drainage is likely to be quite good since the depth of saturation will be overpredicted if the drainage rate is underpredicted and vice versa, thereby adjusting the drainage rate. However, the predicted depth of saturation will be quite different from the measured value.

Improvements should be made to improve the predictions of drainage rates resulting from changes in slope and drainage length. The drainage equation should be modified to increase its applicability to slopes as large as 30 percent and drainage lengths as large as 2000 ft.

Evaluation of the effects of drainage length, slope of the liner, depth of saturation and head above the drain on the drainage rate predicted by the Boussinesq solution should be performed to determine whether the effects observed with the HELP drainage equation are unique or derived from the Boussinesq equation. Similarly, an additional data set of drainage results should be collected to determine whether the effects are unique to this data set. Additional data should be collected for longer drainage lengths and greater slopes and from actual landfill/liner systems.

SECTION 2

INTRODUCTION

BACKGROUND

Landfills have come to be a widely employed means for disposal of municipal, industrial and hazardous solid wastes. Storage of any waste material in a landfill poses several potential problems. Among these is the possible contamination of ground and surface waters by the migration of water or leachate from the landfill to adjacent areas. Given this potential problem, it is essential that the liquids management technology perform as expected over the life of the landfill. It is also essential that the performance of the technology can be simulated or modeled with sufficient accuracy to design landfills to prevent migration of liquids from the facility. The modeling of the moisture movement through landfills also provides important information for review of landfill designs and evaluation of the adequacy of the design and the limitations of the liquids management technology.

This study was conducted to test and verify the liquid management technology for lateral subsurface drainage in covers and leachate collection systems. The specific objective was to verify the lateral drainage component of the Hydrologic Evaluation of Landfill Performance (HELP) Model (1,2) and other regulatory and technical guidance, provisions and procedures developed by the U.S. Environmental Protection Agency (USEPA) (3).

The USEPA regulatory provisions for lateral drainage layers require only that the depth of leachate buildup at the bottom of the landfill should not exceed 1 ft and the construction materials for leachate collection should be resistant to chemical attack and the physical forces exerted on them (3). USEPA technical guidance states that the drainage layer should be constructed to be at least 12 in. thick at a minimum slope of 2 percent and have a hydraulic conductivity of not less than 1×10^{-2} cm/sec. Also, the drainage pipe system should be of appropriate size and spacing to efficiently remove the leachate. It is believed that 4-in.-diameter pipes spaced 50 to 200 ft apart would be adequate for removing leachate (3). The drainage layer in the cover should have the same specifications as above except that pipe drainage systems are not necessary, although free drainage must be provided at the perimeter of the cover (3).

Subsurface drainage has been a subject of interest for at least 200 years as man attempted to drain marshes and reclaim land for health and agricultural purposes. The literature is filled with citations describing drawdown of a water table under steady-state conditions with pipes placed in parallel at a constant elevation. In the majority of these studies the impervious barrier

soil layer was well below the elevation of the drain pipes. Drainage under these conditions has been fully described and can be predicted within 10-percent accuracy. The phreatic surface is elliptical as long as the drains remain unsubmerged and do not restrict drainage.

Drainage from soils where the drainage pipes are placed on the surface of the barrier soil layer is less well defined. In general, the drainage for this condition is considerably slower, and the accuracy of the drainage rate estimate by Dupuit's law (Darcy's law for unconfined flow) is slightly worse, though reasonably good. The drainage rate is smaller because the cross-sectional area through which the water flows toward the drain is smaller. The drainage rate is slightly overestimated because the flow is more curvilinear, violating the parallel flow assumption.

Studies on subsurface drainage from soils above a sloped impervious layer are not widely found in the literature. Preliminary findings on drainage through pipes placed well above the barrier soil layer have been reported, but none of these studies examined drainage from the surface of the barrier soil layer as performed in landfills and in this study. The literature does not present equations to predict the drainage rate or the phreatic surface.

The majority of the drainage equations reported in the literature were developed using a steady-state assumption of a uniform recharge rate equal to the drainage rate. The drainage equation used in the HELP model assumed steady state to develop the basic form of a steady-state equation but was corrected to agree with the results of a numerical model for unsteady drainage. Drainage in the cover of a landfill or from the leachate collection system of an open landfill is clearly transient, and the phreatic surface profile may differ significantly from the elliptical profile obtained under steady-state conditions. The profiles will vary while the drainage layer fills and drains. Consequently, as the profiles vary, the drainage rates vary for the same average depth of saturation.

The prediction of drainage rates is complicated by many factors. At low heads, unsaturated flow controlled by capillary action, soil moisture gradients and gravity can significantly contribute to drainage. Matrix effects between soil layers can affect the drainage between the layers. Air can be entrapped in the layers altering the head, hydraulic conductivity and phreatic surface profile. The unsaturated hydraulic conductivity of soil at a given moisture content varies depending on whether the soil is wetting or drying. Field measurements of hydraulic conductivity, porosity, and field capacity are difficult to perform precisely and accurately. Soils are generally not uniform and homogeneous.

This study examines transient or unsteady drainage from the entire drainage layer above a sloped barrier soil layer to verify the equation used in the HELP model. This equation was developed by extending equations developed in the literature for simpler cases. This study provides much-needed information in three areas where the literature is lacking: transient drainage, drainage from the surface of a barrier soil layer, and drainage from soils above sloped barrier soil layers. This study measured drainage rates as a function of

phreatic surface profile for two sands, three slopes, a range of saturated depths, and two drain spacings.

DESCRIPTION OF HELP MODEL

The HELP model is a computer model that generates water budgets for a landfill by performing a daily sequential simulation of water movement into, through and out of the landfill. The model estimates of depths of saturation and volumes of runoff, evapotranspiration, lateral drainage, and percolation. Lateral drainage is computed in the model as a function of the average depth of saturation above the liner, the slope of the surface of the liner, the length to the drainage collector, and the hydraulic conductivity of the lateral drainage layer (1):

$$Q = \frac{2\,(0.51 + 0.00205\,\alpha\,L)\,K\,\bar{y}\left[\bar{y}\left(\frac{\bar{y}}{\alpha L}\right)^{0.16} + \alpha L\right]}{L^2} \qquad (1)$$

where

Q = average lateral drainage rate for the time period, inches/day (in./day)

α = slope, dimensionless

L = drainage length, inches

K = hydraulic conductivity, in./day

$\bar{y}$ = average depth of saturation, inches

As presented in the HELP documentation report (1), this equation was developed from the Boussinesq equation for unsteady, unconfined laminar flow through porous media. The Boussinesq equation is obtained by combining Darcy's law with the Dupuit-Forchheimer assumptions (also known as Dupuit's law and Dupuit's approximation) with the continuity equation. Dupuit's law is a steady-state equation for lateral flow:

$$q = -K\,y\,(dh/dx) \qquad (2)$$

where

q = flow rate per unit width

y = depth of saturation above the impervious bed

h = height of free surface above the drain

x = horizontal distance from the drain

This law assumes that the flow throughout the depth of saturated soil is horizontal. Thus, the equipotential lines are vertical and the streamlines are horizontal. The second assumption of this law is that the hydraulic gradient is equal to the slope of the free surface and does not vary with depth.

The continuity equation for lateral drainage from porous media may be written as follows

$$f\ (\partial y/\partial t) = -(\partial q/\partial x) + R \qquad (3)$$

where

f = drainable porosity

t = time

R = rate of vertical infiltration or evaporation into or out of the saturated soil

Combining Equations 2 and 3, the Boussinesq equation is obtained:

$$f\ (\partial y/\partial t) = \partial(K\ y\ (\partial h/\partial x))/\partial x + R \qquad (4)$$

This equation applies Dupuit's law for unsteady conditions.

Equations 2, 3, and 4 were developed for systems with horizontal or mildly sloping impervious beds. Landfills typically have liners that are sloped from 2 to 30 percent, which violates the form of Equations 2, 3 and 4. If the flow is assumed to be parallel to the constantly sloped, impervious bed, then the equipotential lines would be perpendicular to the bed. Under these assumptions Equations 2, 3 and 4 can be modified as follows

$$q = -K\ y \cos\theta\ (dh/dl) \qquad (5)$$

$$f\ (\partial y/\partial t) = -(\partial q/\partial l) + R \cos\theta \qquad (6)$$

$$f(\partial y/\partial t) = \partial(K\ y \cos\theta\ (\partial h/\partial l))/\partial l + R \cos\theta \qquad (7)$$

where

θ = slope of the impervious bed

$h = y + l \sin\theta$

l = distance from drain along the bed slope

Equation 7 is the form of the Boussinesq equation used to develop the HELP lateral drainage equation and the equation solved numerically in this study.

To develop the HELP equation, steady state was assumed ($\partial y/\partial t = 0$). This implies that the phreatic surface profile does not differ significantly from the profile during unsteady conditions, particularly during periods when the phreatic surface is falling. Under steady-state conditions the infiltration rate (R) equals the overall average one-dimensional lateral drainage rate (Q); therefore, Equation 7 becomes

$$Q = K\, d[y\ (dh/dl)]/dl \tag{8}$$

This equation is nonlinear since both y and h are functions of l. The boundary conditions for this equation are

$$h = 0 \text{ at } l = 0 \tag{9a}$$

and

$$dh/dl = 0 \text{ at } l = L \tag{9b}$$

where L = length of bed from drain to crest.

Equation 8 was linearized by setting dh/dl equal to the total change in head over the total length divided by the total length:

$$dh/dl = (y_o + L \sin \theta)/L \tag{10}$$

where y_o = depth of saturation at l = L.

Equation 8 becomes

$$Q = K\ (y_o + L \sin \theta)(dy/dl)/L \tag{11}$$

Similarly, dy/dl was set to equal the average depth of saturation divided by half of the drainage length:

$$dy/dl = \bar{y}/(L/2) \tag{12}$$

Therefore, Equation 11 becomes

$$Q = 2\ K\ \bar{y}\ (y_o + L \sin \theta)/L^2 \tag{13}$$

Equation 13 was then converted to replace y_o with a function of $\bar{y}$ since y_o is unknown in the HELP model. It was also corrected to agree with numerical solutions of Equation 8 for periods when the phreatic surface is falling after the profile had reached steady state. The correction was made for saturated depths ranging from 0 to 30 in., for slopes ranging from 1 to 10 percent, and for drainage lengths ranging from 25 to 200 ft. The result of this correction yielded Equation 1 after replacing sin θ with α. The slope, α, in

dimensionless form is equivalent to tan θ, which for small slopes is approximately equal to sin θ.

The spatially averaged depth of saturation is not constant in a landfill with respect to time, and depending on the rainfall intensity, collection system design, and permeability of the soil layers, can vary greatly in several hours. Since the drainage rate is a function of the average depth of saturation, the drainage rate can also vary greatly in several hours.

As lateral drainage occurs from a drain layer without infiltration, the average depth of saturation continuously decreases; the drainage rate does likewise. Therefore, the HELP model solves Equation 1 as a function of time by applying it for a time step, yielding the average drainage rate for the time step. The time steps were 6 hr for lateral drainage from above the top barrier soil layer of the landfill and 24 hr for the lower two barrier soil layers.

The model reports the drainage rate from above each barrier soil layer daily. To obtain the daily value for the top barrier soil layer, the model averages the computed values from the four time steps. The units for drainage are inches/day (volume/day/surface area).

The average drainage rate is a function of the average depth of saturation, which is a function of the average drainage rate. Therefore, the model solves for drainage iteratively by assuming the drainage rate, solving for the average depth of saturation and then solving for the average drainage rate. If the calculated drainage rate differs significantly from the assumed value, a new estimate of the drainage rate is produced and the process is repeated until the estimated and computed values agree within 0.2 percent.

The average depth of saturation is computed by dividing the drainable water in the lowermost unsaturated segment in a subprofile by the drainable porosity of that segment, and then adding this value to the sum of the thicknesses of all saturated segments between that segment and the barrier soil layer. In actuality, the average depth of saturation in a landfill, physical model or a two- or three-dimensional model would be determined by integrating the depth of saturation over the area or along a path to the drain and dividing by the area or the length of the path. This is the method that was used in analyzing data from the physical models in an attempt to verify the drainage equation.

While the model neglects the lateral variation in saturated depth, the drainage equation used in the HELP model was corrected to approximate the numerical solution of the one-dimensional Boussinesq equation as draining occurred. The numerically generated profiles were used to compute the average depths of saturation which were subsequently used to develop Equation 1. Therefore, use of Equation 1 by the HELP model implies that the profiles are the same as those generated by the numerical solutions of the Boussinesq equation.

PURPOSE AND SCOPE

The objective of this study was to verify the lateral drainage component of the HELP model and other USEPA regulatory and technical guidance for leachate collection systems by determining the lateral drainage rate as a function of the hydraulic conductivity, slope, length and depth of saturation of the lateral drainage layer in large-scale physical models. The measured average depths of saturation, drainage rates and drainage times in the physical models were compared with the results predicted by the HELP equations for vertical and lateral drainage.

Two large-scale physical models of landfill liner/drain systems were constructed and filled with a 3-ft sand drain layer overlying a 1-ft clay liner. A 2-in. layer of gravel was placed under the liner to collect seepage from the clay. The models were instrumented to measure the water table profile, subsurface lateral drainage rate, water application, runoff and percolation through the liner. The models have adjustable slope and two drainage lengths, 25.5 ft and 52.5 ft.

Drainage tests were conducted on both models at three slopes--2, 5 and 10 percent. Drainage from two different sands was studied in each model at each slope. Several drainage tests were run on each configuration of the models by applying water as rainfall to the surface of the sand layer and then measuring the water table along the length of the models and the drainage rate as a function of time. The water was applied at several intensities and for several durations.

SECTION 3

MODEL DESIGN, PREPARATION, AND INSTRUMENTATION

MODEL DESIGN AND CONSTRUCTION

Two physical models were designed and constructed to perform the laboratory verification tests. The models, shown in Figures 1 and 2, were constructed at two different lengths to permit the examination of the effects of length on drainage. One model was built to have a usable depth of 5.0 ft, an inside width of 5.3 ft, and a drainage length of 25.4 ft. The other model had the same depth and width but had a drainage length of 52.4 ft.

Both models were constructed of identical materials. The base of the models was constructed of steel soil test cars used for mobility studies. These cars are reinforced 1/4-in. steel tanks that are 27 ft long, 5.3 ft wide and 2.5 ft deep. The sides of the cars were extended upward 4 ft with marine grade, 1/2-in. plywood supported by 2-in. angle iron. Silicone sealant was used to fill the joints and cracks and to seal and prevent leaks.

The models were placed at a 2-percent slope and fitted with supports for attaching 5-ft screw jacks at the upper end. A jacking structure was built to attach to either model which could raise the end of a fully loaded model. The jack could increase the slope of the long model to 11 percent and the short model to 20 percent. The slopes of the models during testing were determined by surveying.

Three troughs, approximately 12 in. deep and extending across the width of the models, were placed inside the lower end of each model as shown in Figure 3. The bottom trough was used to collect seepage through the clay liner. The middle trough collected subsurface lateral drainage at the bottom of the sand drainage layer. The top trough collected runoff from the surface of the sand. The bottom two troughs were constructed of 1/4-in. steel plates welded to the steel soil test car. The top trough was fabricated of galvanized sheet metal and bolted in place to the plywood walls. The sheet metal was sealed to the walls with silicone sealant.

The runoff trough was drained to a 5-ft-deep, 32-in.-diameter (dia) sump tank via 1.5-dia polyvinyl chloride (PVC) pipe. The water level in the tank was measured with a steel measuring tape before and after a simulated rain event to determine the runoff volume. The drainage trough was also drained to a 5-ft-deep, 32-in.-dia sump tank via 1.5-in.-dia PVC pipe. The drainage sump tanks were automatically pumped out when filled to a height of about 44 in., requiring only about 5 minutes (min) to lower the water depth to about 10 in. The minimum time required to fill the tank was about 4 hr. The seepage trough

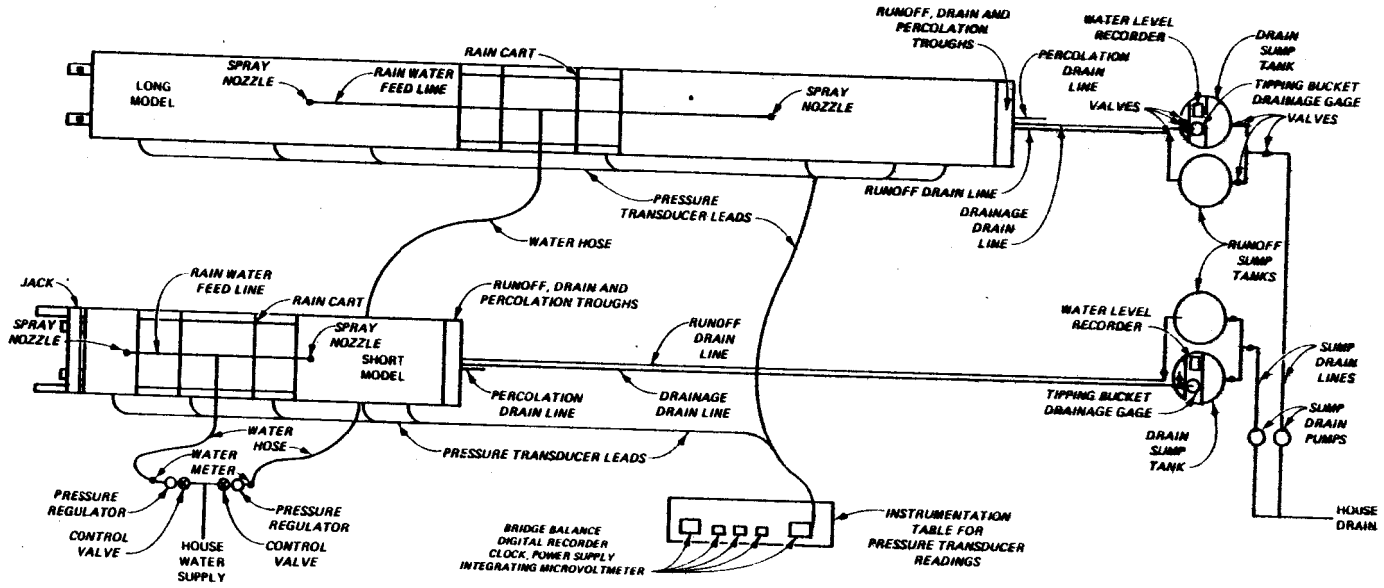

Figure 1. Plan view of experimental components of the physical models.

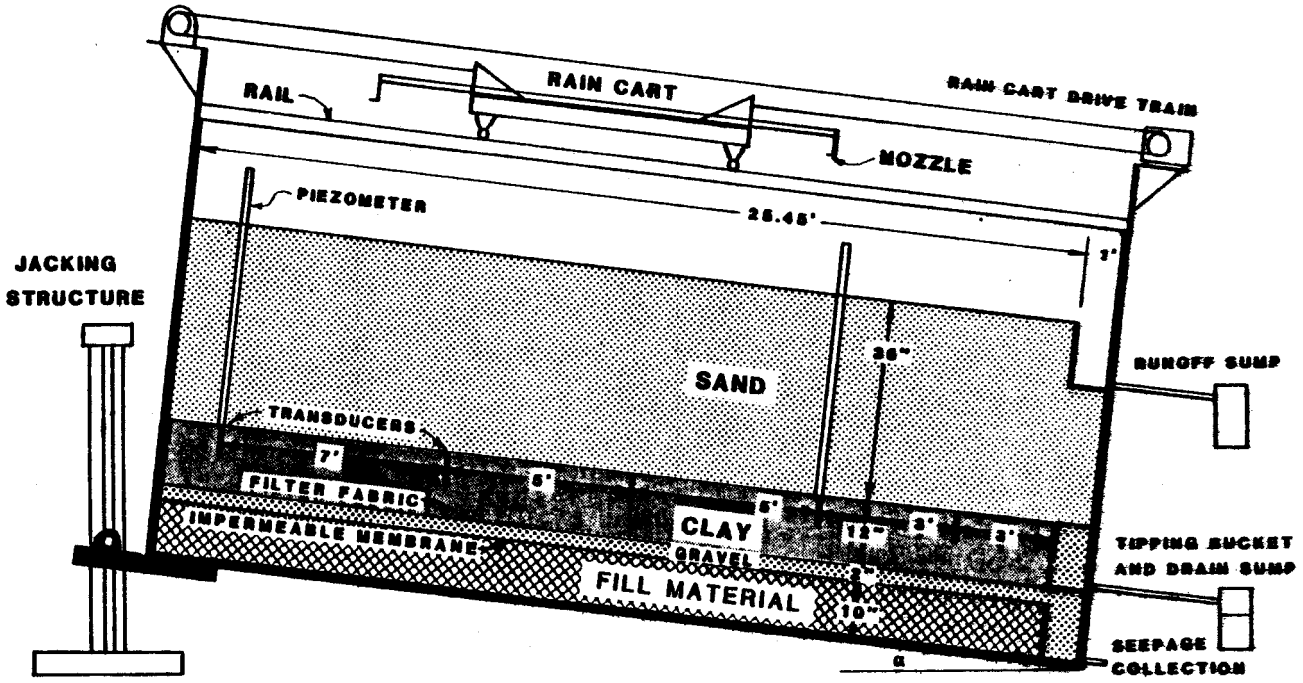

Figure 2. Cutaway side view of physical model.

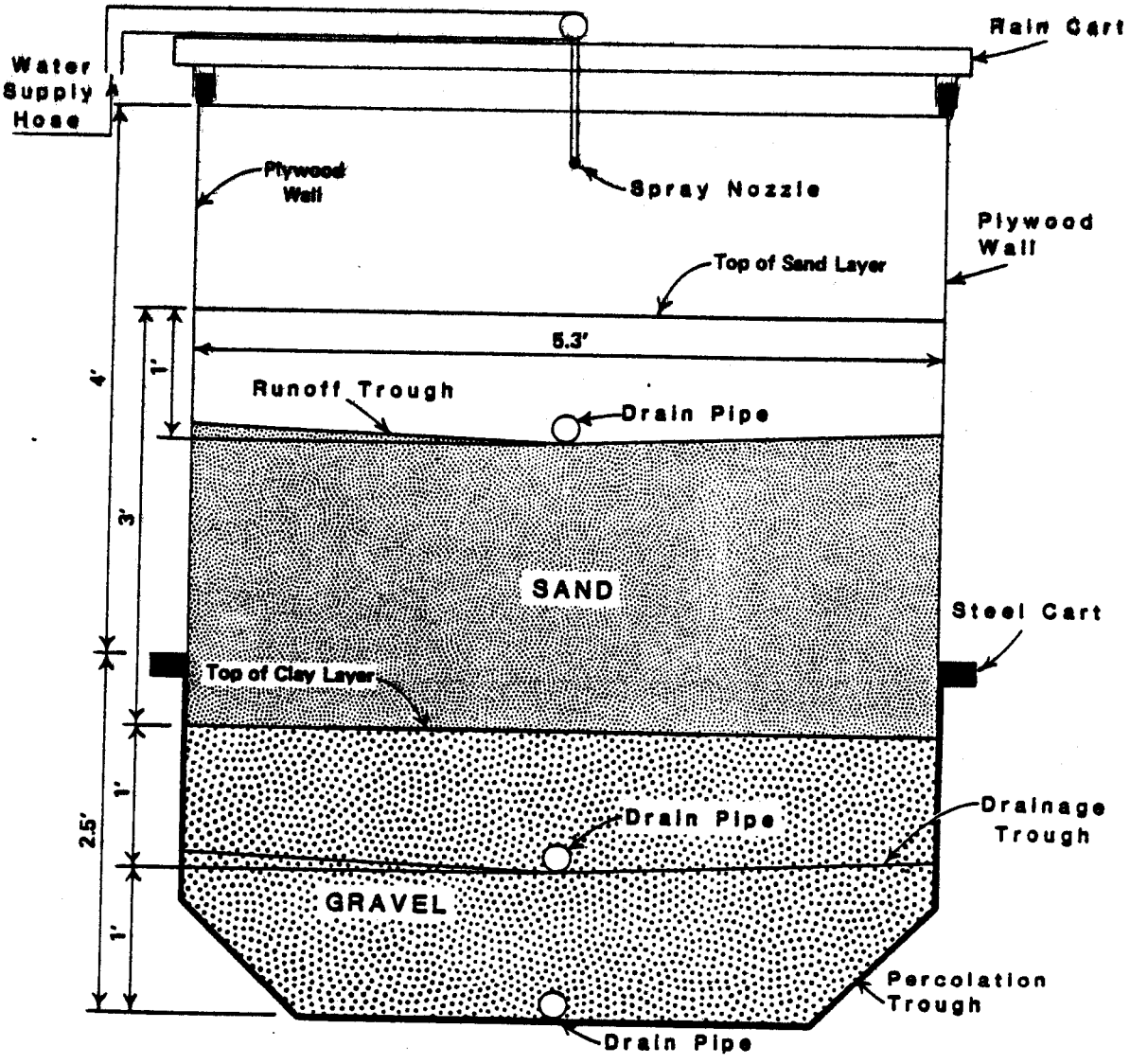

Figure 3. Cutaway end view of physical model at the troughs.

was periodically drained into a 4-liter (ℓ) graduated cylinder to measure the seepage volume. The seepage was drained from the trough via an attached 2-in.-dia rubber hose that was sealed between measurements.

Both models were fitted with a device to spray water uniformly across the length of the surface of the sand drain layer. This device consisted of a 1.5-in.-dia PVC pipe mounted on a 12-ft-long aluminum cart that tracked back and forth on rails that ran the length of the model. A nozzle that sprayed a uniform line of water across the width of the model was attached on each end of the pipe. Each nozzle sprayed on one-half of the model as the cart moved its maximum distance in one direction. The height of the nozzles and the travel limits of the cart were adjustable to ensure that the entire surface of the sand was sprayed. The water application rate or rainfall intensity was adjusted by changing the size of the nozzles or changing the water pressure applied on the nozzles. The intensities of flow rates could be varied between 0.02 and 6 in./hr or 0.06 and 10 gallons/minute (gpm). The intensity during a test was determined by measuring the volume of water applied as a function of time. A stopwatch was used to measure the time and a Badger Meter, Inc., Model Recordall 12 water meter measured the water volume. The nozzles used in the tests were Floodjet 1/8 K.25 316SS through 1/4 K18 316SS that were manufactured by Spraying Systems Co.

Schematics of the models are shown in Figures 1, 2 and 3. Figure 1 shows a plan view of the experimental setup, including the layout of the two models, water and drain lines, instrumentation, and sump tanks. Figure 2 shows a cutaway side view of one model including the troughs, drain lines, sumps, jacking structure and rain cart. Figure 3 shows an cutaway end view of the model illustrating the placement of the trough and the shape of the model.

TEST PREPARATION

After construction was completed, the models were filled with three functional layers and a layer of fill dirt as shown in Figure 2. The top layer was a 3-ft sand layer for lateral drainage. The second layer was a 1-ft compacted clay liner designed to minimize percolation. The third layer was a 2-in. layer of pea gravel to transmit the seepage from the clay liner to a drain. The bottom layer was a 10-in. layer of fill dirt to build up the pea gravel layer to promote drainage.

Fill material 10 in. deep was compacted in the bottom of the steel test car to fill the trapezoidal section of the model and to reduce the volume of pea gravel required. The fill material was covered with a 30-mil, butyl rubber membrane, T-16 manufactured by Firestone. The membrane was glued to the walls of the steel car to prevent percolation into the fill material. The glue was G-580, a synthetic rubber resin dispersed in solvent and manufactured by Pittsburgh Paint & Glass.

A 2-in. layer of washed creek pea gravel was placed on the impermeable membrane and in the seepage collection trough. This layer was designed to have a high permeability and low storage potential in order to transmit the small volume of seepage rapidly to the collection trough. The layer was

covered with Bidim Type C34 filter fabric manufactured by Monsanto to prevent migration of fines from the clay liner into the pea gravel, thereby protecting the ability of the pea gravel to transmit seepage. The filter fabric was glued to the walls of the steel car to ensure that the fabric and pea gravel did not move during placement of the clay liner. Both the gravel and fabric were wetted during placement of the liner. Wetting reduced the seepage required to sufficiently deplete the storage volume of the pea gravel and rubber membrane for transmission of the seepage to begin.

A 12-in. clay liner was placed above the seepage transmission layer. Buckshot clay, a local, well-defined clay, was used. The clay was spread on a concrete strip and cut into small clods using a scarifier. The clay was then wetted to a moisture content of about 27 percent and placed in the model in 2-in. lifts. Each lift was compacted with a gasoline-powered, hand-operated compactor manufactured by Wacker. The compactor had a compacting area of about 0.5 square foot (sq ft). Additional water was added during compaction to ensure good blending and to prevent drying. At least four passes were made on each lift with the compactor, after which no additional compaction could be discerned by additional passes.

After placement of the clay liner was completed, a sample of the top 3 in. was taken. Its water content was 27.1 percent, its dry density was 94.9 pounds per cubic foot (lbs/cu ft or pcf), and its coefficient of permeability was 1.67×10^{-7} cm/sec. A second sample, taken at a depth of 6 in. while filling, had a moisture content of 28.3 percent and a dry density of 91.0 pcf. Nuclear density probe measurements indicated a moisture content of 34.5 percent and a dry density 89 pcf. The nuclear density measurements were made with a Troxler Electronic Laboratories, Inc. Model 3411B nuclear density gage using the procedures outlined in its instruction manual. The moisture content read by the nuclear density meter is much higher because it includes water of crystallization and hydration which could not be measured by the standard moisture content test. Buckshot clay is known to have a high content of bound water. In all of the samples, the dry densities were very high for the moisture content (as shown in Figure 4), which indicates very good compaction. The soil testing was performed in accordance with ASTM-accepted procedures as outlined in Laboratory Soils Testing, Engineer Manual 1110-2-1906 (4).

While placing the clay liner, a flap of the T-16 rubber membrane was glued to the walls of the steel car at 8 in. above the base of the clay and 4 in. below the eventual top of the clay liner. This flap extended 4 in. into the clay. The purpose of the flap was to prevent seepage from occurring between the car and the clay by diverting the water into the clay in the event that the clay shrunk or cracked at the walls.

A 3-ft layer of sand was placed above the clay liner. The sand was placed in 4-in. lifts and each lift was vibrated until no additional compaction could be discerned. In general, four passes were made with a hand-operated, gasoline-powered sand compactor manufactured by Wacker. The size of the vibrating plate on the compactor was about 2 sq ft.

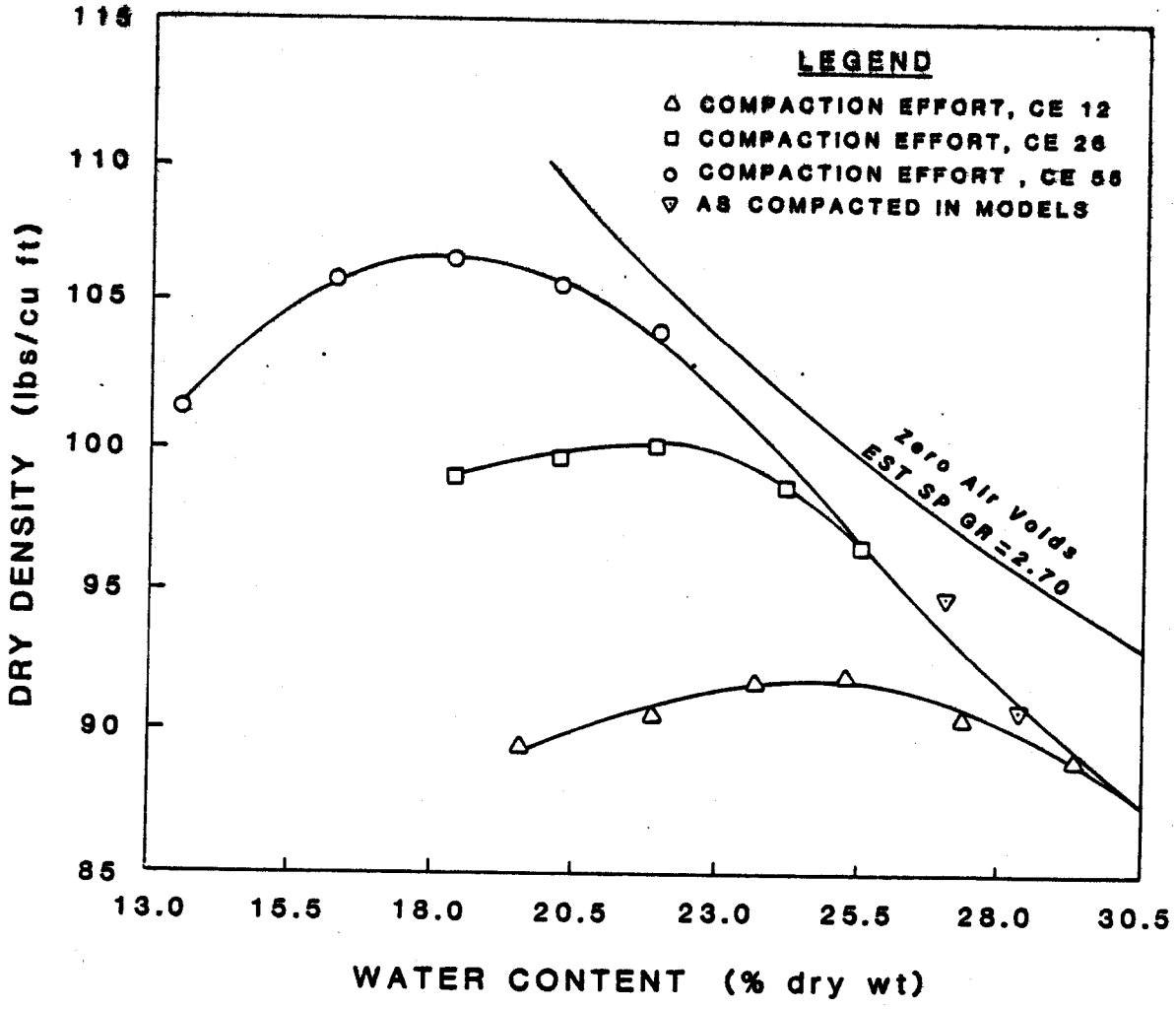

Figure 4. Compaction curves for buckshot clay soil.

Two different sands were used in the tests. One sand was Reid-Bedford sand with Windham clay nonuniformly dispersed throughout. The clay content was about 10 percent in the short model and about 13 percent in the long model. The dry density, as placed, was 106 pcf. This is a relative density of 96 percent, indicating very good compaction. The specific gravity was 2.7, and the coefficient of permeability measured in the soils laboratory was about 3.5×10^{-3} cm/sec. The porosity was 0.37, the maximum drainable porosity was between 0.21 to 0.25, and the wilting point was about 0.07. The grain-size distribution of the sand with the clay is shown in Figure 5.

The other sand was a local, ungraded washed creek sand. The dry density, as placed, was 107 pcf in the long model and 110 pcf in the short model, indicating both were highly compacted. The specific gravity of the sand was 2.7, and the coefficient of permeability measured in the soils laboratory was 2.2×10^{-1} cm/sec. The porosity was 0.35 in the short model and 0.36 in the long model. The maximum drainable porosity was between 0.24 to 0.28 and the wilting point was about 0.04 to 0.05. The grain-size distribution is shown in Figure 5.

INSTRUMENTATION

Description and Installation

The lateral drainage rate from the sand layer was determined by two devices, one for low flow rates and the other for high flow rates. Low flow rates (below 0.08 gpm or 0.05 in./hr for the short model and 0.02 in./hr for the long model) were determined by measuring the drainage volume as a function of time using a Weathertronics Model 6010 tipping bucket rain gage. The tipping bucket collected the water from the end of the PVC pipe draining the drainage trough and discharged the water into the drainage sump tank. A bypass was placed in the PVC pipe to divert the drainage directly into the sump tank during periods of very high flow rates. Higher flow rates (greater than 0.08 gpm) were determined by measuring the water level in the drainage sump tank as a function of time using a Weather Measure Corporation Model F553-A water level recorder powered at 12 volts by a ELCO Model 1060S low ripple battery eliminator and charger.

Pore-pressure transducers were placed in the clay liner with the transducer exposed upward toward the sand layer. The face of the transducer was set slightly below the surrounding top surface of the clay. To install a transducer, a hole about 5 to 6 in. deep and 6 in. in diameter was dug in the clay. The transducer and wire lead were placed in the hole and the removed clay was tamped back in place. The transducer was about 2.5 in. long and 1 in. in diameter. The wire lead from the transducer was placed just below the surface of the clay to prevent interference with the lateral drainage from the sand layer. The tranducer installation is shown in Figure 6.

Six transducers were placed in the long model and five were placed in the short model. Consolidation Electrodynamics Corporation Type 4-312 pressure pickups were fitted in a brass body with a porous stone so the pressure transducer could only measure pore pressure, which in this case was the head of

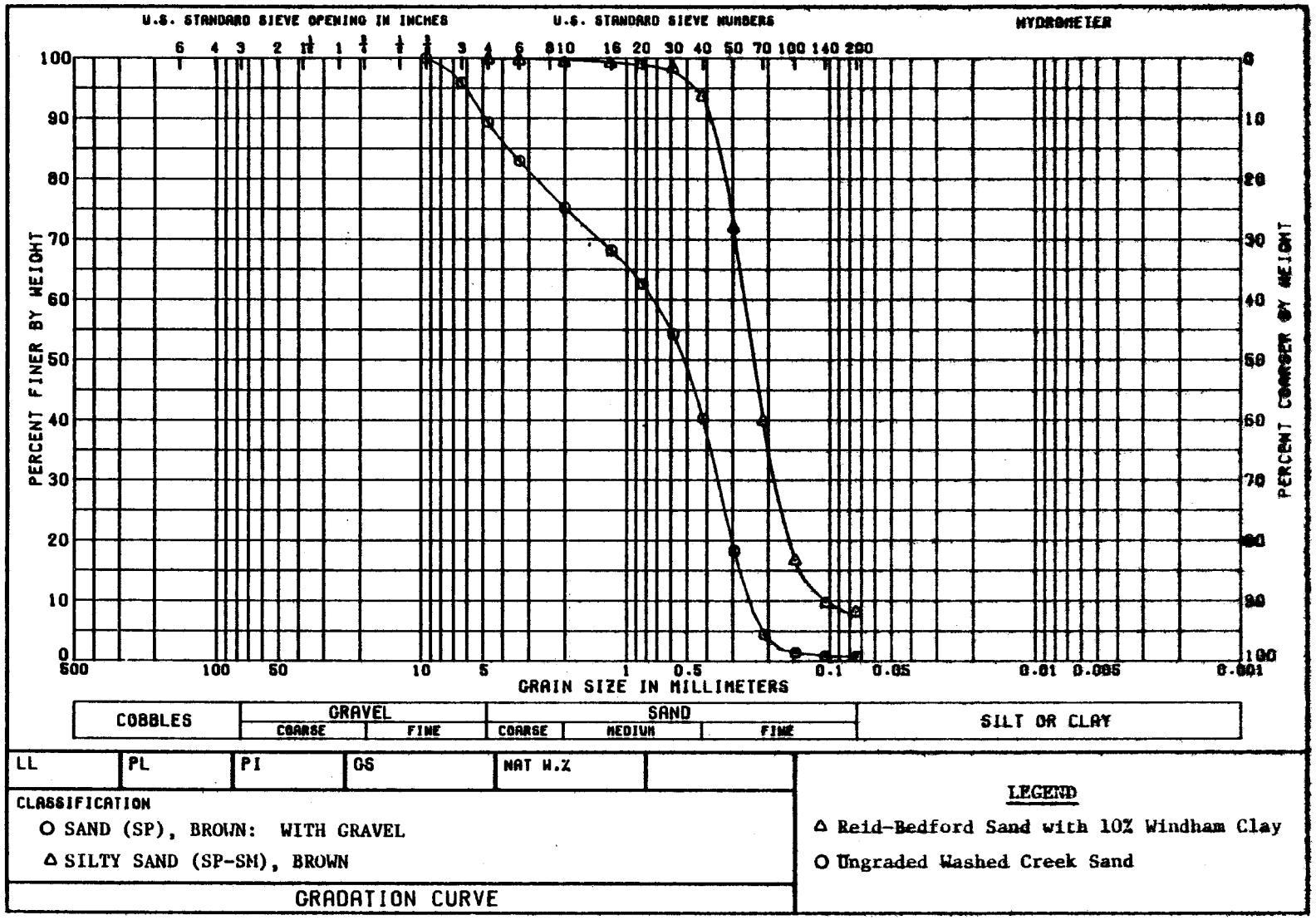

Figure 5. Grain-size distributions of the sand drainage media.

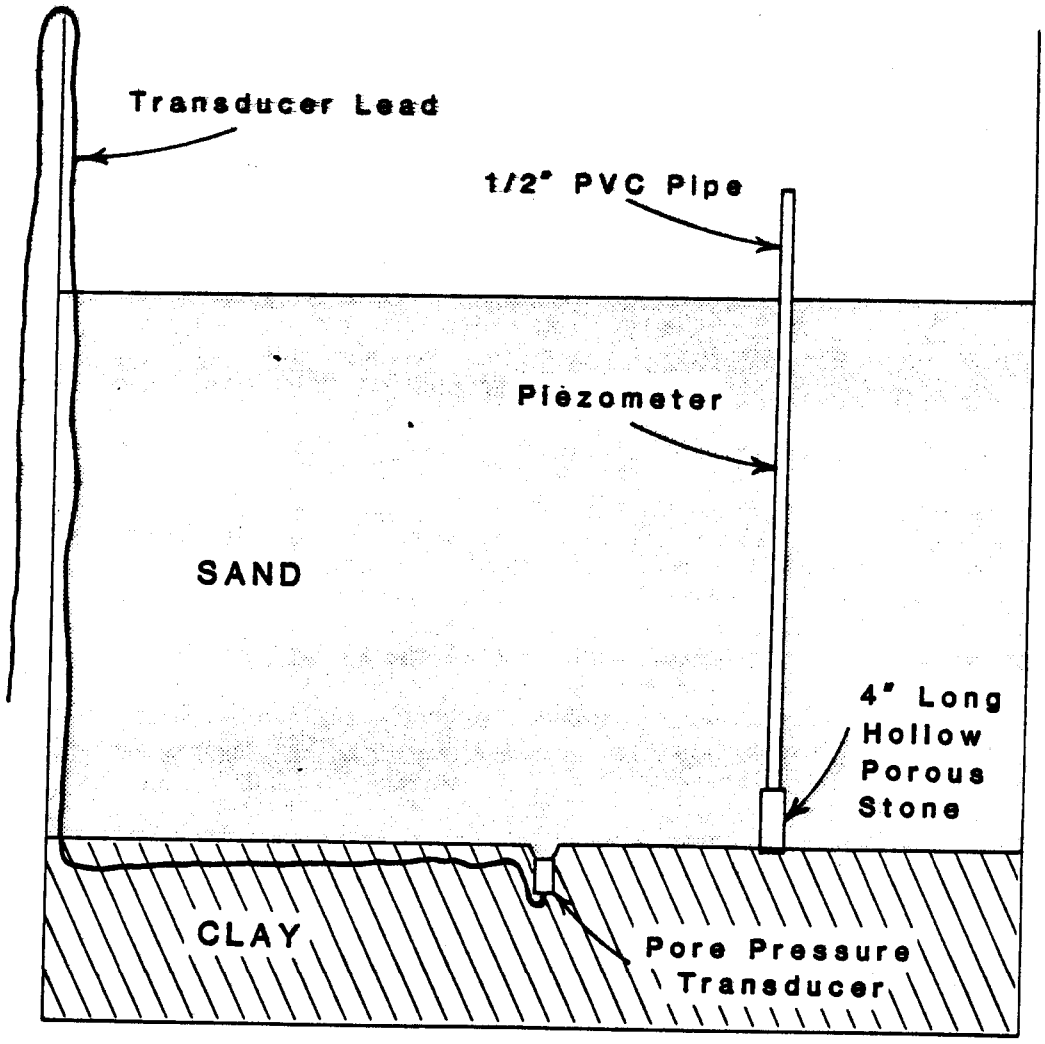

Figure 6. Sketch of piezometer and transducer installation.

water on the transducer. The locations of the transducers were approximately 3, 6, 11, 16 and 23 ft from the lip of the drainage trough in the short model and 3, 6, 11, 23, 35 and 50 ft from the trough in the long model, as shown in Figure 2. The transducers were placed on the centerline dividing the width of the models. The elevations and locations of the transducers were determined by surveying.

Piezometers were installed in the sand layer to provide a backup method for measuring the depth of saturation above the clay liner. These measurements were also used to calibrate the pressure transducers and to check the accuracy of the transducers throughout the testing. Piezometers were constructed by attaching 1.5 in.-dia, 4-in. long-cylindrical porous stones to 1/2-in.-dia PVC pipes of approximately 4-ft lengths. The piezometers were installed with the stone end placed flush with the top of the clay liner and with the pipe extending straight up through the sand layer. The depth of saturation was determined by measuring the depth to the water surface from the end of the pipe and then subtracting that value from the total length of the piezometer. Piezometers were placed at the locations of the second and last transducers from the lip of the drainage trough in the short model, and at the second, fourth and last transducers in the long model. A sketch of the piezometer installation is shown in Figure 6.

Calibration

Instrumentation was used to measure the water applied as rain on the models, to measure the runoff, lateral drainage and seepage from the model, and to measure the depth of saturation above the clay liner. Each of these instrumentation systems was calibrated or used calibrated devices of known accuracy.

The water applied as rain was metered on a Badger Meter which was calibrated at the factory. The meter was accurate within 1 percent at all flow rates. The accuracy was checked by filling a 5-gallon (gal) bucket with water and then carefully measuring the volume of water using a graduated cylinder. The measured volume was within 1 percent of the volume measured by the meter.

Runoff was measured by measuring the change in the water level in the runoff sump tank. The volume of the tank was measured as a function of the water level. Water was added to the tank in increments to raise the water level about 5 in. The quantity of water added was measured using the calibrated meter for the rainfall, and the water level was measured using a steel measuring tape. The procedure was repeated until the tank was full.

Lateral drainage was measured in two ways. For high flow rates the water level in the drainage sump tank was measured as a function of time using a Weather Measure Corporation Model F553-A water level recorder. The volume of water in the drainage tank and the response of the recorder were measured as a function of the water level using the same procedure used to calibrate the runoff sump tank. For low flow rates the volume of drainage was measured as a function of time using a Weathertronics Model 6010 tipping bucket rain gage. The volume per tip was calibrated at the factory and checked by slowly pouring a measured volume of water from a graduated cylinder through the tipping

bucket. The number of tips was counted and compared with the number recorded on the water level recorder. The drainage rates computed from the tipping bucket data and the water level recorder data were compared at the midrange of the flow rates and agreed well with each other.

Seepage was collected in the model for a week or longer and then drained into a 5-gal bucket or a graduated cylinder. The volume of seepage was measured with a graduated cylinder.

The depth of saturation above the clay liner was measured in two ways--manually using piezometers and automatically using pore pressure transducers. The piezometers were calibrated by measuring the length of each piezometer and surveying the location and elevation of each piezometer with respect to the lips of the runoff and drainage troughs and the clay liner. The end of each piezometer was placed flush with the surface of the clay liner.

Prior to installation, the transducers were calibrated in the instrumentation laboratory to determine the linear response factors for a unit increase in head and the readings for zero head. The responses from the transducers were recorded using a Digitrend Model 210 digital recorder with a Hewlett Packard Model 6113A 5-volt DC power supply, a Doric Model 214 digital clock and a Doric Model DS-100 integrating microvoltmeter. A Consolidated Electrodynamics Corporation Type 8-108 DC bridge balance was used to convert the millivolt signals from the transducers to pressure readings in pounds per square inch for the experiments with the Reid-Bedford sand. This same equipment was used both in the instrumentation laboratory and in the model tests.

After installation, the locations and elevations of the transducers were surveyed with respect both to the lips of the runoff and drainage troughs and the clay liner. After the sand was placed above the transducers, the transducers were calibrated again in place to establish the readings which corresponded to zero head of water on the clay liner since the transducers were not placed flush with the surface of the liner. The transducers were also checked to determine if the linear response factors for a unit increase in head were the same as in the instrumentation laboratory. The zeros and response factors were determined in place by saturating the sand layer and flooding the surface to establish free water surfaces of known elevations above the sand. Using the surveying data and the linear response factors, the zeros were calculated. The linear response factors were checked by computing the changes in the readings for several known changes in water level and comparing them with the factors determined in the instrumentation laboratory. The response factors agreed well with the instrumentation laboratory data but the zeros varied considerably.

The piezometers were read periodically throughout the testing to provide a backup for the transducers. The readings of the piezometers were compared with those of the transducers to better define the zeros for the transducers. After testing was completed, corrections to the zeros were determined from the comparisons. The corrections ranged from about -2 to 2 in. (±5 percent of maximum), though half of the transducer readings required little or no correction. The zero of one transducer drifted with time in a constant manner, and the correction was made as a function of time. After correcting the readings

of the transducers which had piezometers associated with them, the readings of the other transducers were corrected. These readings were corrected by plotting the readings to form a profile of the saturation at about five different average heads for each test. A smooth curve was drawn through the previously corrected readings and zero at the trough. The offset of the other readings for each plot was noted to determine whether the offset was constant at all average heads and for each test. A constant offset at all heads and for each test indicated that the zero was off and required correction equal to the offset. If the offsets changed continuously, particularly in one direction, it would indicate that the readings drifted. Readings of only one transducer drifted and the transducer was located at a piezometer. If the offsets increased or decreased uniformly with increasing average head, it would indicate that the linear response factor was incorrect. None of the linear response factors required correction. Nonsystematic changes in the offsets indicated the variance in the transducer readings. The standard deviations of the readings were about ±0.25 in.

SECTION 4

EXPERIMENTAL DESIGN AND PROCEDURES

EXPERIMENTAL DESIGN

A complete block experimental design was used to examine the effects of drainage length, slope, hydraulic conductivity, depth of saturation, rainfall intensity and rainfall duration on the lateral subsurface drainage rates. The block design was selected because it provided the most data with the least time and expense for construction and model preparation. Only two models could be built due to their costs, and only two sands could be examined due to the unavailability of another of significantly different permeability. Several slopes and rainfall events could be examined quickly since very little time was required for changing these test conditions. Also, the time requirements and costs for running an additional test with a different slope or rainfall were less than 10 percent of the requirements for preparing the model for a different sand. Additional rainfall events were examined in lieu of replicates since the lateral drainage rate as computed by Equation 1 does not directly consider the effects of rainfall intensity or duration. Also, since a complete block design was used, the effect of a change in a variable is directly examined under multiple test conditions, reducing the need for replicates.

A summary of the model tests is presented in Tables 1, 2 and 3. Two drainage lengths were compared—25.4 ft and 52.4 ft. Three slopes were examined—approximately 2, 5 and 10 percent. Sands of two hydraulic conductivities were used—4×10^{-3} cm/sec (fine sand) and 2.2×10^{-1} cm/sec (coarse sand). Four rainfall events were examined—a 1-hr rainfall at 0.50 in./hr, a 2-hr rainfall at 1.50 in./hr, a 6-hr rainfall at 0.50 in./hr and a 24-hr rainfall at 0.125 in./hr. Also, water was applied to the sand for a long period of time (generally more than 36 hr) at a rainfall intensity that would maintain the average depth of saturation in the sand at 12 in. In addition to these drainage tests, the sand was saturated, predominantly from the bottom up for several test conditions, and then allowed to drain.

The order of the testing was arranged to accommodate manpower and equipment restrictions. All tests were performed on a given sand before replacing the sand since it would have been very costly and time-consuming to continually change the sand. Also, the placement of the sand would not have been identical each time, which would have been a source of error in the comparisons of the other variables such as drainage length and slope.

All rain events were performed for a given test condition before changing the slope of the model. This was done to minimize manpower requirements and

TABLE 1. EXPERIMENTAL CONDITIONS FOR UNSTEADY DRAINAGE TESTS WITH RAINFALL

Test Setup	Type of Sand	Model Length (ft)	Slope (%)	Rainfall Intensity (in./hr)	Rainfall Duration (hr)	Rainfall Volume (gal)
1A	Fine*	25.45	1.8	0.58	1.0	48.5
1B	"	"	"	1.69	2.0	284.2
1C	"	"	"	0.56	6.0	284.4
1D	"	"	"	0.14	24.1	287.0
1E	"	"	"	1.69	2.0	282.2
2A	"	"	4.9	0.58	6.0	291.6
3A	"	"	10.4	0.56	1.0	48.6
3B	"	"	"	1.74	2.0	291.7
3C	"	"	"	0.57	6.0	291.1
3D	"	"	"	0.14	24.0	291.0
4A	"	52.45	2.1	0.57	1.0	98.5
4B	"	"	"	1.70	2.0	588.0
4C	"	"	"	0.54	6.3	593.0
4D	"	"	"	0.14	23.5	587.0
5A	"	"	5.0	0.57	6.0	591.0
6A	"	"	10.3	0.57	1.0	98.6
6B	"	"	"	1.70	2.0	589.2
6C	"	"	"	0.54	6.2	581.0
6D	"	"	"	0.14	24.6	592.2
7A	Coarse**	25.45	1.9	0.58	1.0	48.6
7B	"	"	"	1.73	2.0	291.6
7C	"	"	"	0.58	6.0	291.6
7D	"	"	"	0.14	27.9	338.7
7E	"	"	"	0.14	24.2	290.9
8A	"	"	5.4	1.73	2.0	291.4
8B	"	"	"	0.59	5.9	291.1
9A	"	"	10.0	0.58	1.0	48.6
9B	"	"	"	1.73	2.0	291.0
9C	"	"	"	0.58	6.0	291.6
9D	"	"	"	0.12	29.6	290.9
9E	"	"	"	0.14	24.0	291.0

(Continued)

TABLE 1. (CONCLUDED)

Test Setup	Type of Sand	Model Length (ft)	Slope (%)	Rainfall Intensity (in./hr)	Rainfall Duration (hr)	Rainfall Volume (gal)
10A	Coarse**	52.45	2.3	0.57	1.0	98.4
10B	"	629.4	"	1.70	2.0	589.2
10C	"	"	"	0.56	6.1	591.0
10D	"	"	"	0.14	24.0	591.0
11A	"	"	5.2	1.62	2.1	589.4
11B	"	"	"	0.57	6.0	590.4
12A	"	"	9.9	0.57	1.0	98.6
12B	"	"	"	1.71	2.0	589.2
12C	"	"	"	0.57	6.2	581.0
12D	"	"	"	0.14	24.0	590.4
12E	"	"	"	1.70	2.0	589.4

* Hydraulic conductivity = 3×10^{-3} cm/sec
** Hydraulic conductivity = 2.2×10^{-1} cm/sec

TABLE 2. EXPERIMENTAL CONDITIONS FOR STEADY-STATE DRAINAGE TESTS

Test Setup	Type of Sand	Model Length (ft)	Slope (%)	Avg. Depth of Saturation (in.)	Rainfall Rate (in./hr)	Drainage Rate (in./hr)
1	Fine*	25.45	1.8	12.6	0.0446	0.0336
2	"	"	10.4	13.2	0.0714	0.0543
3	"	52.45	10.3	12.7	0.0589	0.0249
4	Coarse**	25.45	1.9	11.4	0.0928	0.0708
5	"	"	10.0	11.3	0.2070	0.1688
6	"	52.45	2.3	11.3	0.0464	0.0330
7	"	"	9.9	11.8	0.1212	0.1050

* Hydraulic conductivity = 3×10^{-3} cm/sec
** Hydraulic conductivity = 2.2×10^{-1} cm/sec

TABLE 3. EXPERIMENTAL CONDITIONS FOR DRAINAGE TESTS USING PRESATURATED SAND

Test Setup	Type of Sand	Model Length (in.)	Slope (%)	Initial Avg. Depth of Saturation (in.)
1	Fine*	305.4	1.8	20.95
2	"	"	"	16.79
3	"	629.4	2.1	27.35
4	"	"	"	24.74
5	"	"	"	9.24
6	Coarse**	305.4	1.9	29.79
7	"	"	10.0	19.14
8	"	"	"	2.44
9	"	629.4	2.3	27.75
10	"	"	"	21.18
11	"	"	"	14.62

* Hydraulic conductivity = 3×10^{-3} cm/sec
** Hydraulic conductivity = 2.2×10^{-1} cm/sec

because it would have been difficult to achieve exactly the same slope again. The order in which the slopes were tested was not constant to accommodate manpower and equipment scheduling. The scheduling introduced some randomness into the order of testing the effects of slope. Similarly, the order of the rainfall events for different test conditions was varied to accommodate the work schedules for personnel. This scheduling introduced some randomness into the order of testing the effects of differences in rain events.

TEST PROCEDURE AND DATA COLLECTION

Each test was run in one of three manners. Lateral drainage was measured from a presaturated sand; from a sand before, during, and after a simulated rainfall event; or from a sand while attempting to maintain a constant average depth of saturation of 12 in. The test procedures for the three manners were very similar; only the procedure for applying the water to the model varied.

The procedures for running a test were as follows:

1. Prepare model for testing. This included preparing the sand by placing or leveling; preparing the rainfall cart for desired rainfall intensity by changing nozzles, nozzle heights and end stops; changing the slope of the model; draining sump tanks; and preparing the recorders.

2. Initialize test. This included starting the recorders, setting the time, draining the lateral drainage trough, recording test conditions, measuring initial depth of water in runoff sump tank, and recording the initial water meter reading.

3. Apply water to the model as prescribed for the test. This included adjusting the water application rate and the spray pattern.

4. Note peculiarities of the test including unusual environmental conditions, problems, and variations from the test procedure.

5. After the rainfall was completed and runoff ceases, measure the final depth of water in runoff sump tank.

6. Measure water levels in piezometers periodically.

7. Drain tanks as required.

8. Continue testing until the heads become so low as to nearly expose a transducer to air and then stop drainage or start a new test.

9. Collect data from recorders and reduce the data.

Prior to calibration of the pore pressure transducers, water was added slowly to both ends of the model. In this manner the sand was saturated primarily from the bottom up, which forced the air out of the sand. Following the calibration, the sand was drained and the drainage rate and heads were measured continuously while draining. Drainage from presaturated sand was measured for only four test conditions since saturation was required only for calibration.

For the tests in which a constant average head of 12 in. was maintained, water was applied to the model to increase the head rapidly to 12 in. This water was applied at a rate of about 0.5 in./hr. After reaching a head of 12 in., the rainfall intensity was decreased to the intensity estimated as necessary to maintain the head. The desired intensity was determined by adding the evaporation rate, the rate of leakage and seepage, and the drainage rate which corresponded to an average head of 12 in. during a previous rainfall for the same physical test conditions. The intensity was adjusted during the test if the head did not remain constant near 12 in. The rain was continued for at least 12 hr after the head remained nearly constant.

The evaporation rate ranged from about 0.2 to 0.3 in./day while raining, as estimated by the differences in the water application rate and the lateral drainage rate during the steady-state drainage tests. The rate was dependent on building temperature and on the spray nozzle. The building temperature

ranged from about 58°F to 90°F, but for most tests the temperature ranged between 70°F and 82°F.

Leakage varied directly as a function of head. Both models leaked, but the short model was more watertight than the long model. The leakage rates for the short model were measured to be about 0.02 in./day at a head of 20 in. and about 0.01 in./day at a head of 12 in., while the leakage rates for the long model were measured to be about 0.12 in./day at a head of 20 in. and about 0.07 in./day at a head of 12 in. Neither model leaked at heads below 6 in. since all of the seams in the model were above this depth. The long model leaked more because it suffered greater deflections upon loading due to its greater length. This caused more seams to rupture and leak. These leakage rates were used to correct the water budgets for each test.

The majority of the drainage tests encompassed measurements before, during, and after a specified rainfall event. In these tests, a specified quantity of water, either 48.5 or 291 gal for the short model and either 98.5 or 591 gal for the long model, was sprayed across the entire surface of the sand in a specified period of time--1, 2, 6 or 24 hr. These quantities of water correspond to about 0.57 in. and 3.4 in. of rain, respectively, for both models. During these tests, the head increased from a starting point of about 4 in. to a peak value occurring about 30 min after the rainfall ceased, and then returned to about 4 in. when the test was stopped. Several tests were allowed to continue until the head was nearly zero inches.

DATA REDUCTION

The readings of the pressure transducers were recorded on a digital recorder at an interval ranging from 10 to 60 min. The reading for each transducer was converted into head of water at the location of each transducer. The reading was converted by subtracting the zero for the transducer and then multiplying this value by the linear response factor for the transducer to convert the millivolt value to pressure head in inches of water. The head was then corrected for changes in the barometric pressure and temperature using the readings from a transducer installed to monitor these changes. The heads were then corrected for the differences between the elevations of the transducers and the elevations to the surrounding clay liner. After the actual heads were computed, the heads throughout each model at each time period were averaged using the trapezoidal rule. The head at the lip of the drainage trough was assumed to be zero, and at the upper end the head was assumed to be the same as at the uppermost transducer.

The volume of drainage was recorded continuously on a strip chart. The drainage rate was determined by reading the change in volume of drainage collected in the sump tank for an interval of time or the volume of drainage, as tips, passing through the tipping bucket during an interval of time. These volumes were then divided by the interval of time to yield the average drainage rate. This rate was recorded as the drainage rate at the center of the time interval. The intervals ranged from 15 min to 3 hr depending on how rapidly the drainage rate was changing. The drainage rate was then correlated with the heads by matching the time of the readings.

SECTION 5

PHYSICAL MODEL RESULTS

This section presents the results of the drainage tests. These results include measurements of the saturated depth as a function of distance from drain, measurements of saturated depth and drainage rate as a function of time and, similarly, measurements of drainage rate as a function of saturated depth. Explanations of these results are presented in the next section along with comparisons between these results and the HELP model predictions.

SATURATED-DEPTH PROFILES

The depth of saturation was measured using pressure transducers at various distances from the drain. Plots of depth of saturation versus distance from the drain are shown in Figures 7-10 for various times during the experiments. The depth measurements at a given time were used to compute the average saturated depth ($\bar{y}$) for that time by the trapezoidal rule. The values of $\bar{y}$ are noted in the figures for all saturated-depth profiles shown. A comparison of profile shapes indicates significant differences between the rising saturated-depth profile (fill conditions) and the falling saturated-depth profile (drain conditions) for the same $\bar{y}$. The profiles are steeper near the drain when filling than when draining. The difference is greater for higher infiltration rates. Profile plots are shown in Figure 11 for steady-state discharge at slopes of 2 and 10 percent (α = 0.02 and 0.10) when $\bar{y}$ equaled approximately 12 in. Steady-state profiles are very similar to the profiles for draining. Similar plots for the hydraulic head above the drain profiles are shown in Figures 12-16. All profiles shown in Figures 7-16 were taken from the 6-hr rainfall experiments, except for the fine sand profiles in the short model at 2-percent slope, which were taken from the 24-hour rainfall experiment.

DRAINAGE RATE AND SATURATED DEPTH

The variations in average saturated depth and drainage rate with time are shown in Figures 17-22. Again, these figures represent 6-hr rainfall experiments with the exception noted above. In some cases, the entire thickness of the drainage layer approached saturation prior to the end of rainfall. As a result, the curve of average depth versus time for a few cases approaches a plateau near the point of maximum average depth.

The same $\bar{y}$ and drainage rate data are presented in Figures 23 and 24. Here the drainage rate is plotted as a function of $\bar{y}$ for the same point in time throughout both the filling and draining portion of each experiment. The resulting curves show hysteresis in the filling and draining cycles for the

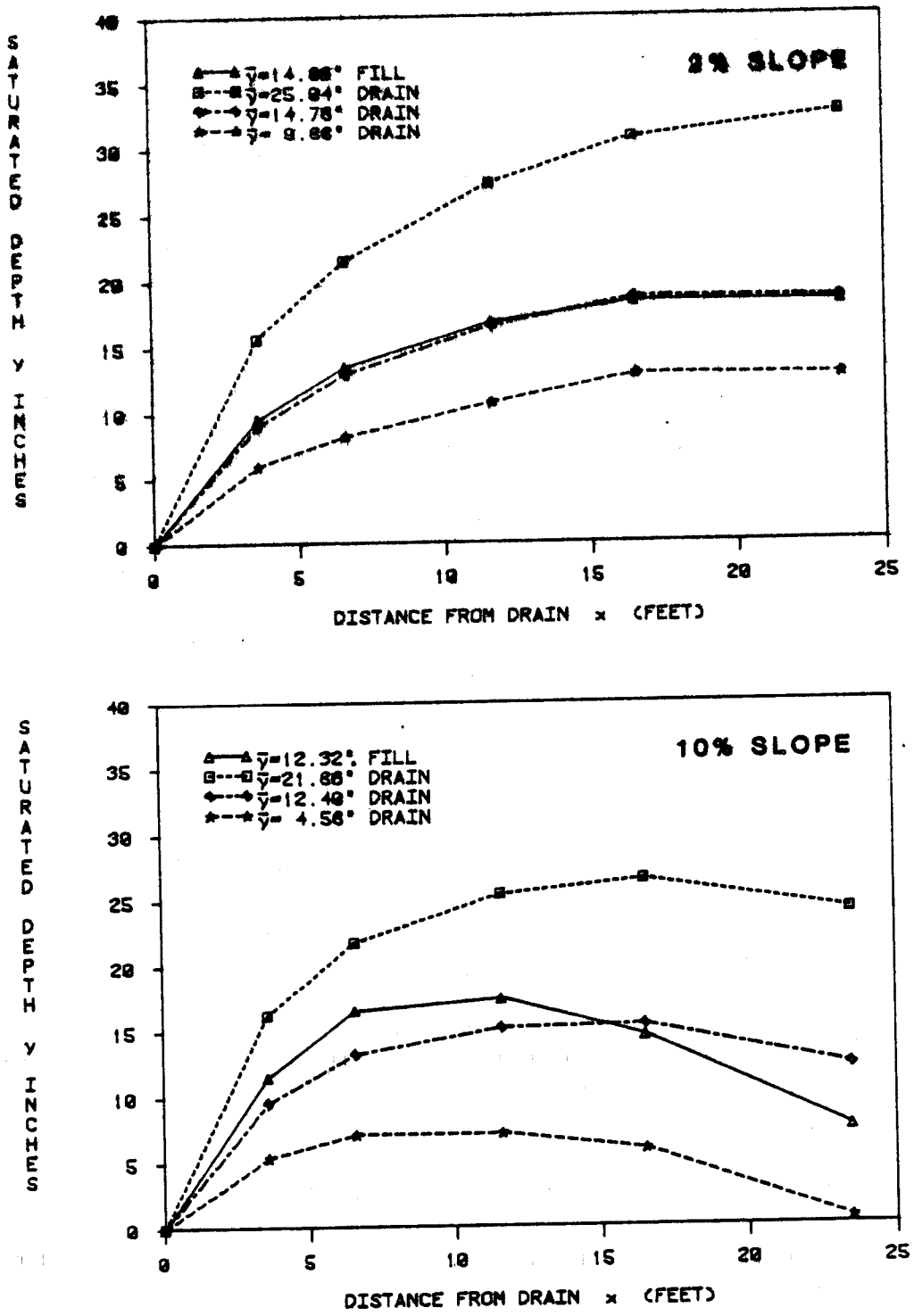

Figure 7. Saturated depth profiles for unsteady drainage during 24-hr rainfall test at 2-percent slope and during 6-hr rainfall test at 10-percent slope using fine sand in short model.

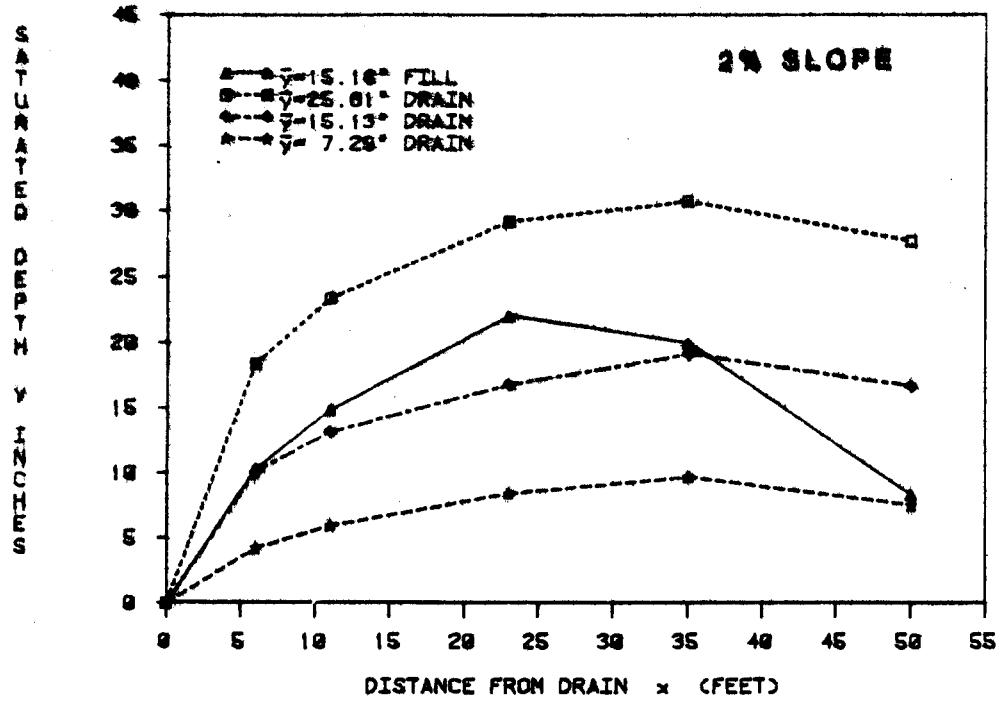

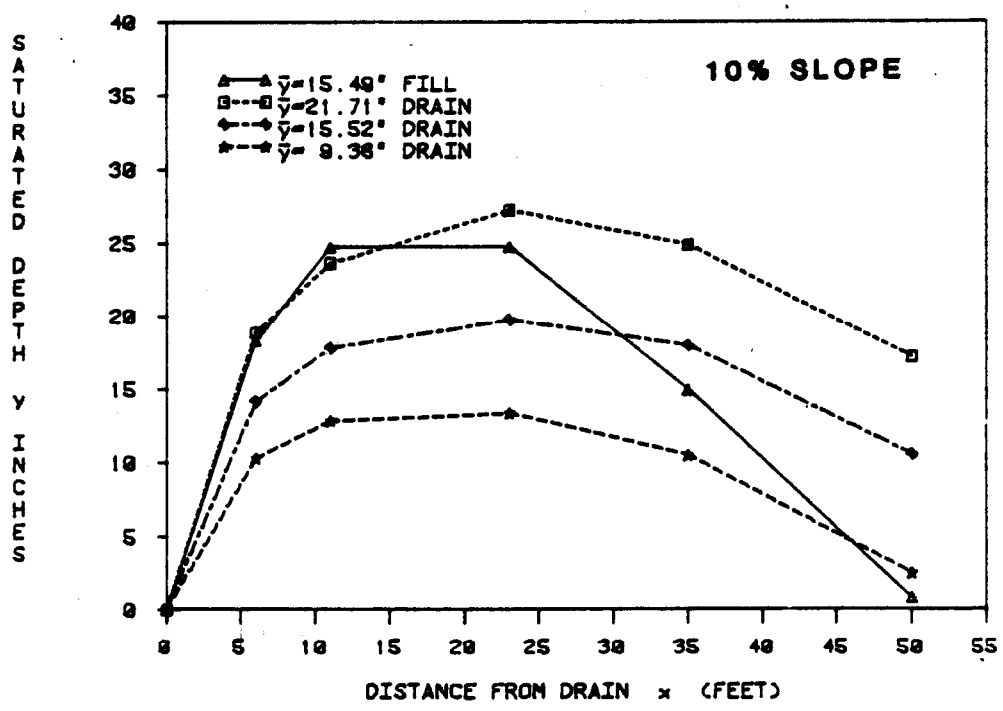

Figure 8. Saturated depth profiles for unsteady drainage during 6-hr rainfall test using fine sand in long model at slopes of 2 and 10 percent.

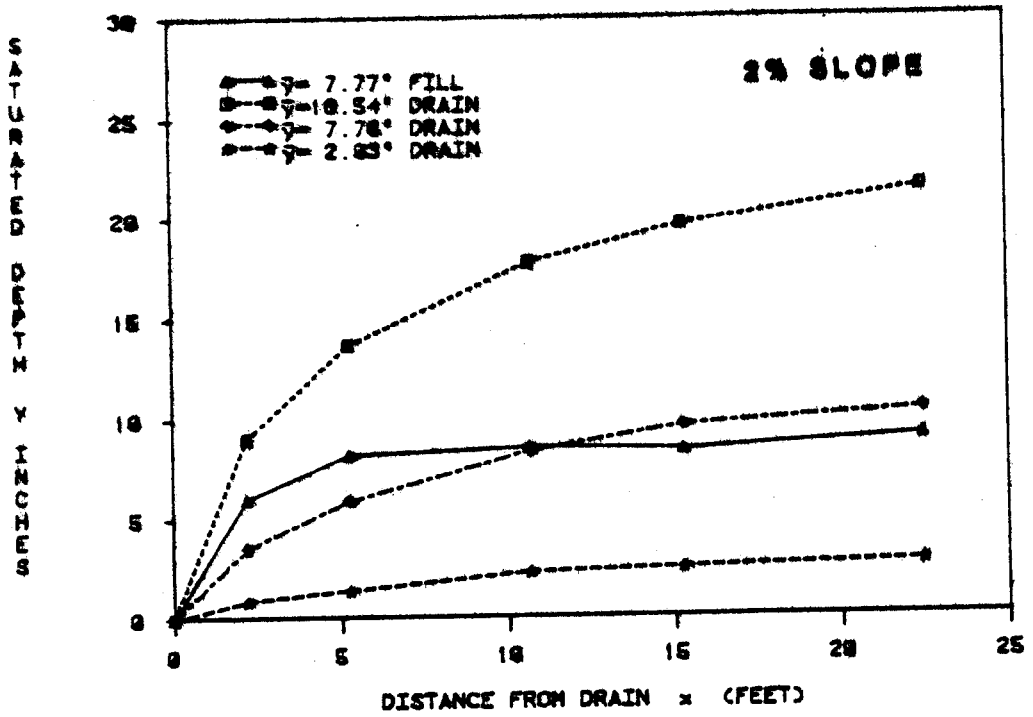

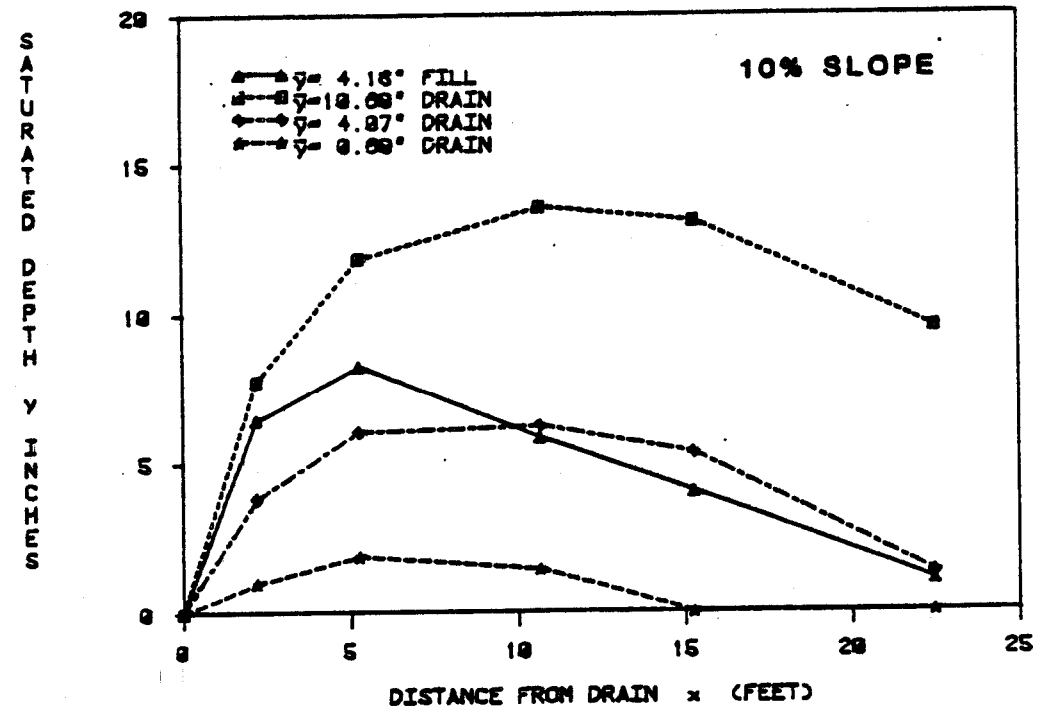

Figure 9. Saturated depth profiles for unsteady drainage during 6-hr rainfall test using coarse sand in short model at slopes of 2 and 10 percent.

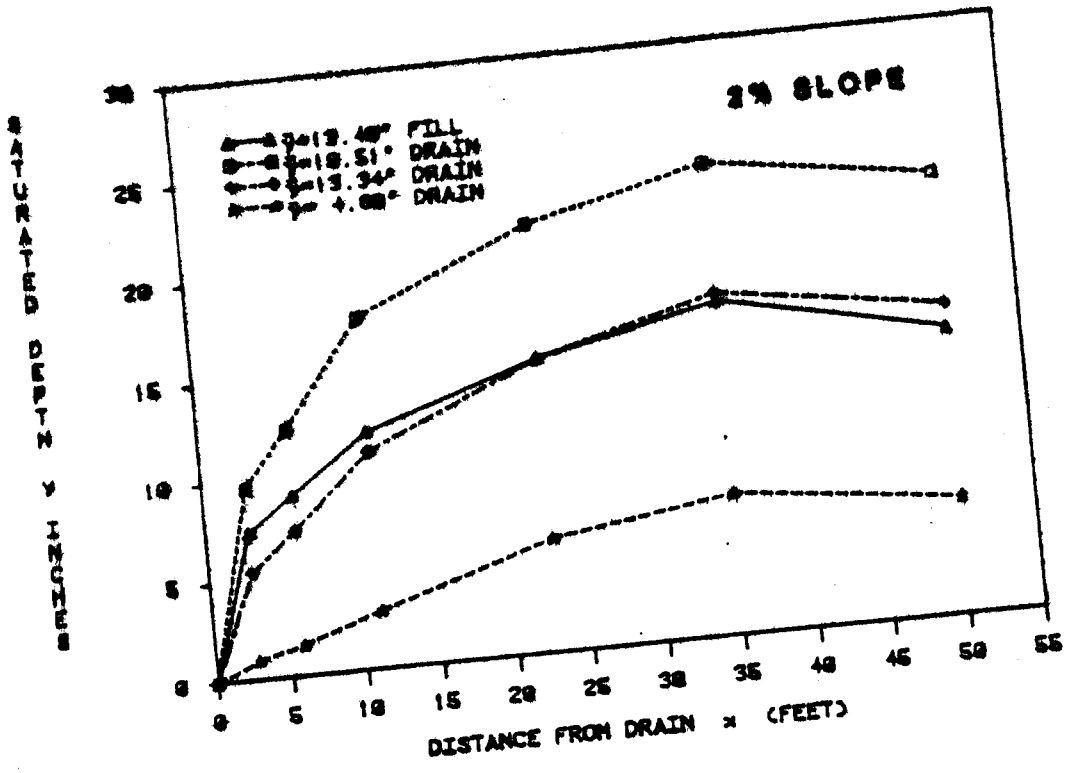

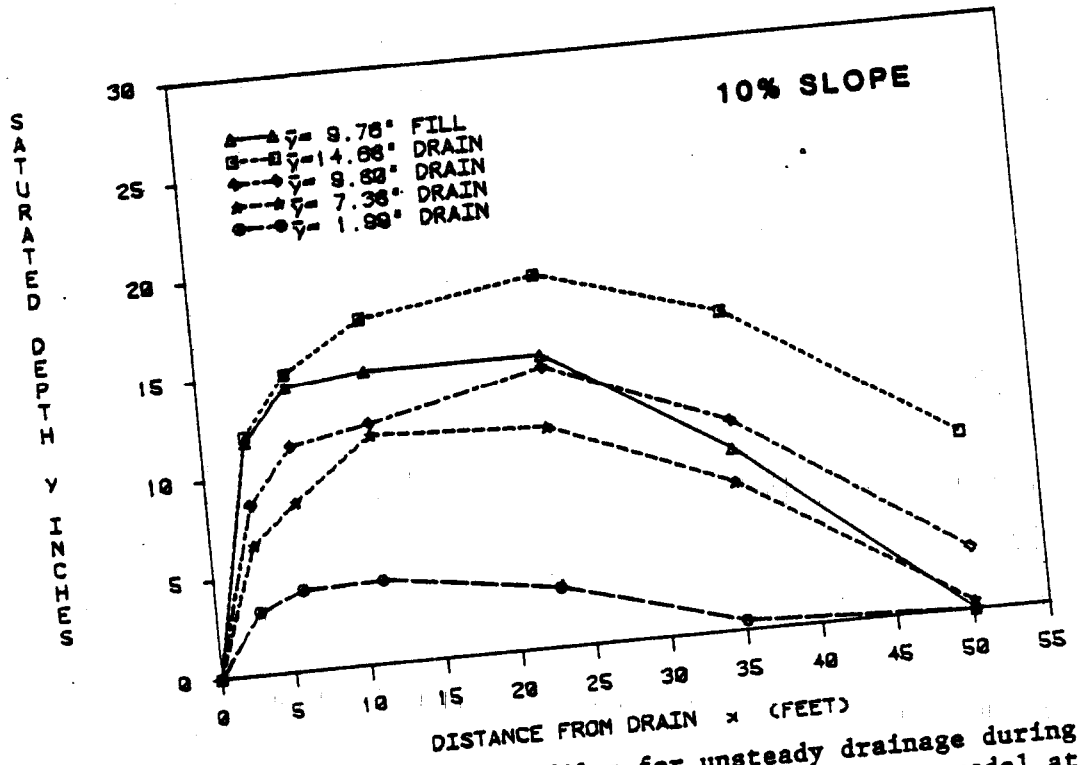

Figure 10. Saturated depth profiles for unsteady drainage during 6-hr rainfall test using coarse sand in long model at slopes of 2 and 10 percent.

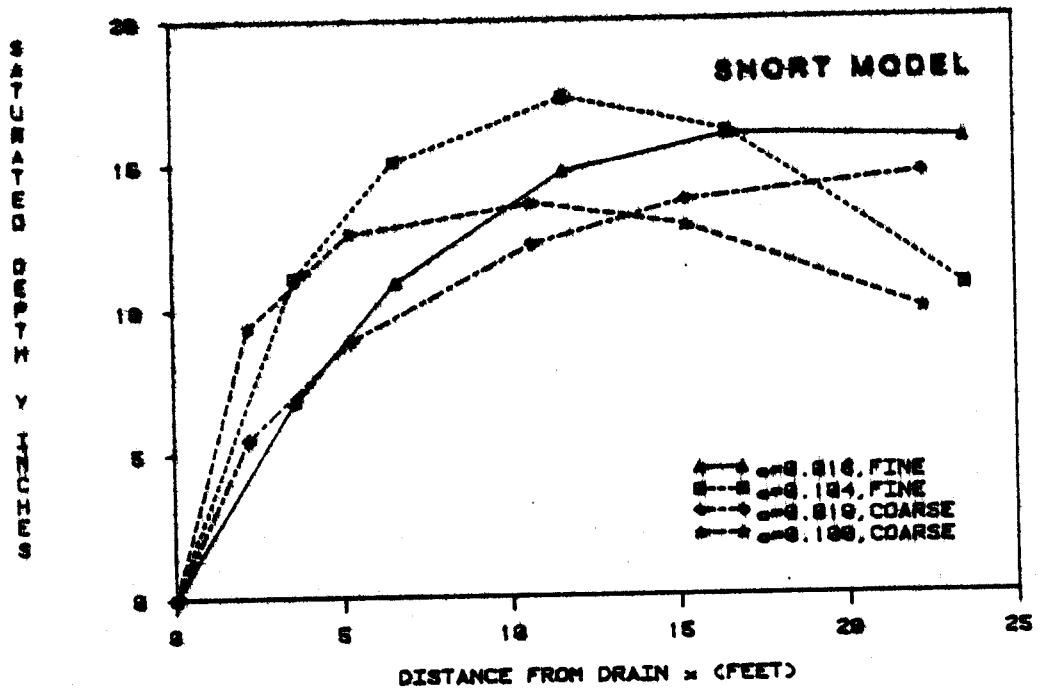

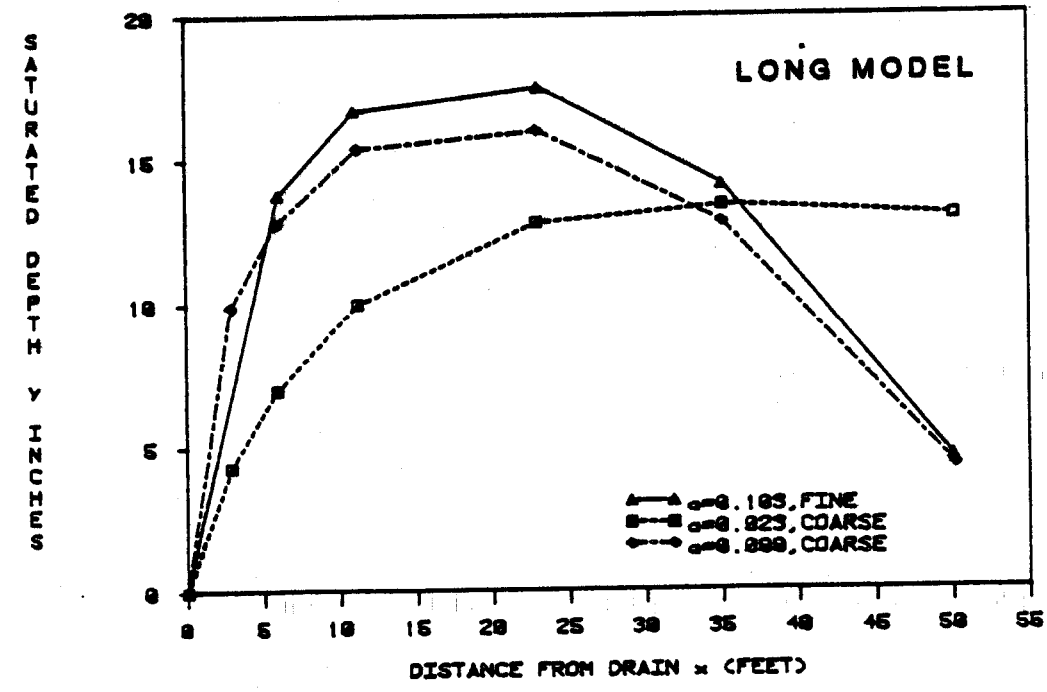

Figure 11. Saturated depth profiles for steady-state drainage in both physical models.

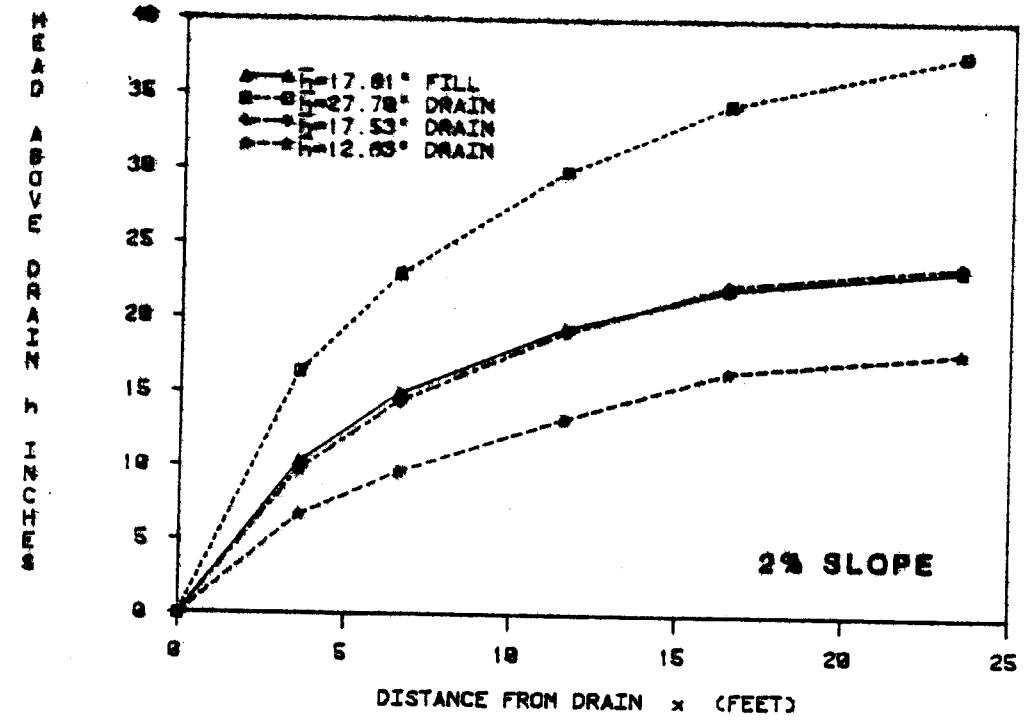

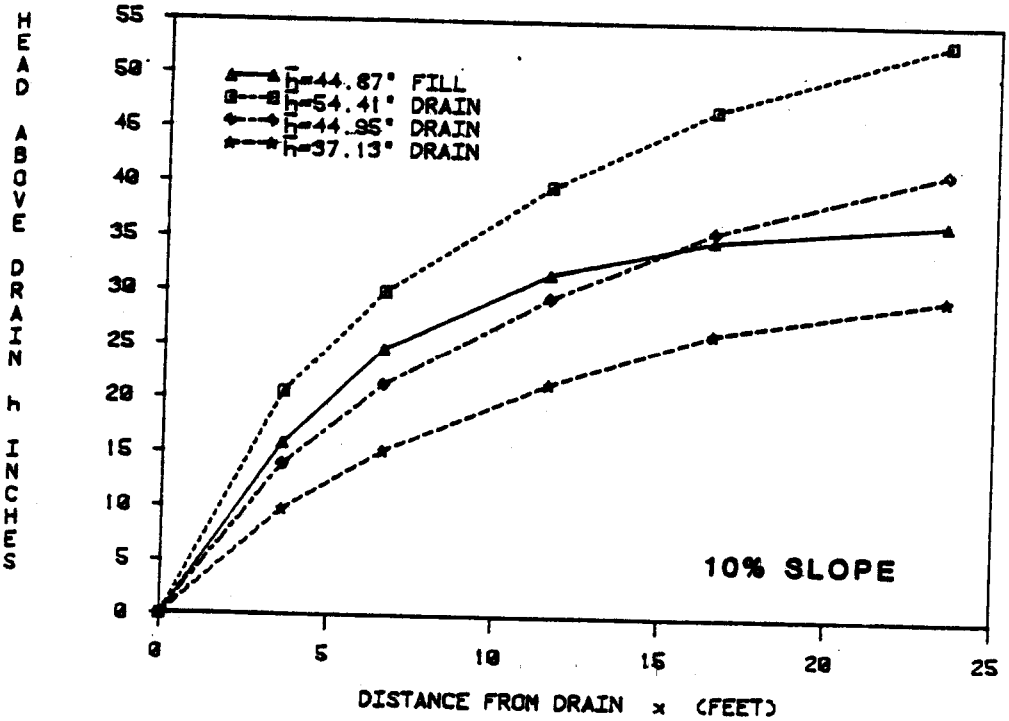

Figure 12. Head profiles for unsteady drainage during 24-hr rainfall test at 2-percent slope and during 6-hr rainfall test at 10-percent slope using fine sand in short model.

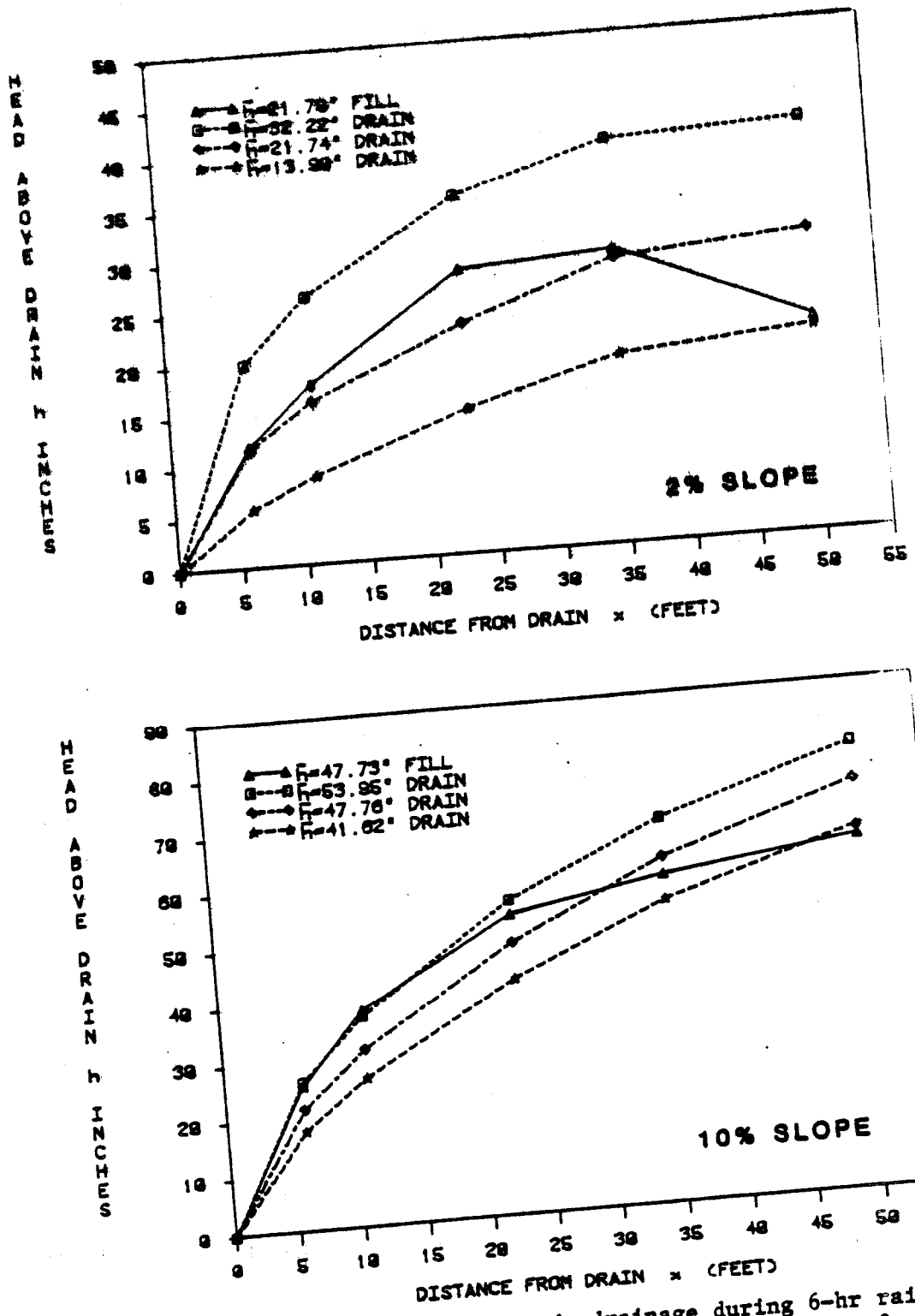

Figure 13. Head profiles for unsteady drainage during 6-hr rain test using fine sand in long model at slopes of 2 an 10 percent.

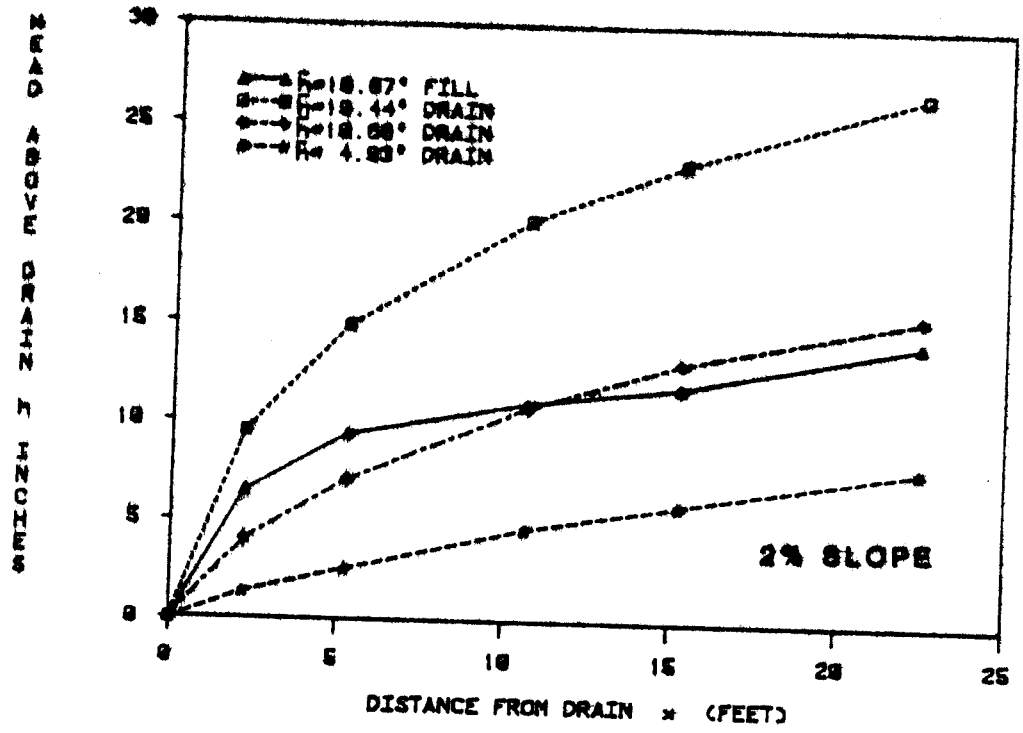

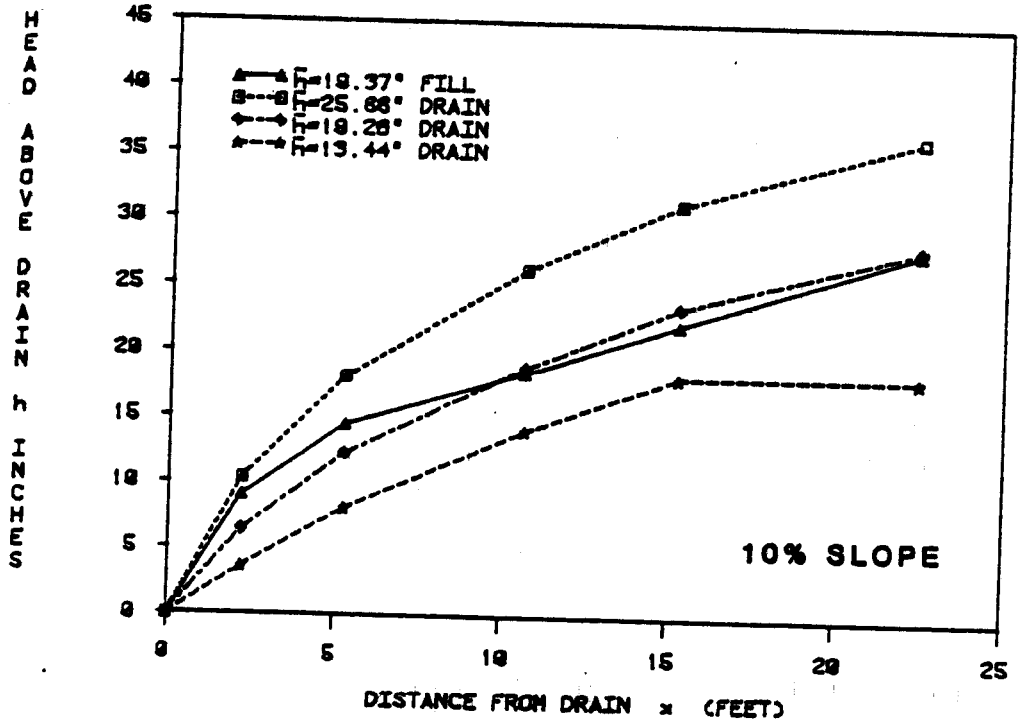

Figure 14. Head profiles for unsteady drainage during 6-hr rainfall test using coarse sand in short model at slopes of 2 and 10 percent.

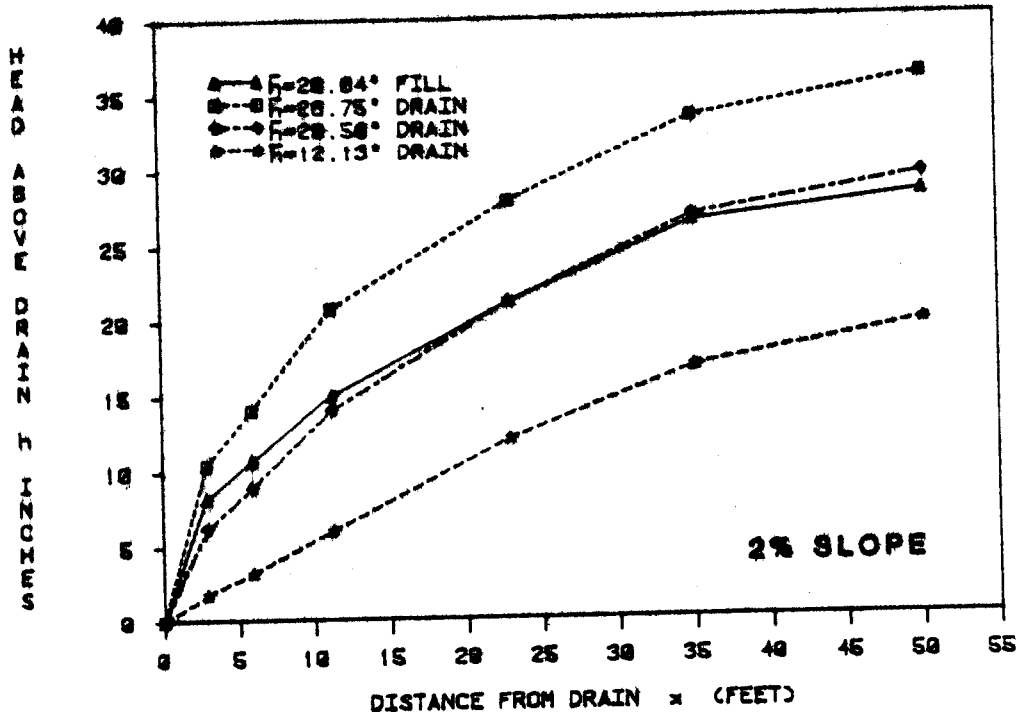

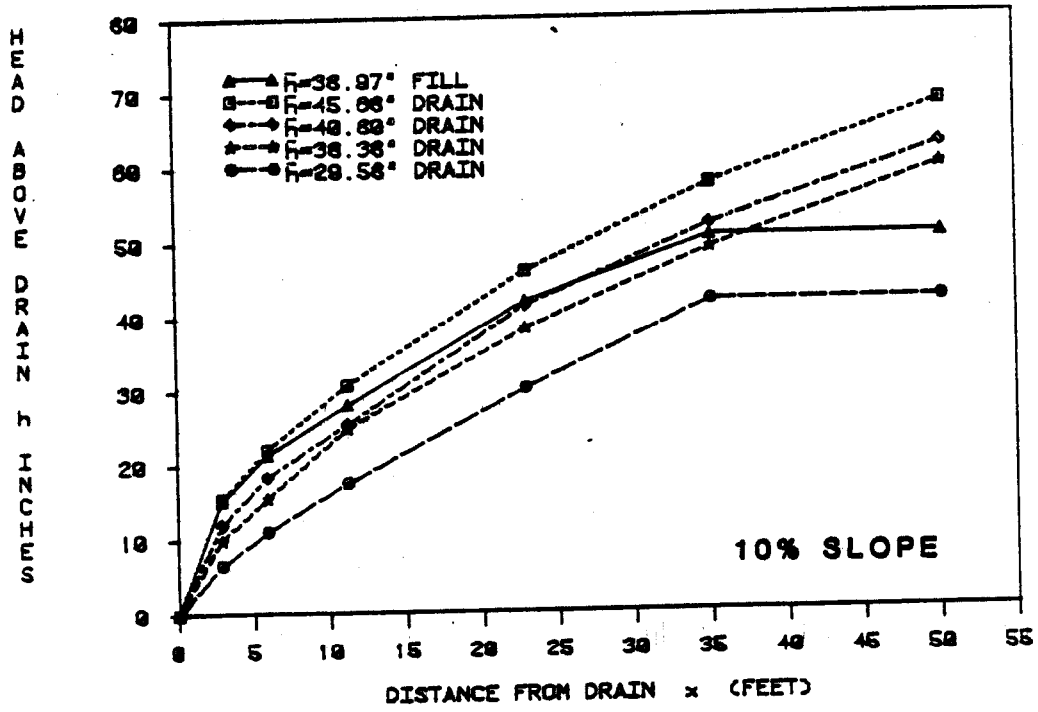

Figure 15. Head profiles for unsteady drainage during 6-hr rainfall test using coarse sand in long model at slopes at 2 and 10 percent.

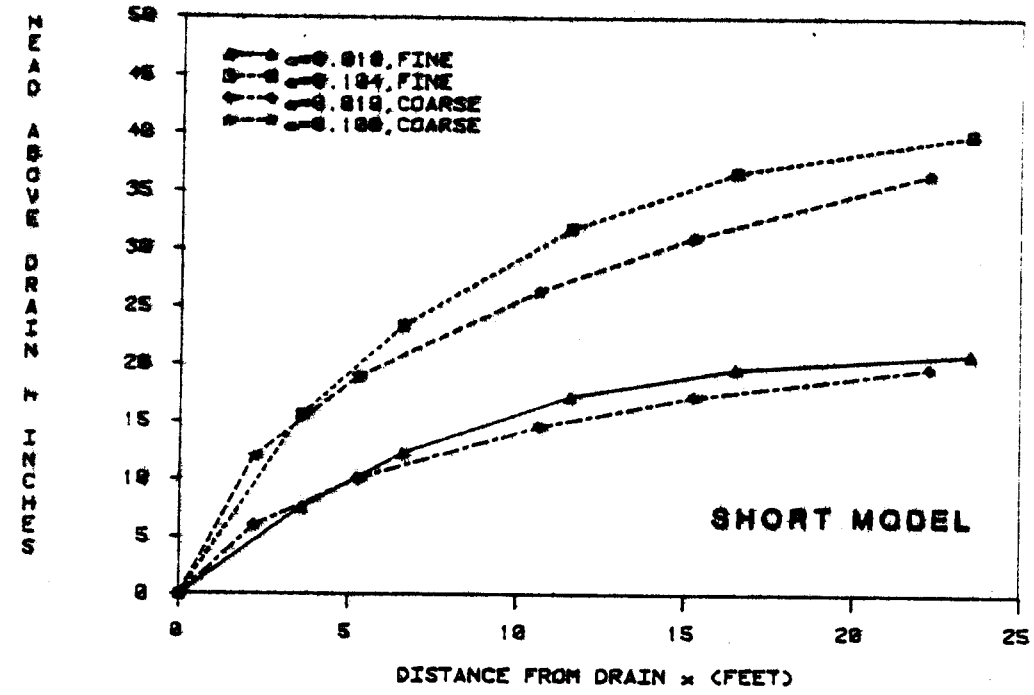

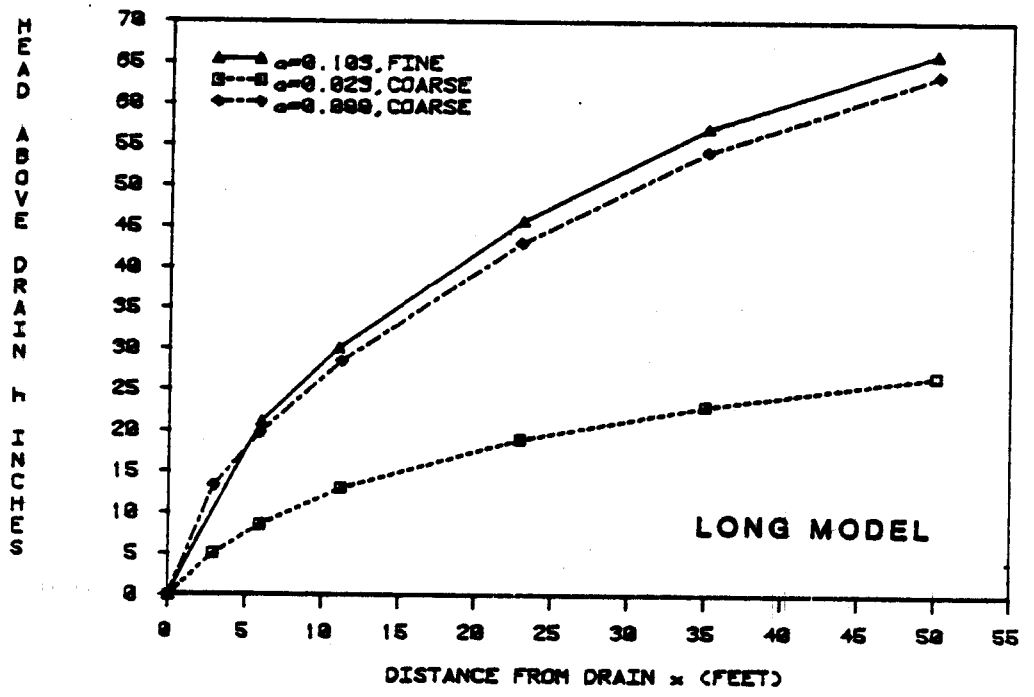

Figure 16. Head profiles for steady-state drainage in both physical models.

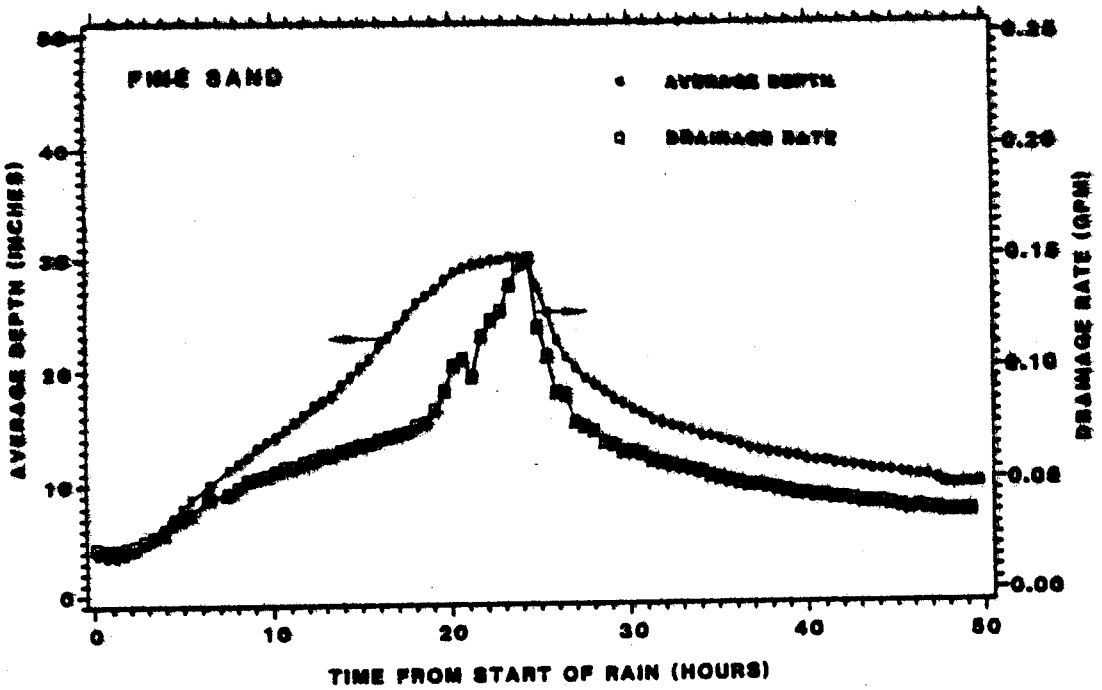

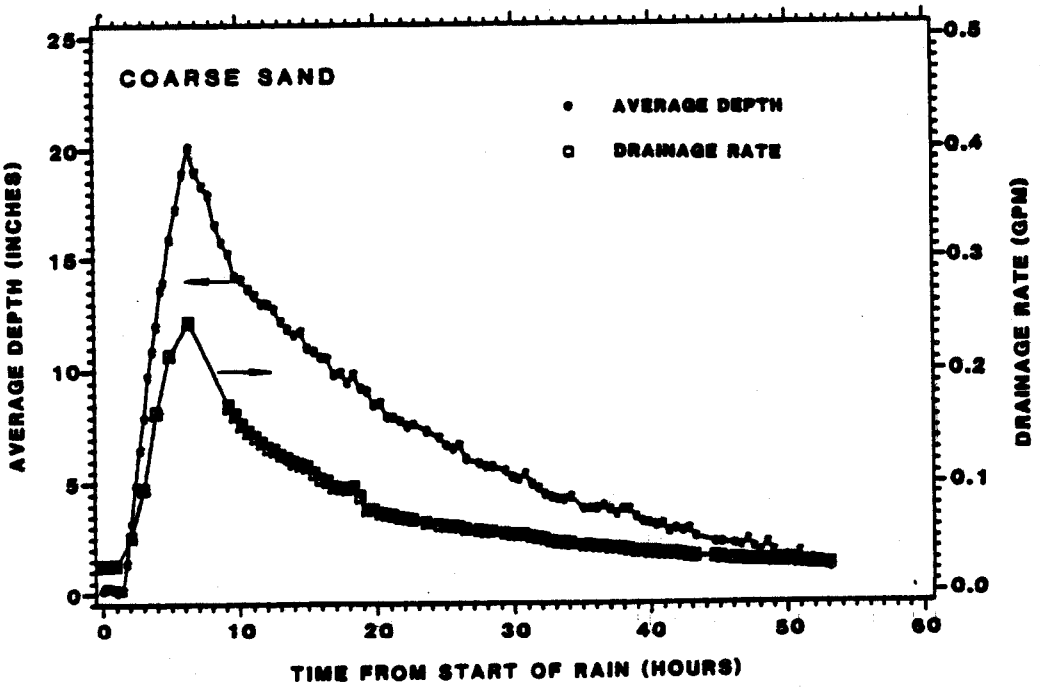

Figure 17. Average saturated depth and drainage rate as a function of time for 24-hr rainfall test using fine sand and for 6-hr rainfall test using coarse sand in short model at 2-percent slope.

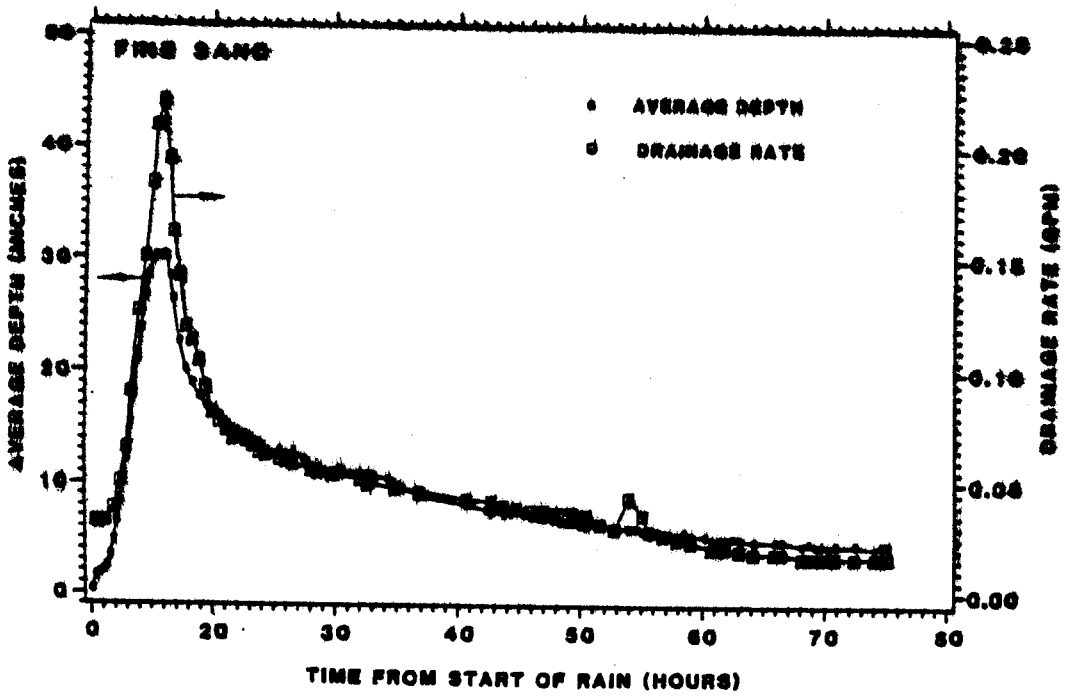

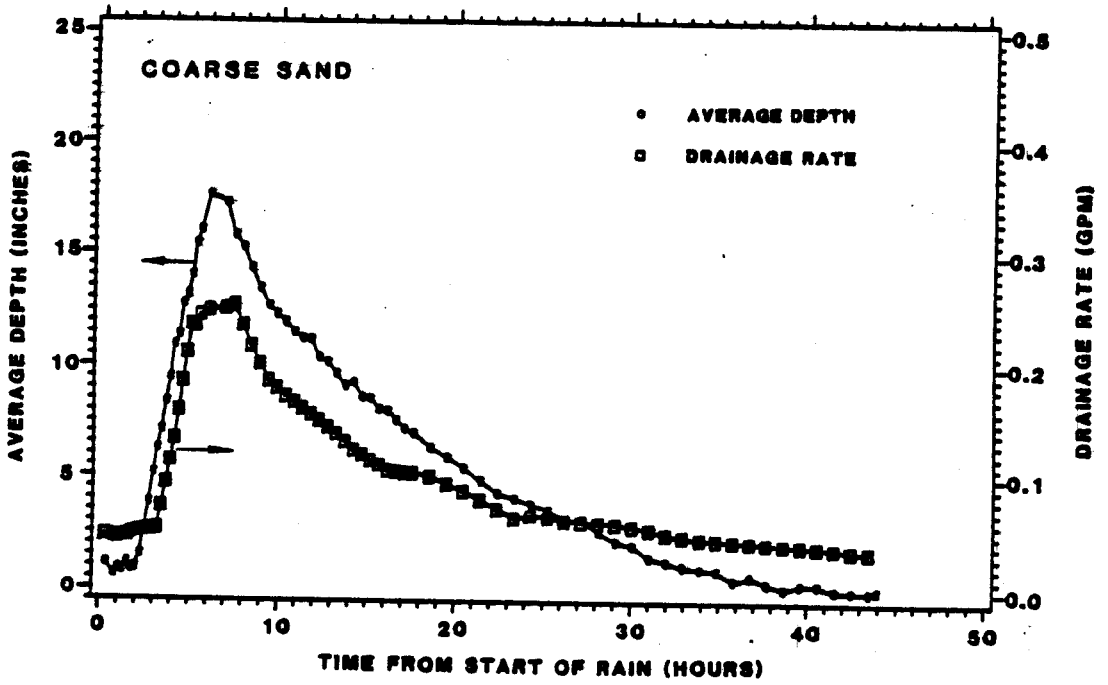

Figure 18. Average saturated depth and drainage rate as a function of time for 6-hr rainfall test using both sands in short model at 5-percent slope.

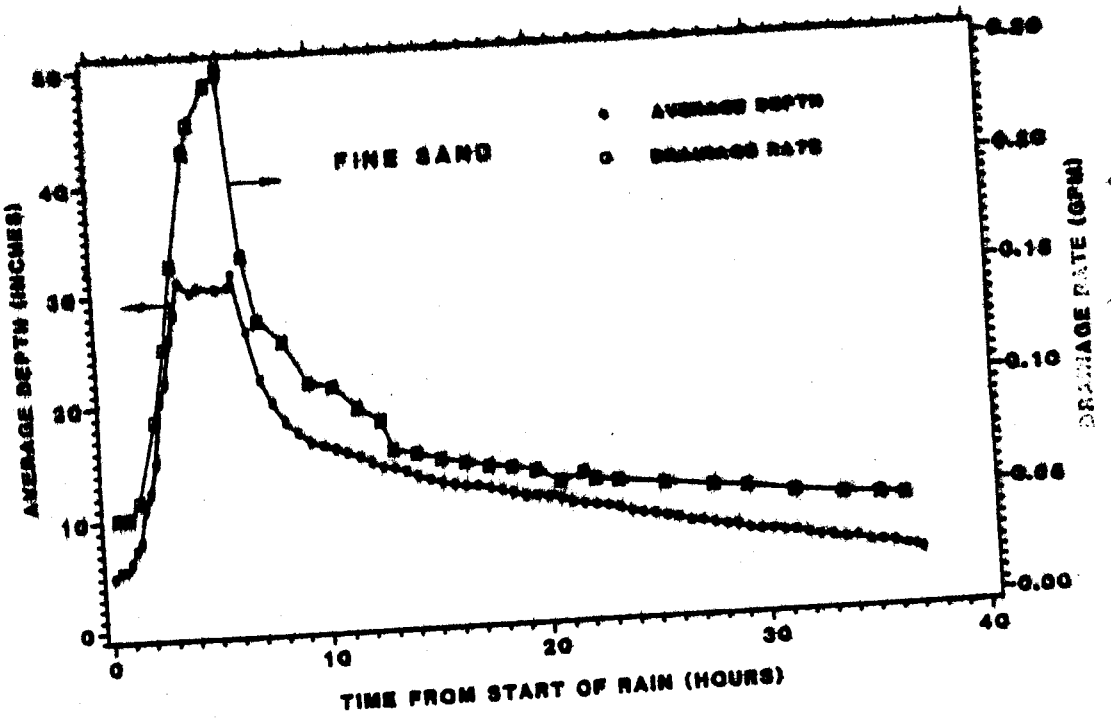

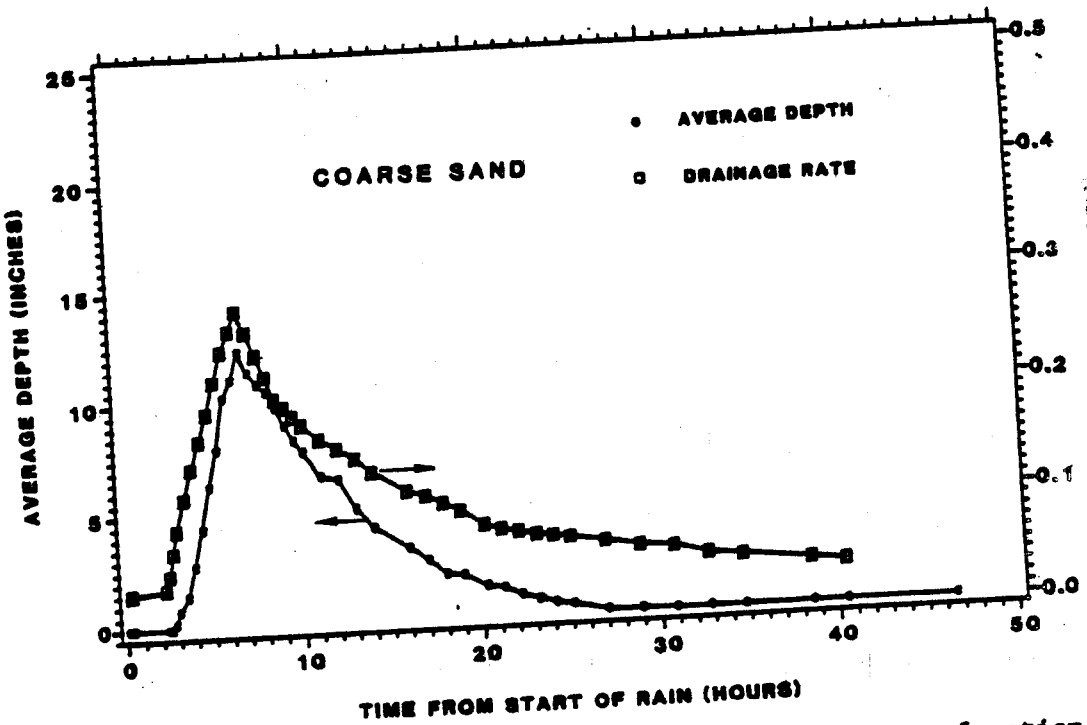

Figure 19. Average saturated depth and drainage rate as a function time for 6-hr rainfall test using both sands in short model at 10-percent slope.

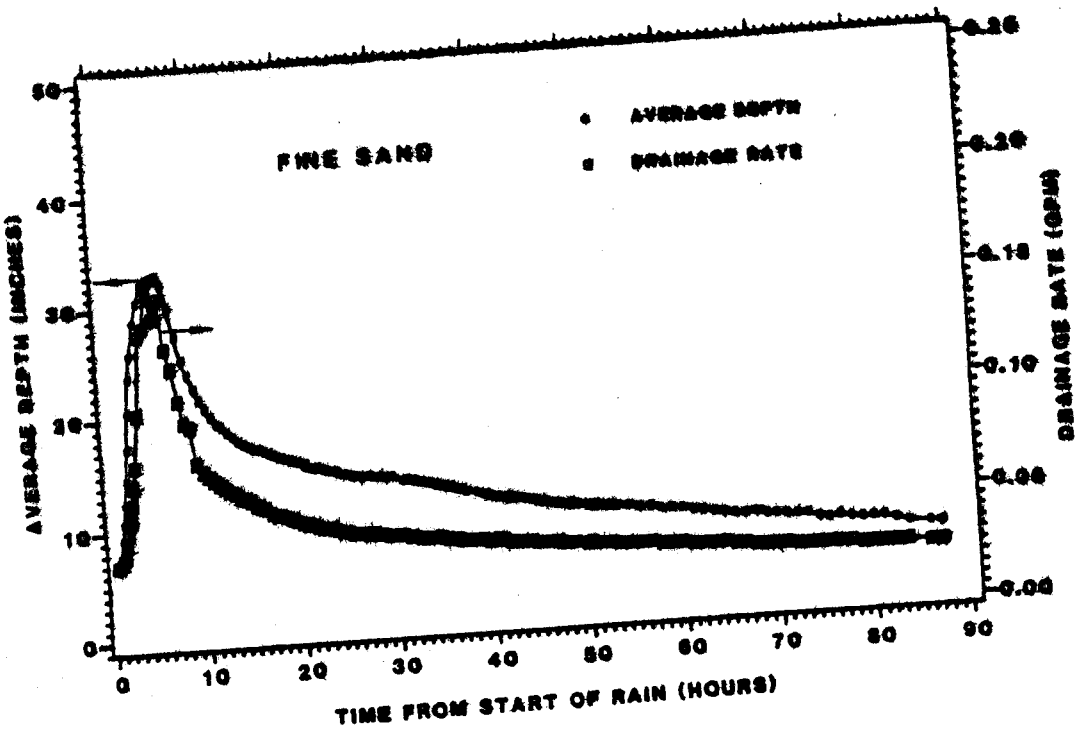

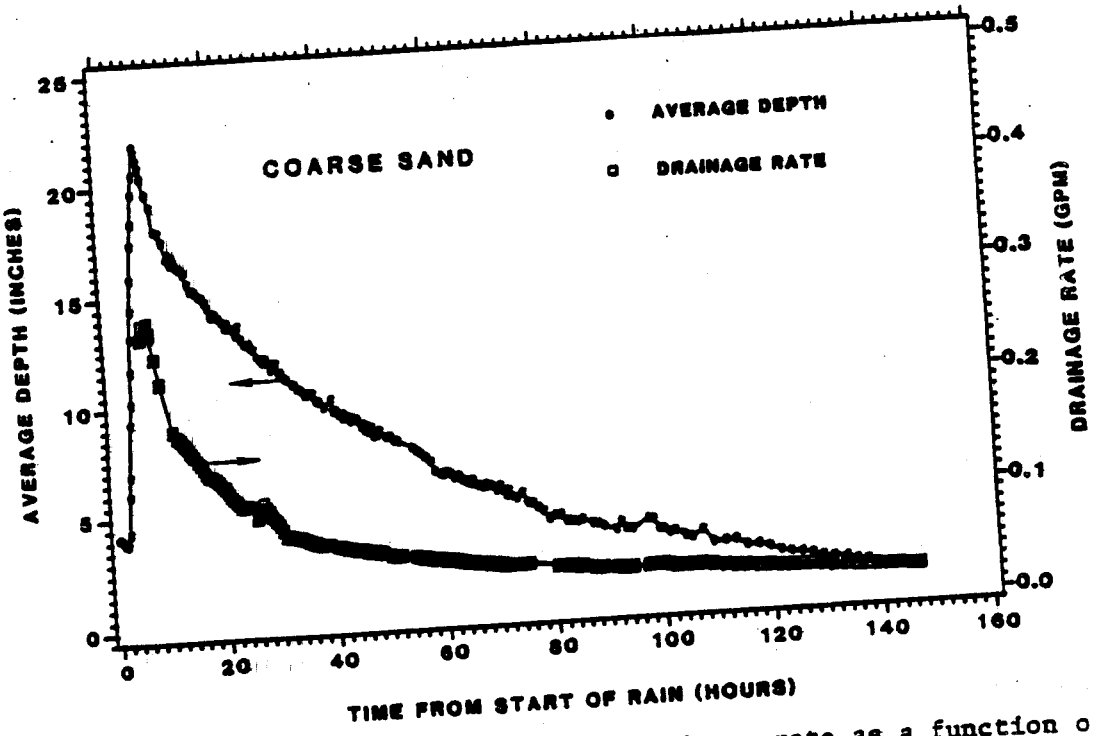

Figure 20. Average saturated depth and drainage rate as a function o time for 6-hr rainfall test using both sands in long mode at 2-percent slope.

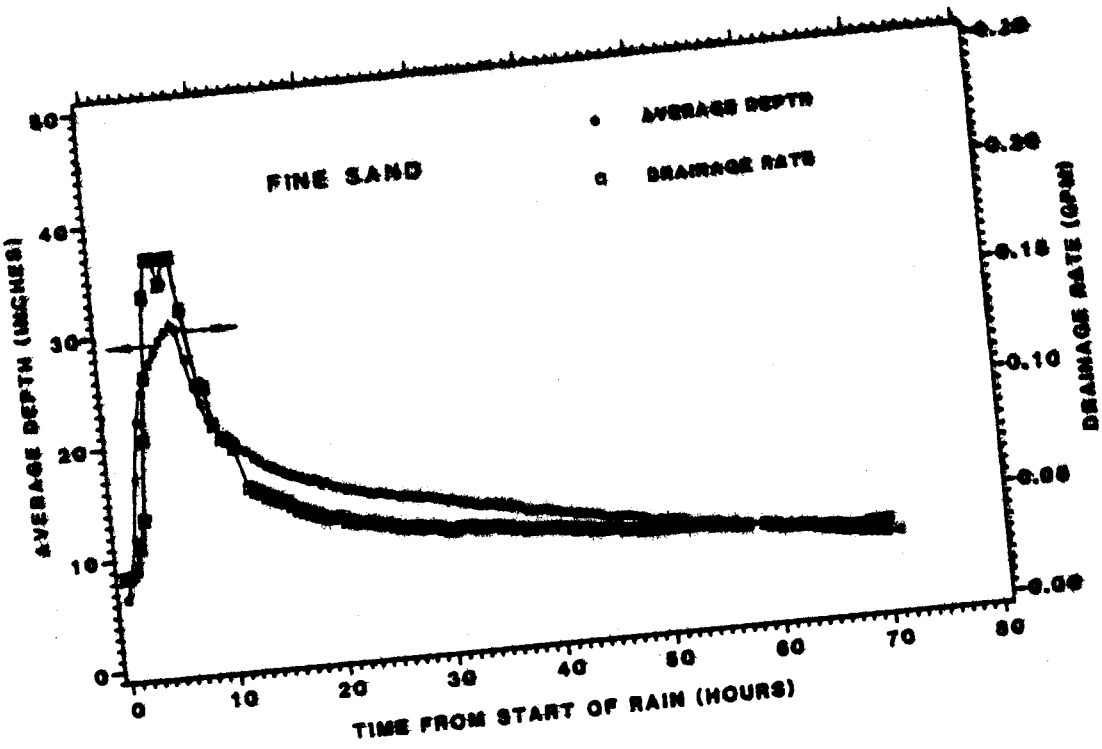

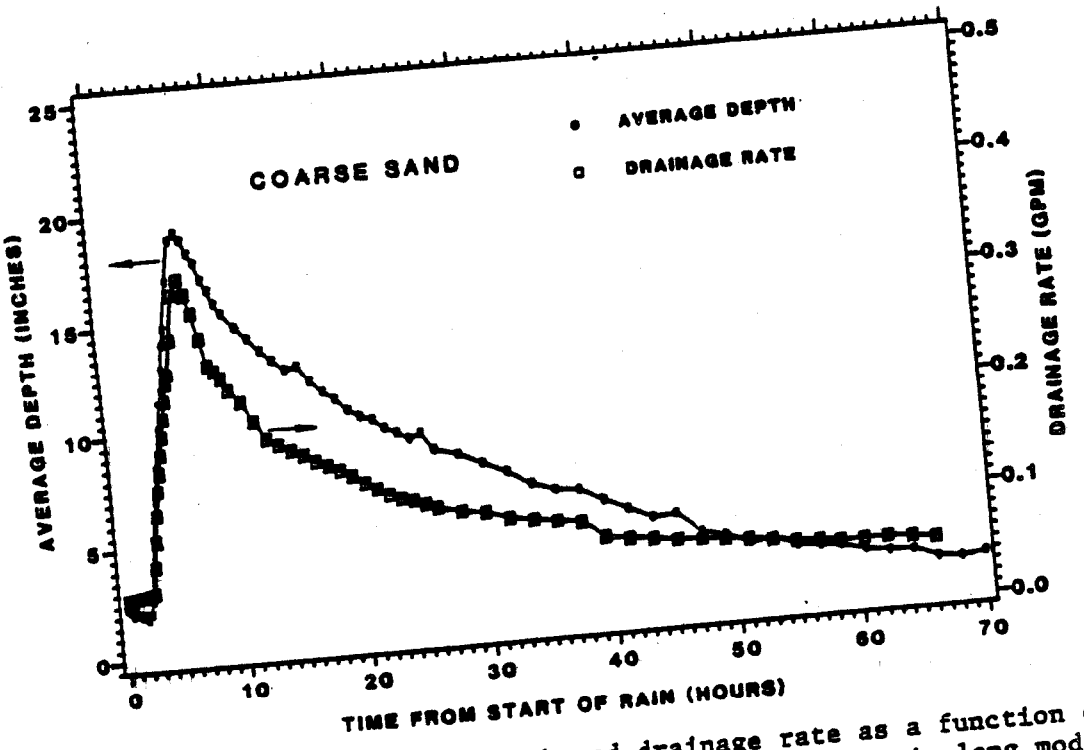

Figure 21. Average saturated depth and drainage rate as a function of time for 6-hr rainfall test using both sands in long model at 5-percent slope.

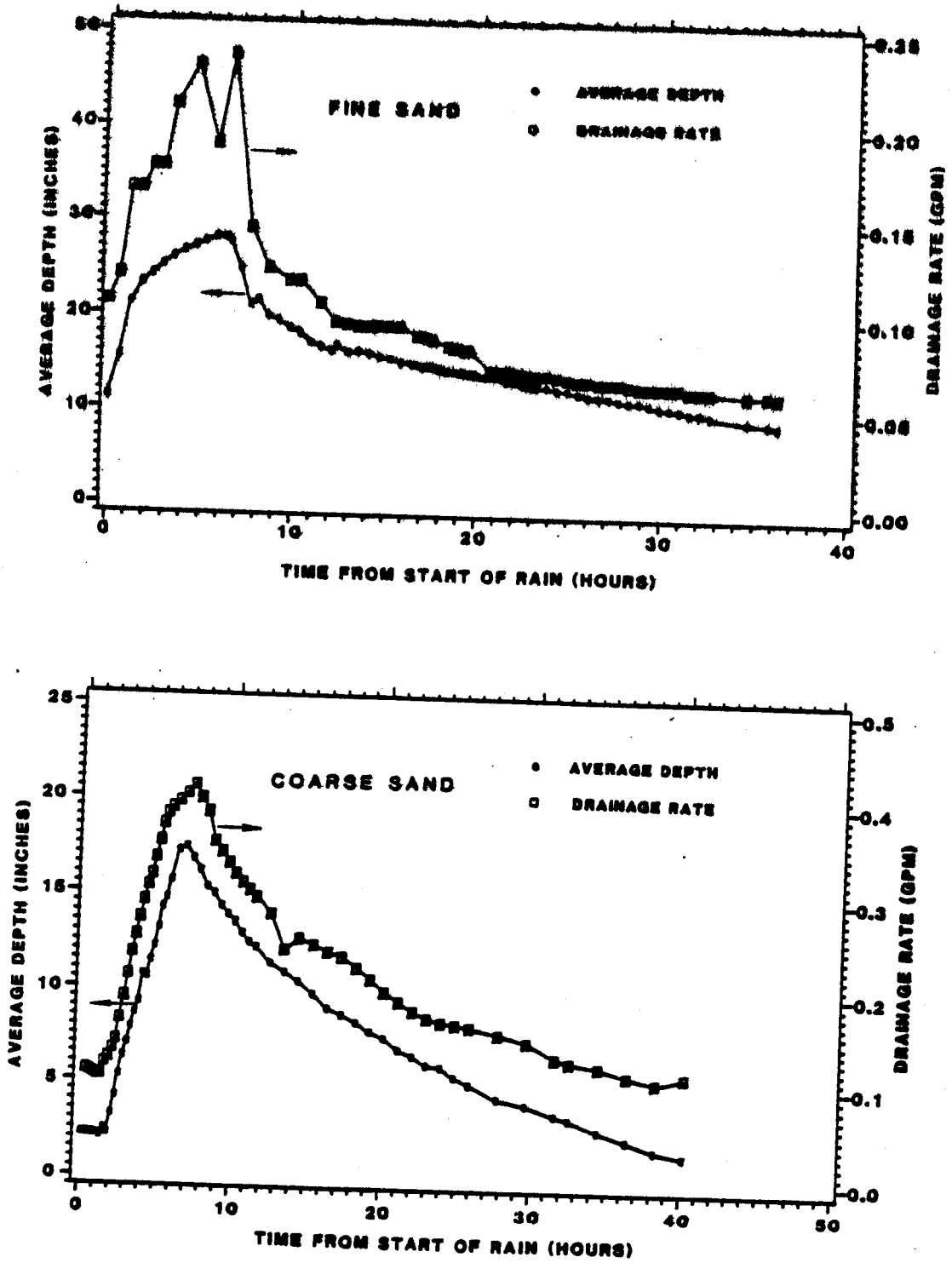

Figure 22. Average saturated depth and drainage rate as a function of time for 6-hr rainfall test using both sands in long model at 10-percent slope.

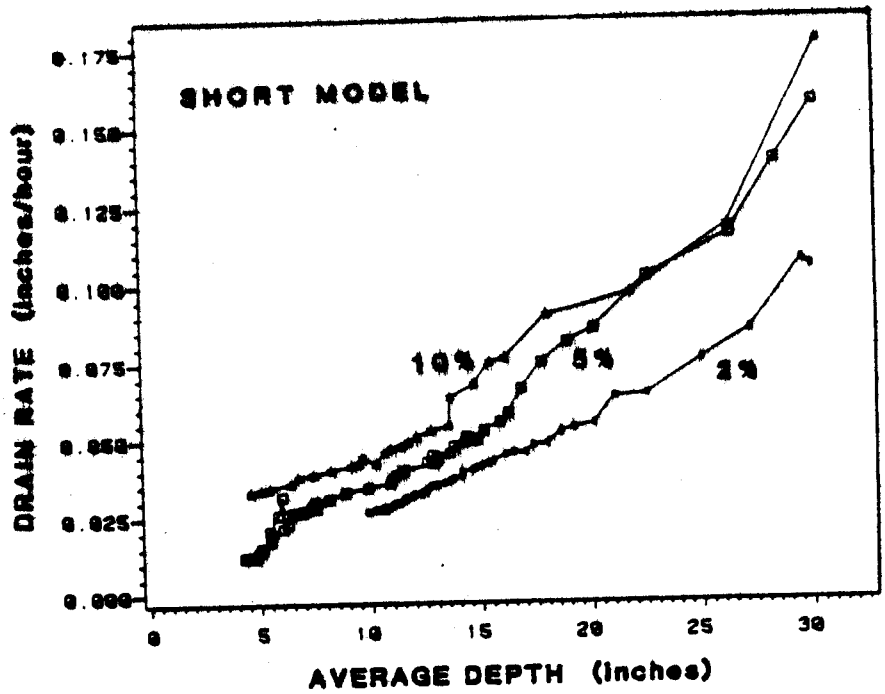

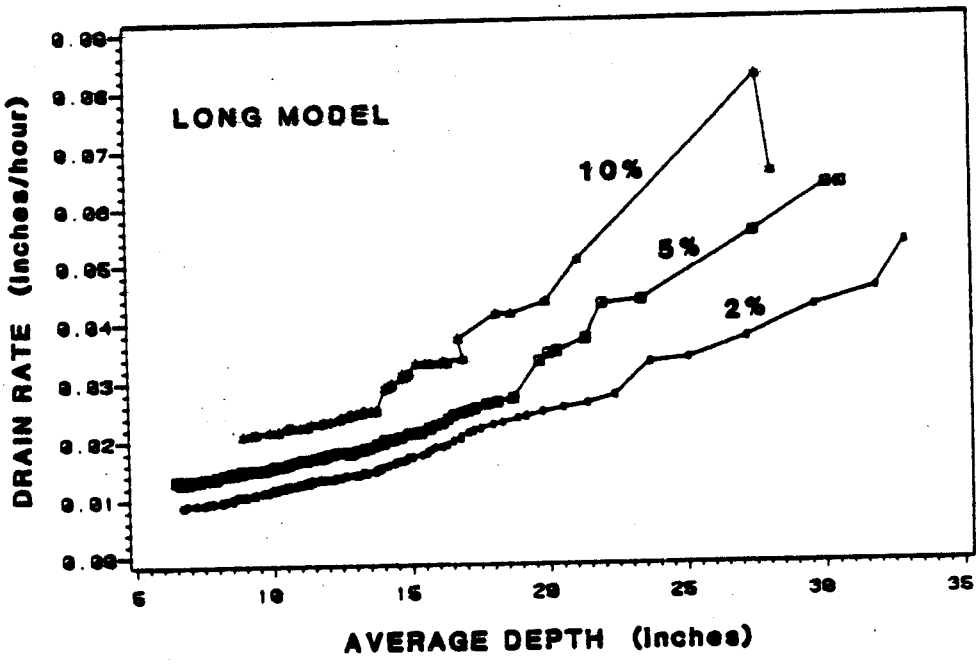

Figure 23. Unsteady drainage rate as a function of average saturated depth for fine sand in both physical models.

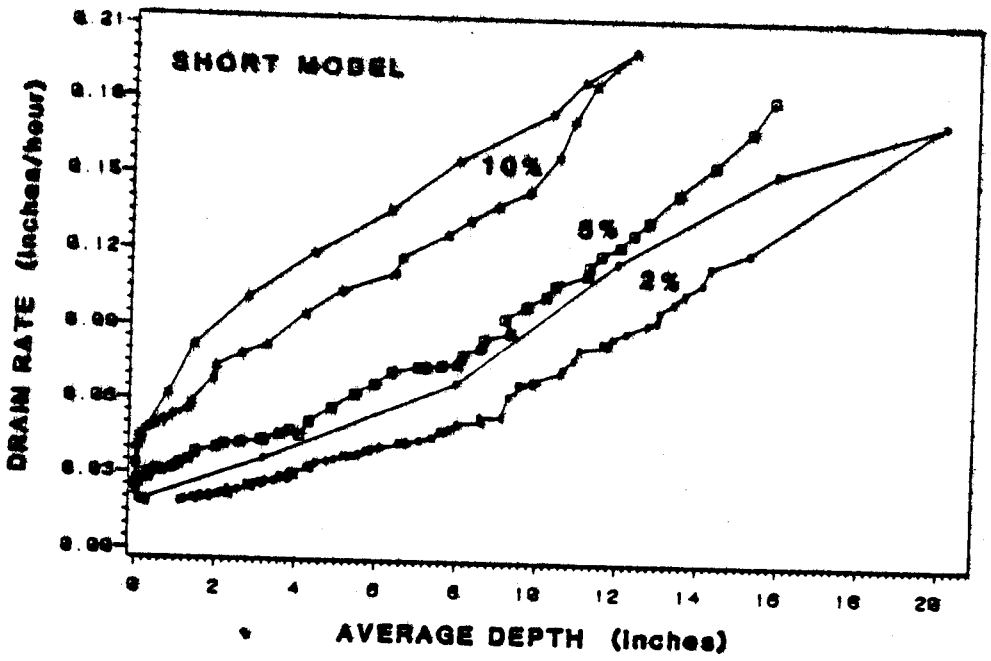

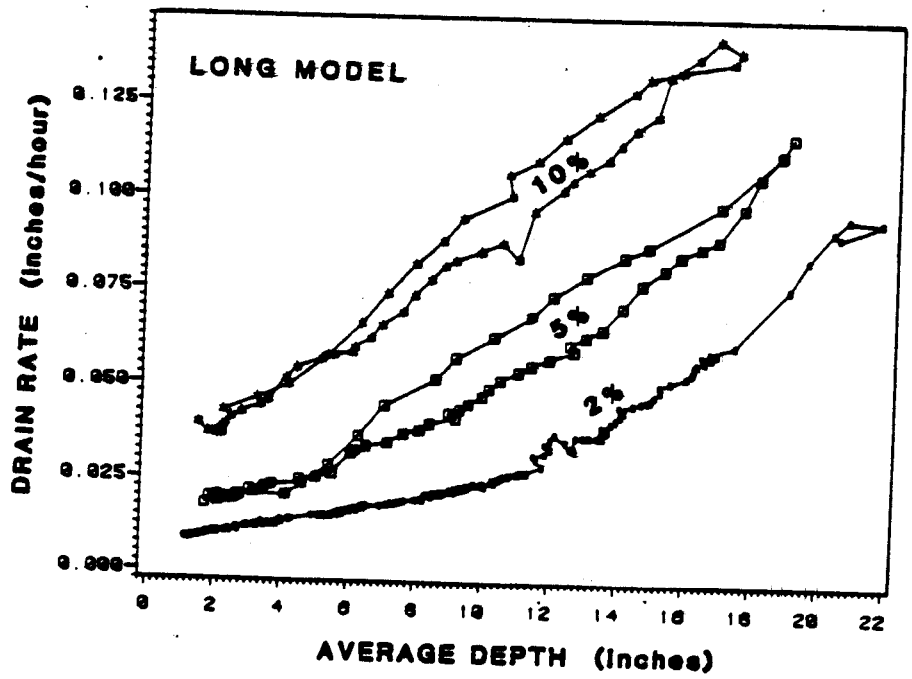

Figure 24. Unsteady drainage rate as a function of average saturated depth for coarse sand in both physical models.

coarse sand. Similar hysteresis occurred with the fine sand. The data for the filling cycle were not plotted because they crossed over the lines for higher slope. For the same $\bar{y}$, the drainage rate during filling is greater than during draining. This is consistent with the profiles in Figures 7-16, which show steeper hydraulic gradients near the drain for filling conditions. The curves also show that drainage continues after $\bar{y}$ has essentially reached zero. This is presumed to be drainage of capillary water, commonly called delayed yield. An estimate of this capillary water volume when $\bar{y}$ had just drained to 0 in. based on an analysis of the experimental data is about 0.1 in. (cubic inches per square inch) for the fine sand and 0.3 in. for the coarse sand.

DRAINABLE POROSITY

The $\bar{y}$ and drainage rate data presented in Figures 17-22 were used to compute drainable porosity at various heights within the model. The volume of drainage water collected while the average saturated depth fell from $\bar{y}_1$ to $\bar{y}_2$ was divided by the total volume contained in the model between $\bar{y}_1$ and $\bar{y}_2$. This number was used as an estimate of the drainable porosity within the region between $\bar{y}_1$ and $\bar{y}_2$. The results are shown in Table 4. It is apparent that the drainable porosities in Table 4 (ranging from 0.01 to 0.20) are less than those cited in Section 3 (ranging from 0.21 to 0.28). The latter values were maximum values based on soil moisture and porosity measurements taken after all experiments were concluded. The values in Table 4, particularly for high $\bar{y}$ values, are low due to delayed yield and capillary effects resulting from the high drainage rate. Nevertheless, significant reductions in drainable porosity appeared to exist with increasing height above the clay liner. A closer examination of these data using regression analysis resulted in the following predictive equation for drainable porosity (DP) at a point located a vertical distance y (in inches) above the clay liner:

$$DP = DPC\ (0.959 - 0.0327\ y) \qquad (14)$$

where DPC = drainable porosity constant. Values for DPC are listed in Table 5 for eight experimental cases. Based on an examination of the data, a lower limit for DP was set for this study at 0.0271 DPC. It is assumed that the presence and vertical distribution of entrapped air were primarily responsible for the change in drainable porosity with height, although no measurements of entrapped air were obtained.

Table 6 shows the time for $\bar{y}$ to fall from one level to another. As expected, the time for $\bar{y}$ to fall from 18 to 12 in. was significantly less than from 12 to 6 in. because of the larger discharge rates at larger $\bar{y}$ values. However, the smaller drainable porosities at larger $\bar{y}$ values also contributed to the shorter drain times. For the coarse sand experiments, the times for $\bar{y}$ to fall from 12 to 2 in. ranged from 0.5 to 1.4 days for the 25.4-ft-long model and from 1.1 to 4.0 days for the 52.4-ft-long model. The fine sand experiments experienced much longer drain times and therefore were not monitored long enough for $\bar{y}$ to reach 2 in. In all experiments, $\bar{y}$ drained from 18 to 12 in. in less than about 1 day.

TABLE 4. DRAINABLE POROSITY

Type of Sand	Slope (%)	Drain Length (ft)	Drainable Porosity Between $\bar{y}_1$ and $\bar{y}_2$*					
			$\bar{y}_1 = 30$ $\bar{y}_2 = 25$	$\bar{y}_1 = 25$ $\bar{y}_2 = 20$	$\bar{y}_1 = 20$ $\bar{y}_2 = 15$	$\bar{y}_1 = 15$ $\bar{y}_2 = 10$	$\bar{y}_1 = 10$ $\bar{y}_2 = 5$	$\bar{y}_1 = 5$ $\bar{y}_2 = 2$
Fine	2	25.4	0.029	0.020	0.050	0.093	-	-
Fine	5	25.4	0.017	0.015	0.039	0.117	0.137	-
Fine	10	25.4	0.017	0.016	0.052	0.099	0.109	-
Fine	2	52.4	0.007	0.015	0.043	0.088	-	-
Fine	5	52.4	0.010	0.020	0.047	0.094	-	-
Fine	10	52.4	-	0.015	0.058	0.085	-	-
Coarse	2	25.4	-	-	0.088	0.143	0.151	0.187
Coarse	5	25.4	-	-	-	0.090	0.133	0.186
Coarse	10	25.4	-	-	-	-	0.109	0.171
Coarse	2	52.4	-	-	0.094	0.131	0.136	0.209
Coarse	5	52.4	-	-	-	0.127	0.161	0.201
Coarse	10	52.4	-	-	-	0.132	0.153	0.185

* Values for $\bar{y}_1$ and $\bar{y}_2$ expressed in inches.

TABLE 5. VALUES FOR DRAINABLE POROSITY CONSTANT, DPC

Type of Sand	Slope (%)	Drain Length (ft)	DPC
Fine	2	25.4	0.161
Fine	10	25.4	0.147
Fine	2	52.4	0.153
Fine	10	52.4	0.148
Coarse	2	25.4	0.215
Coarse	10	25.4	0.196
Coarse	2	52.4	0.220
Coarse	10	52.4	0.200

TABLE 6. DRAINAGE TIMES*

Type of Sand	Slope (%)	Drain Length (ft)	Time to Drain from $\bar{y}_1$ to $\bar{y}_2$ (hrs)		
			$\bar{y}_1 = 18$** $\bar{y}_2 = 12$	$\bar{y}_1 = 12$ $\bar{y}_2 = 6$	$\bar{y}_1 = 6$ $\bar{y}_2 = 2$
Fine	2	25.4	11.0	-	-
Fine	5	25.4	10.5	16.5	-
Fine	10	25.4	8.0	15.8	-
Fine	2	52.4	24.4	>50	-
Fine	5	52.4	21.6	>37	-
Fine	10	52.4	16.2	-	-
Coarse	2	25.4	7.0	12.1	20.6
Coarse	5	25.4	4.3	9.2	10.9
Coarse	10	25.4	-	5.0	6.2
Coarse	2	52.4	19.0	36.5	60.5
Coarse	5	52.4	8.7	21.5	27.0
Coarse	10	52.4	-	12.0	13.9

* Drainage times in this table were taken from 6-hr rainfall experiments, except for the fine sand, 2-percent slope, 25.4-ft drain length case which was taken from a 24-hr rainfall experiment. Dashes indicate that data were not available.

** Values for $\bar{y}_1$ and $\bar{y}_2$ expressed in inches.

SECTION 6

VERIFICATION OF THE HELP MODEL

Comparisons between the HELP model predictions and the actual measurements are made in this section to assess the accuracy of the HELP lateral drainage equation. All parameters required to compute the drainage rate by the HELP equation except the hydraulic conductivity were measured for each drainage test. Hydraulic conductivity measured in a permeameter in the soils laboratory differed significantly from hydraulic conductivity calculated from data on drainage rates and depth of saturation measured in the large-scale physical models. This is thought to be due to differences in placement, compaction, and preparation of the sand drainage media, and due to entrapment of air in the sand. As described in the documentation report for the HELP model (1), the lateral drainage equation was developed to approximate numerical solutions of the Boussinesq equation for one-dimensional, unsteady, unconfined flow through porous media (5). Therefore, the actual hydraulic conductivity for the drainage tests was estimated by adjusting its value while solving the Boussinesq equation until the results matched the measured drainage rates and saturated depths. The hydraulic conductivity estimates are summarized in Appendix A. Determining the hydraulic conductivity in this manner provided the best estimate obtainable for each test since the Boussinesq solution is the commonly accepted representation of the actual drainage process. Comparisons were made for both steady-state drainage during rainfall and unsteady drainage following cessation of rainfall.

Comparisons between the Boussinesq solution predictions and the actual measurements are made in the Appendix B to determine how well the most commonly used theoretical representation of the lateral drainage process performs. The numerical solution of the Boussinesq equation used in this study was developed by Skaggs (5). In addition, the Boussinesq solution predictions are compared with the HELP model predictions in Appendix C. These comparisons are very important because they define the limits of modeling and demonstrate how well the HELP equation represents the Boussinesq solution.

COMPARISONS BY HYDRAULIC CONDUCTIVITY

First, the results of the steady-state cases are described. The rainfall rate was adjusted until the average head on the liner (which is also the average depth of saturation, $\bar{y}$) reached a steady-state height of approximately 12 in. Using this measured value of $\bar{y}$ and the corresponding measured value of the steady-state drainage rate, the hydraulic conductivity was computed explicitly using the HELP drainage equation (Equation 1) with the slope and drainage length employed in the drainage test. To compute the hydraulic conductivity using the Boussinesq solution, a series of numerical Boussinesq runs

were made changing the hydraulic conductivity until the computed steady-state $\bar{y}$ having the measured steady-state drainage rate matched the measured value. A comparison of these values is shown in Table 7. Overall, the computed hydraulic conductivity using the HELP equation exceeded that using the Boussinesq solution by an average of 44 percent. Consequently, the HELP model underestimates the drainage rate by 30 percent as predicted by the Boussinesq solution under steady-state conditions. For fine sand, computed values of hydraulic conductivity by the HELP equation exceeded the measured values using permeameters by an average of 31 percent; for coarse sand, the average computed value was 10 percent of the measured value.

TABLE 7. COMPARISON OF COMPUTED HYDRAULIC CONDUCTIVITIES FOR STEADY-STATE DRAINAGE

Type of Sand	Slope (%)	Length (ft)	Rainfall Rate (in./hr)	Hydraulic Conductivity K_{H*} (cm/sec)	K_{B**} (cm/sec)	$K_{L\dagger}$ (cm/sec)
Fine	2	25.4	0.034	0.008	0.006	0.004
Fine	10	25.4	0.054	0.006	0.004	0.004
Fine	10	52.4	0.025	0.006	0.004	0.005
Coarse	2	25.4	0.071	0.021	0.015	0.220
Coarse	2	52.4	0.033	0.030	0.021	0.220
Coarse	10	25.4	0.169	0.025	0.015	0.220
Coarse	10	52.4	0.105	0.027	0.021	0.220

* Computed hydraulic conductivity using the HELP equation.
** Computed hydraulic conductivity using the numerical Boussinesq solution.
† Hydraulic conductivity measured in laboratory permeameters.

For unsteady drainage following cessation of rainfall, hydraulic conductivity was computed explicitly using the HELP drainage equation for instantaneous measured values of $\bar{y}$ and drainage rate. To compute hydraulic conductivity using the Boussinesq solution, the following steps were followed: (a) Unsteady drainage from the physical model was simulated using the numerical Boussinesq solution with an estimated hydraulic conductivity; (b) at a given value of $\bar{y}$, a correction factor was computed by dividing the measured drainage rate by the simulated drainage rate; and (c) the estimated hydraulic conductivity was multiplied by the correction factor to obtain the final computed hydraulic conductivity for the given value of $\bar{y}$. Successive estimates used in the Boussinesq solution showed that the correction factor adjusted the initial guess to within 5 percent of the best estimate of the hydraulic

conductivity. Hydraulic conductivities were computed by these two methods at various values of $\bar{y}$ for each experimental case.

Overall, the computed hydraulic conductivity using the HELP equation exceeded that using the Boussinesq solution by an average of 13 percent. Consequently, the HELP equation underestimates the drainage rate by 11 percent as predicted by the Boussinesq solution under unsteady conditions. These results were determined using a paired-sample t test to determine whether the differences in hydraulic conductivity values between the two methods were statistically different from zero. Table 8 summarizes these results. The test using all data from all experimental cases concluded that the two methods did produce hydraulic conductivity values that were statistically different. Similarly, the two methods produced statistically different hydraulic conductivities using the data for only coarse sand or only fine sand; for only short model or only long model; and for only 2-percent slope or 10-percent slope. However, when the test was conducted for individual experimental cases, the test concluded that in five out of eight cases, the two methods produced hydraulic conductivity values that were not statistically different. The five cases were: coarse sand in both physical models at 2-percent slope, coarse sand in the long model at 10-percent slope, and fine sand in both models at 10-percent slope.

For both steady and unsteady drainage, the hydraulic conductivity computed by the HELP model was shown to exceed that computed by the more rigorous Boussinesq solution. Consequently, the HELP model might be expected to underestimate the drainage rate from a drainage system where porous media properties were accurately known. However, in field applications, the magnitude of this underestimation would probably be much less than the uncertainties in the in-place porous media properties. This difficulty was highlighted in this study by the large differences between laboratory measurements using permeameters and apparent in-place hydraulic conductivities. Also, the difference between the two solution methods was much less for the unsteady case--the case which generally occurs in field systems.

The computed hydraulic conductivity of the sand during steady-state drainage by the Boussinesq solution was about 61 percent of the value during unsteady drainage. Consequently, if the hydraulic conductivity for unsteady drainage was used in the HELP model for all types of drainage conditions, the lateral drainage rate would be underestimated by 11 percent during unsteady drainage and overestimated by 14 percent during steady-state drainage.

EFFECTS OF ENTRAPPED AIR

In analyzing the computed hydraulic conductivity values, it was apparent that hydraulic conductivity decreased with increasing $\bar{y}$. Table 4 shows that the drainable porosity also decreased with increasing $\bar{y}$. Lower drainable porosity could have resulted by two mechanisms: greater air entrapment or greater compaction. Compaction was 97 percent of maximum throughout the sand layer; therefore, air entrapment must have caused the decrease in drainable porosity. Lower drainable porosity results in lower cross-sectional area contributing to drainage; consequently, the hydraulic conductivity decreases.

TABLE 8. COMPARISON OF COMPUTED HYDRAULIC CONDUCTIVITIES FOR UNSTEADY DRAINAGE

Data Group*	No. of Data Points**	Mean Value of $(K_B - K_H)$ (cm/sec)	Standard Deviation of $(K_B - K_H)$† (cm/sec)	t†† Statistic	$t_{\alpha/2}$ ($\alpha = 0.05$)	Statistical Significance of $(K_B - K_H)$ at $\alpha = 0.05$
All data	93	-0.00309	0.00693	-4.300	-1.960	Not equal to zero
C	43	-0.00589	0.00943	-4.098	-1.960	Not equal to zero
F	50	-0.00608	0.00101	-4.740	-1.960	Not equal to zero
2	51	-0.00083	0.00135	-4.375	-1.960	Not equal to zero
10	30	-0.00584	0.01055	-3.033	-2.045	Not equal to zero
S	49	-0.00314	0.00815	-2.697	-1.960	Not equal to zero
L	44	-0.00303	0.00534	-3.765	-1.960	Not equal to zero
C2S	10	-0.00067	0.00107	-1.981	-2.262	May equal zero
C10S	8	-0.01609	0.01491	-3.053	-2.365	Not equal to zero
C2L	11	-0.00104	0.00233	-1.479	-2.228	May equal zero
C10L	6	-0.00749	0.00746	-2.459	-2.571	May equal zero
F2S	17	-0.00054	0.00047	-4.782	-2.120	Not equal to zero
F10S	8	-0.00031	0.00073	-1.222	-2.365	May equal zero
F2L	13	-0.00114	0.00127	-3.235	-2.179	Not equal to zero
F10L	8	0.00012	0.00061	0.552	2.365	May equal zero

* C = coarse sand; S = short model; 2 = 2% slope.
F = Fine sand; L = long model; 10 = 10% slope.

** Each data point represents one $(K_B - K_H)$ value at particular $\bar{y}$.

† K_B = Computed hydraulic conductivity using the numerical Boussinesq solution.

†† K_H = Computed hydraulic conductivity using the HELP equation.

$$t = \frac{\bar{x} - Mu}{s/\sqrt{n}}$$

where $\bar{x}$ = mean value of $(K_B - K_H)$.
Mu = hypothetical population mean = 0.
s = standard deviation of $(K_B - K_H)$.
n = number of data points.

To determine whether variability in the estimates of the hydraulic conductivity was a function of other variables in addition to average saturated depth, a series of unequal three-way analysis of variance (ANOVA) tests was run on the both sets of estimates. This procedure permits analysis of experiments that have three variables called treatments, which produce variance in the measured variable. ANOVA also permits determination of interaction between variables. The variance and the number of duplicates of treatments did not have to be equal in the procedure. The analyses were performed using the Statpro software by Penton Software Inc. (6). The test variables include type of sand, average saturated depth, slope, drainage length, rainfall duration and rainfall intensity. No effects of rainfall duration and intensity could be discerned by inspection; therefore, the initial ANOVAs were run using depth, slope and length as the variables for data sets containing hydraulic conductivity estimates for one type of sand. These ANOVAs indicated that the hydraulic conductivity estimates by HELP varied only as a function of average saturated depth for coarse sand and of average saturated depth and slope for fine sand. Running ANOVAs on the estimates generated by the Boussinesq solution, the estimates varied significantly with depth and slope for both sands.

No physical reasons are apparent for the variability of the hydraulic conductivity as a function of slope. Therefore, the variability arises from inaccuracies in the manners in which the effects of slope are modeled by the Boussinesq equation and the HELP equation. This difference is presented in greater detail later in this section and in Appendices B and C.

A regression analysis was conducted to investigate the relationship between hydraulic conductivity and $\bar{y}$. Hydraulic conductivity, K, was fitted to a power function of $\bar{y}$ such that

$$K = a\,\bar{y}^{b} \qquad (15)$$

where values of the regression coefficients a and b are listed in Table 9 for 10 of the experimental cases. This equation applies only to $\bar{y}$ values ranging from 2.5 to 30 in. in these drainage tests. In Equation 15, the units for K are centimeters per second and the units for $\bar{y}$ are inches. The relationship between drainable porosity and height above the liner is presented in Section 5.

COMPARISON OF DRAINAGE RATES

To further test the accuracy of the HELP lateral drainage equation, the relationship between drainage rate and $\bar{y}$ as predicted by the HELP drainage equation was compared to measured results for unsteady drainage following cessation of rainfall. The comparisons are shown in Figures 25 and 26. Measured results are represented by the shaded area which defines the range of all measured data for the given sand, slope and drainage length. Three computed curves are also plotted. One curve represents the HELP drainage equation using the hydraulic conductivity measured in the laboratory permeameters. A second curve represents the HELP drainage equation using the mean of hydraulic conductivity estimates obtained from the Boussinesq solution for all unsteady drainage tests performed with the given sand, slope and length. The third

TABLE 9. REGRESSION COEFFICIENTS FOR HYDRAULIC CONDUCTIVITY AS A POWER FUNCTION OF $\bar{y}$*

Type of Sand	Slope (%)	Drain Length (ft)	a	b
Fine	2	25.4	0.0951	-0.8650
Fine	10	25.4	0.0248	-0.6166
Fine	2	52.4	0.0677	-0.7252
Fine	10	52.4	0.0048	0.0964
Coarse	2	25.4	0.1297	-0.6934
Coarse	5	25.4	0.0675	-0.4359
Coarse	10	25.4	0.0477	-0.2892
Coarse	2	52.4	0.1057	-0.5383
Coarse	5	52.4	0.0313	-0.2444
Coarse	10	52.4	0.0395	-0.1896

* The regression equation is $K = a\,\bar{y}^{-b}$ where K = hydraulic conductivity in centimeters per second, $\bar{y}$ = average depth of saturation or head on the liner in inches, and a,b = regression coefficients.

curve also represents the HELP equation but uses Equation 15 for hydraulic conductivity. The curves based on laboratory measurements of hydraulic conductivity resulted in poor fits except for the few cases where the measured hydraulic conductivity was close to the computed values. This again highlights the difficulty in estimating in-place hydraulic conductivity from laboratory measurements. The curves based on a mean value of hydraulic conductivity fit reasonably well within a relatively narrow band representing the $\bar{y}$ region for which the mean hydraulic conductivity was computed. Outside this band, the predicted curves tended to deviate, especially for the short model. The curve based on Equation 15 generally fit well for $\bar{y}$ values less than 15 to 20 in. for the fine sand and less than 12 to 15 in. for the coarse sand. These also represent the $\bar{y}$ ranges for which Equation 15 and Table 9 were derived. None of the predicted curves fit well at $\bar{y}$ values close to zero due to the measured capillary water drainage which the HELP equation does not model.

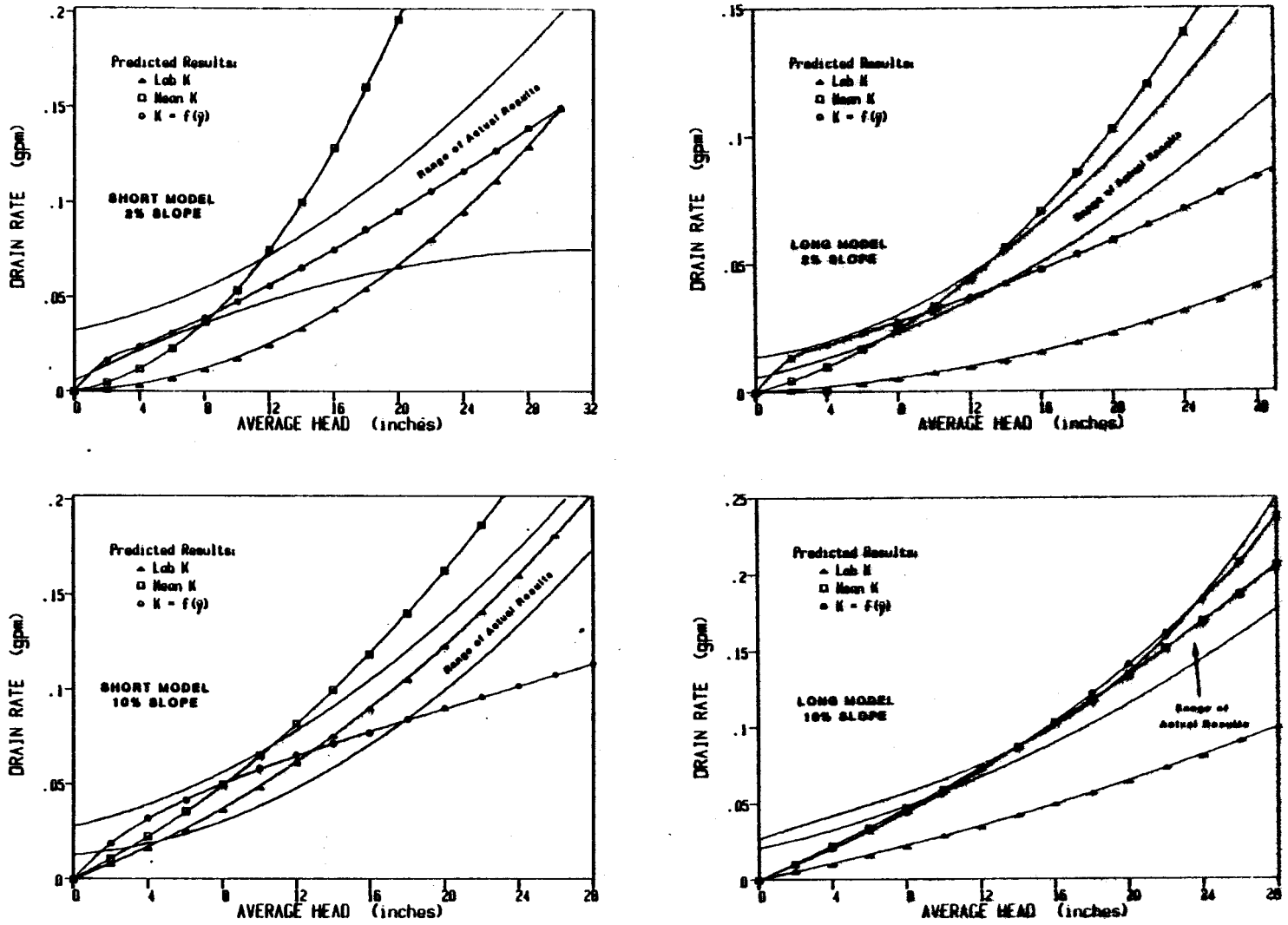

Figure 25. Measured drainage rate following rainfall vs. average head above the liner compared to HELP drainage equation predictions for fine sand in both physical models at slopes of 2 and 10 percent.

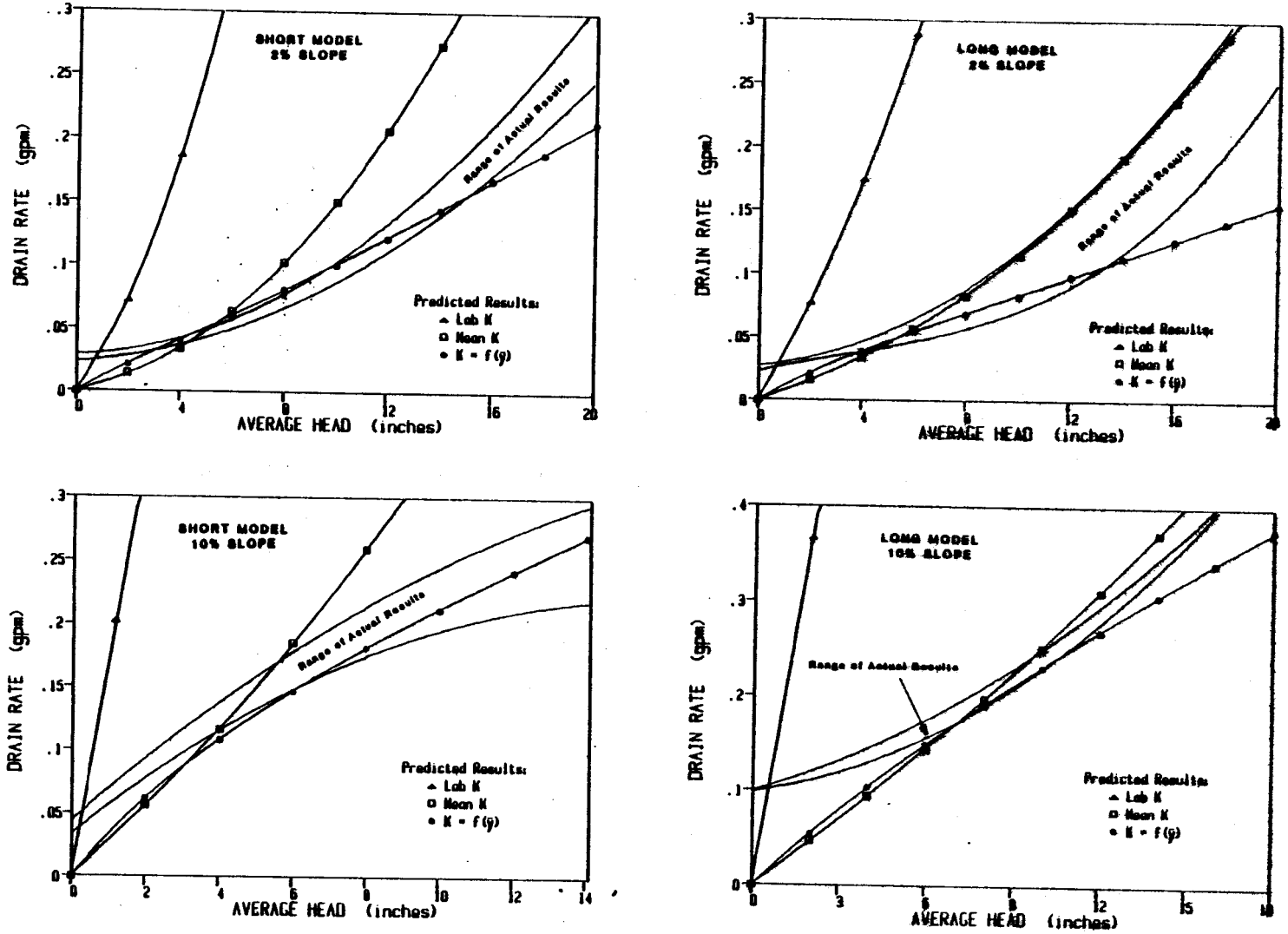

Figure 26. Measured drainage rate following rainfall vs. average head above the liner compared to HELP equation predictions for coarse sand in both physical models at slopes of 2 and 10 percent.

SIMULATIONS BY HELP MODEL

Figures 27-30 show how well the drainage equation in the HELP model predicted drainage rates versus time throughout an entire rainfall experiment. Similar comparisons for average depth of saturation (average head on liner) versus time are also shown in these figures. The predicted curves were computed using both drainable porosity and hydraulic conductivity as functions of $\bar{y}$ (Equations 14 and 15). The volume of drainage is not necessarily equal for both the predicted and actual curves because evaporative losses had to be estimated in the prediction. Similarly, since evaporative and runoff losses are time dependent, the rate of change in depth and drainage rate during the experiment may be affected by the estimation of these losses. Nevertheless, the figures should demonstrate the overall performance of the simulations.

The peak drainage rate and depth of saturation were generally overpredicted for the drainage tests performed at a slope of 10 percent while the predictions for tests conducted with a slope of 2 percent agreed well with the measured results. The HELP equation appears to underpredict the drainage rate for a given depth of saturation in the models at 10-percent slope. This increases the storage requirement and consequently the peak average depth since water that has not been drained is still stored in the sand and contributes to the head. The overpredicted peak depth produces a peak drainage rate that is also overpredicted. The prediction disagrees with the measured results most significantly during the period the sand layer is filling with water. However, an experimental factor may have also contributed to the discrepancy. As mentioned earlier, the fine sand layer approached complete saturation in portions of the model at peak discharge. Consequently, the head profile was forced to shift, becoming steeper near the drain, which produces drainage rates in excess of those expected from a thicker sand layer with more available storage capacity. The HELP simulation was conducted without a limitation on the depth of saturation and thus produced lower drainage rates at the larger values of $\bar{y}$.

A detailed evaluation of the HELP drainage equation based on these comparisons is complicated by the estimates of hydraulic conductivity and drainable porosity that were involved. Changes in these values would have produced different results. Lower values of hydraulic conductivity would have produced smaller drainage rates and larger values of $\bar{y}$. Lower values of drainable porosity would have produced larger drainage rates and larger values of $\bar{y}$. Figures 31 and 32 represent predicted curves where mean values for hydraulic conductivity and drainable porosity were used instead of functions of $\bar{y}$. Significant changes in these predicted curves can be observed.

ANALYSIS OF DRAINAGE EQUATION

Finally, an analysis was conducted to determine how well the drainage equation in the HELP model accounts for the effects of drainage length (L), slope (α), average depth of saturation ($\bar{y}$), and αL in the estimation of the drainage rate. The measured drainage rates used in this analysis were averages of the drainage rate measured during various unsteady drainage tests having the same sand, slope, drainage length and average depth of saturation but having different rainfall durations and intensities. These tests are

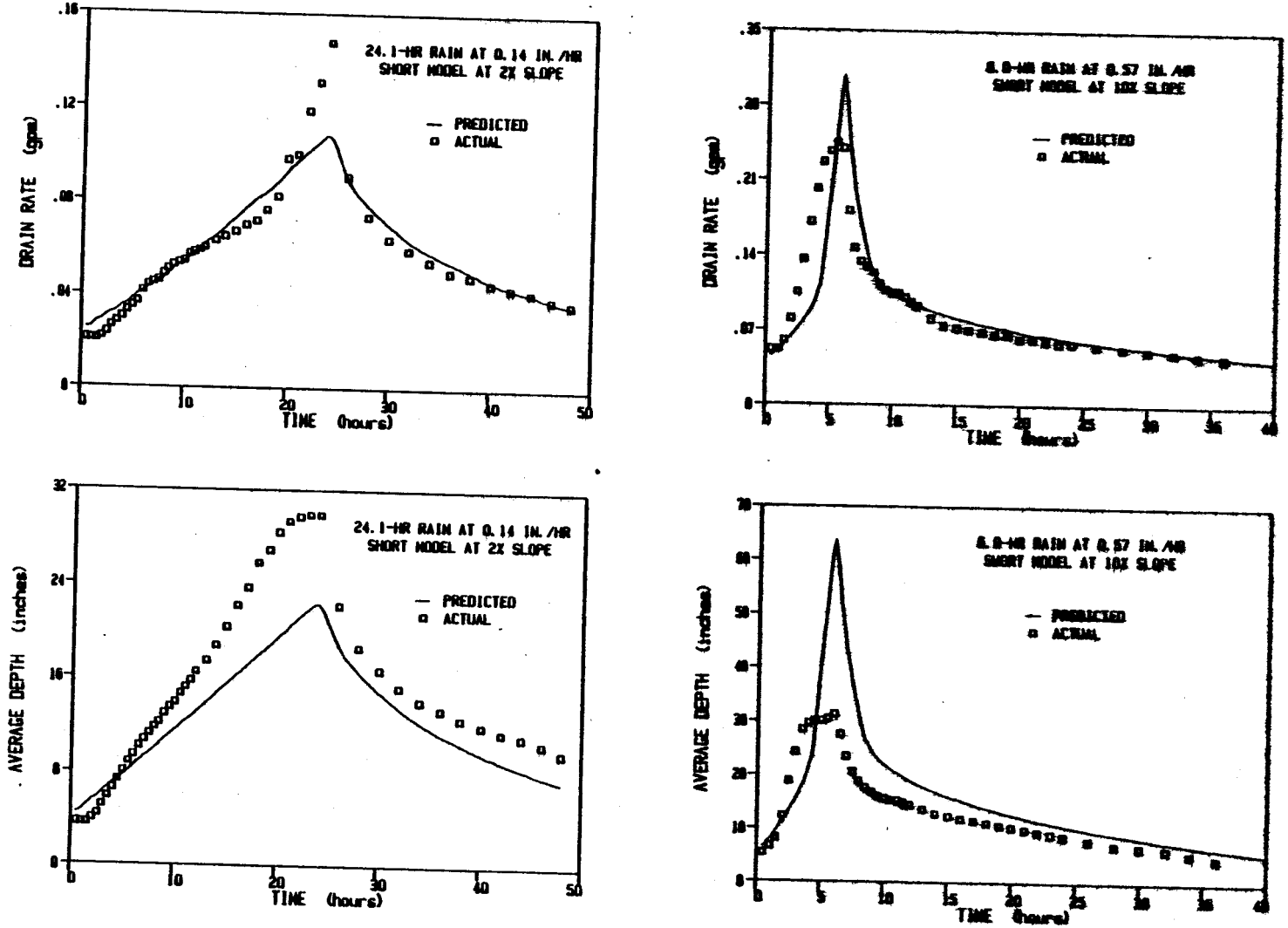

Figure 27. Measured drainage rate and average saturated depth vs. time compared to HELP prediction for fine sand in the short model at slopes of 2 and 10 percent.

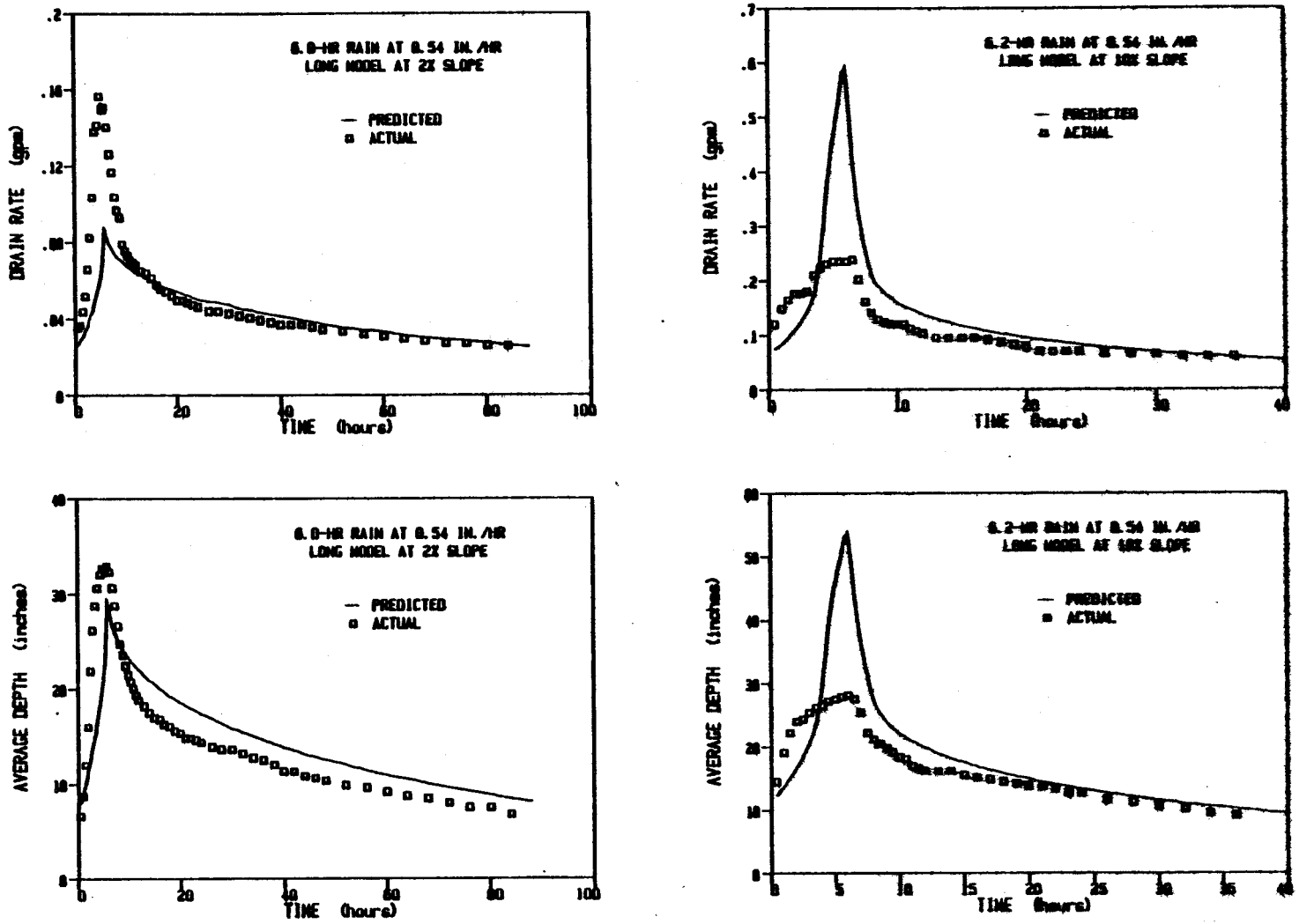

Figure 28. Measured drainage rate and average saturated depth vs. time compared to HELP prediction for fine sand in the long model at slopes of 2 and 10 percent.

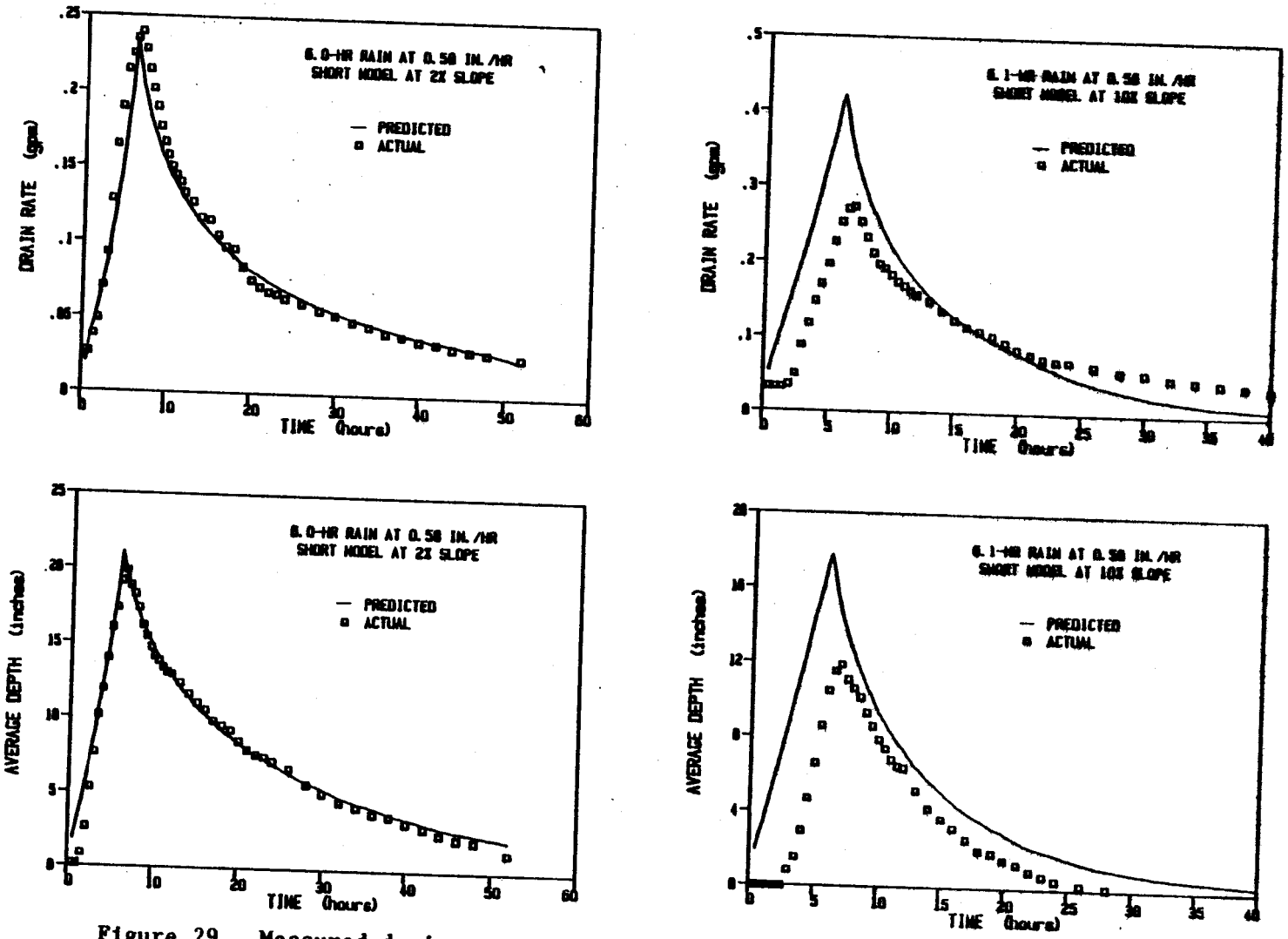

Figure 29. Measured drainage rate and average saturated depth vs. time compared to HELP prediction for coarse sand in the short model at slopes of 2 and 10 percent.

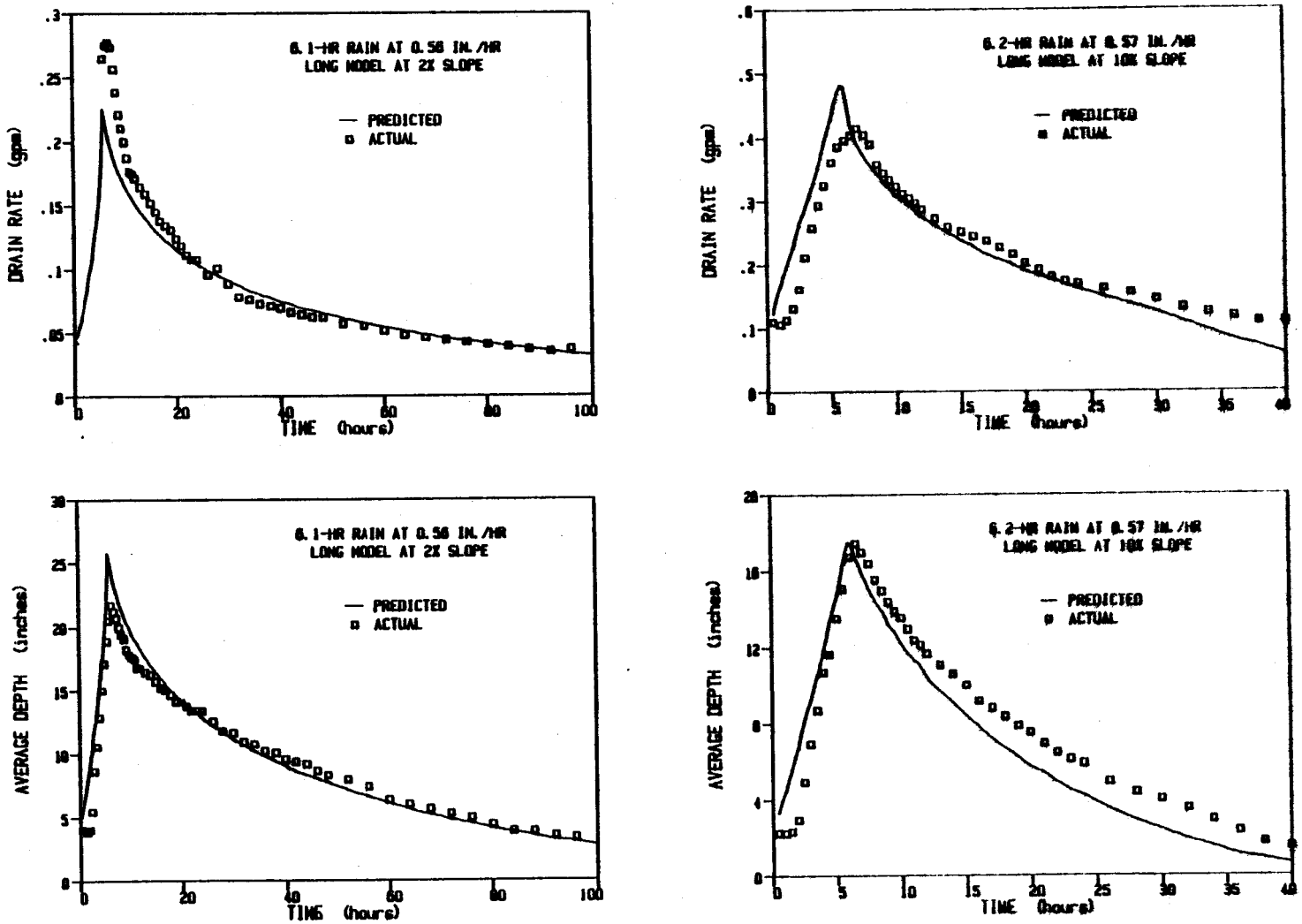

Figure 30. Measured drainage rate and average saturated depth vs. time compared to HELP prediction for coarse sand in the long model at slopes of 2 and 10 percent.

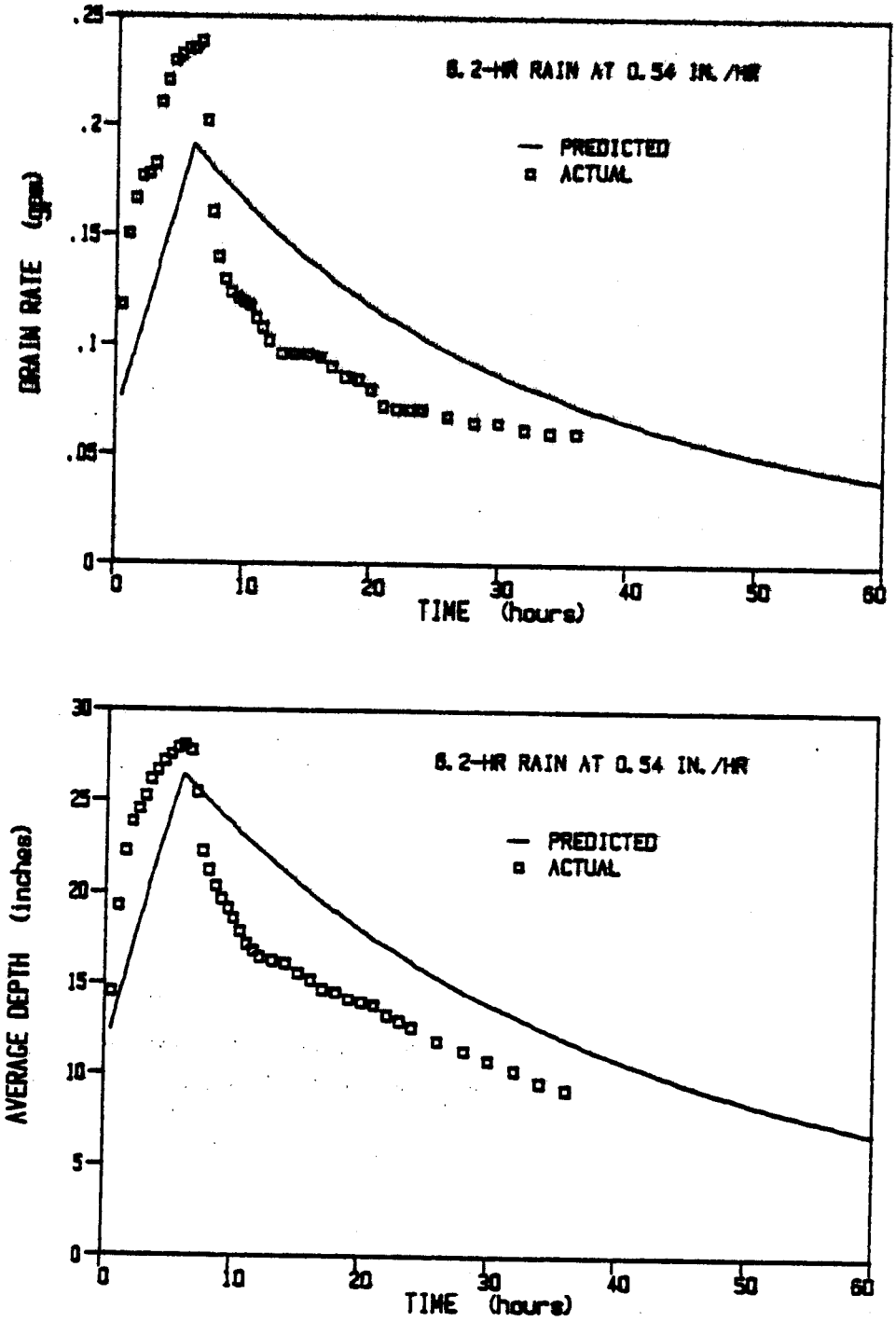

Figure 31. Measured drainage rate and average saturated depth vs. time compared to HELP prediction for fine sand in the long model at 10-percent slope using mean values for hydraulic conductivity and drainable porosity.

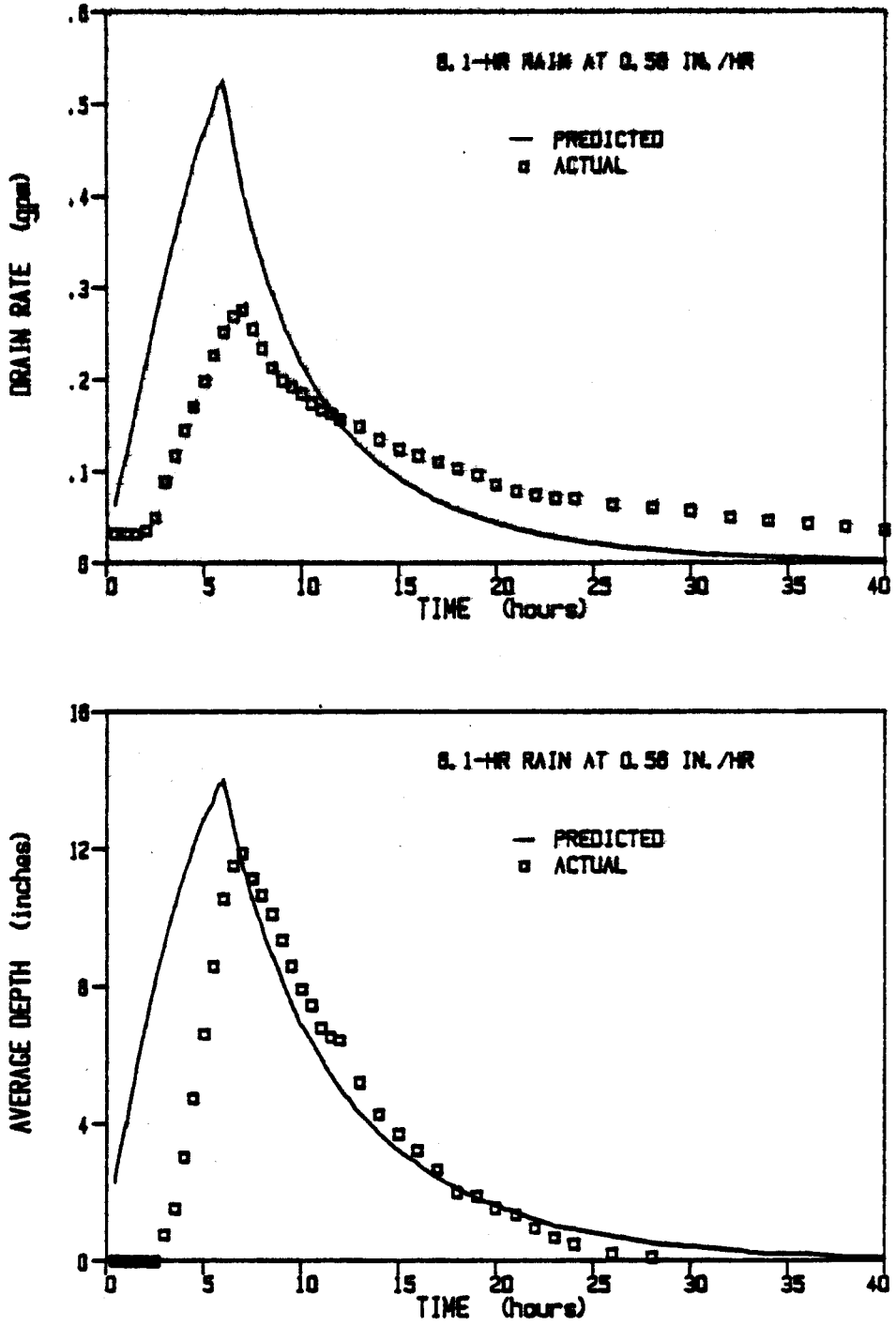

Figure 32. Measured drainage rate and average saturated depth vs. time compared to HELP prediction for coarse sand in the short model at 10-percent slope using mean values for hydraulic conductivity and drainable porosity.

treated as duplicates in this analysis. First, the effect of drainage length was isolated by using Equation 1 to compute the ratio of drainage rate for the long model (Q_L) to drainage rate for the short model (Q_s) given the same drainage media and constant values for α and $\bar{y}$. This ratio was multiplied by the measured Q_s to predict Q_L. The difference between measured and predicted Q_L was assumed to be due to a combination of experimental error and simplifying assumptions used in the derivation of the HELP drainage equation. Table 10 summarizes these comparisons, and Figure 33 plots the predicted Q_L versus measured Q_L. A regression analysis was conducted using the data in Table 10 and Figure 33 to find the slope of the best-fit line which also passed through the origin. The regression analyses performed to evaluate the HELP equation are summarized in Table 11. The resulting slope was 0.82 with a coefficient of determination (r^2) of 0.99. The 95-percent confidence interval for the slope did not include the value of 1.00. The slope should equal 1.00 and the intercept should equal 0.0 if the predicted and actual results are identical and the predictive method is accurate. Therefore, Q_L as measured in the unsteady drainage tests and as predicted by the HELP equation based on a measured Q_s are statistically different. The HELP lateral drainage equation overestimates the decrease in drainage rate resulting from an increase in length given the same sand, slope, and $\bar{y}$.

The effect of slope was similarly isolated by using Equation 1 to compute the ratio of drainage rate for the 10-percent slope ($Q_{10\%}$) to the drainage rate for the 2-percent slope ($Q_{2\%}$) given the same sand and constant values for L and $\bar{y}$. This ratio was multiplied by the measured $Q_{2\%}$ to predict $Q_{10\%}$. Table 12 summarizes these comparisons, and Figure 34 plots the predicted $Q_{10\%}$ versus measured $Q_{10\%}$. A regression analysis was conducted using the data in Table 12 and Figure 34 to find the slope of the best-fit line which also passed through the origin. The resulting slope was 1.30 with $r^2 = 0.98$. The 95-percent confidence interval for the slope of this line did not include the value of 1.00. Therefore, $Q_{10\%}$ as measured in the laboratory and as predicted by the HELP equation based on a measured $Q_{2\%}$ are statistically different. The HELP lateral drainage equation overestimates the increase in drainage rate resulting from an increase in slope.

Similarly, Equation 1 was used to compute the ratio of drainage rate for $\bar{y}$ = 12 in. ($Q_{12"}$) to drainage rate for $\bar{y}$ = 6 in. ($Q_{6"}$) given the same sand and constant values for L and α. In the calculation of this ratio it was assumed that the hydraulic conductivity at $\bar{y}$ = 12 in. was equal to 0.732 times the hydraulic conductivity at $\bar{y}$ = 6 in. based on Equation 15. This ratio was multiplied by the measured $Q_{6"}$ to predict $Q_{12"}$. Table 13 summarizes these comparisons, and Figure 35 plots the predicted $Q_{12"}$ versus measured $Q_{12"}$. The slope of the best-fit line passing through the origin was 1.02 with $r^2 = 0.99$. The 95-percent confidence interval for the slope of this line included the value 1.00. Therefore, $Q_{12"}$ as measured in the laboratory and as predicted by the HELP equation based on a measured $Q_{6"}$ are not statistically different. The HELP lateral drainage equation accounts for the effect of changes in $\bar{y}$ very well.

In the HELP lateral drainage equation (Equation 1) the slope (α) and drainage length (L) occur as a product several times. This product physically represents the head above the drain contributed by the slope of the liner.

TABLE 10. EFFECT OF LENGTH IN THE HELP DRAINAGE EQUATION*

Type of Sand	$\bar{y}$ (in.)	Slope (%)	Q_L/Q_s from HELP Equation	Measured Q_s (gpm)	Measured Q_L (gpm)	Predicted** Q_L (gpm)
Fine	6	2	0.737	0.030	0.025	0.022
	8	2	0.689	0.044	0.030	0.030
		5	0.868	0.043	0.040	0.037
		10	1.005	0.058	0.061	0.058
	12	2	0.626	0.056	0.039	0.035
		5	0.802	0.058	0.051	0.047
		10	0.956	0.072	0.070	0.069
	14	2	0.604	0.067	0.045	0.040
		5	0.775	0.068	0.057	0.053
		10	0.933	0.082	0.081	0.077
Coarse	6	2	0.737	0.056	0.052	0.041
		5	0.909	0.098	0.094	0.089
		10	1.033	0.164	0.166	0.169
	8	2	0.689	0.070	0.067	0.048
		5	0.868	0.123	0.116	0.107
		10	1.005	0.183	0.204	0.184
	12	2	0.626	0.119	0.106	0.074
		5	0.802	0.177	0.168	0.142
		10	0.956	0.244	0.287	0.233
	14	2	0.604	0.151	0.139	0.091
		5	0.775	0.218	0.210	0.169
		10	0.933	0.264	0.334	0.246

* Q_L = Drainage rate from long model.
Q_s = Drainage rate from short model.

** Predicted Q_L = (Q_L/Q_s from HELP Equation) x (Measured Q_s).

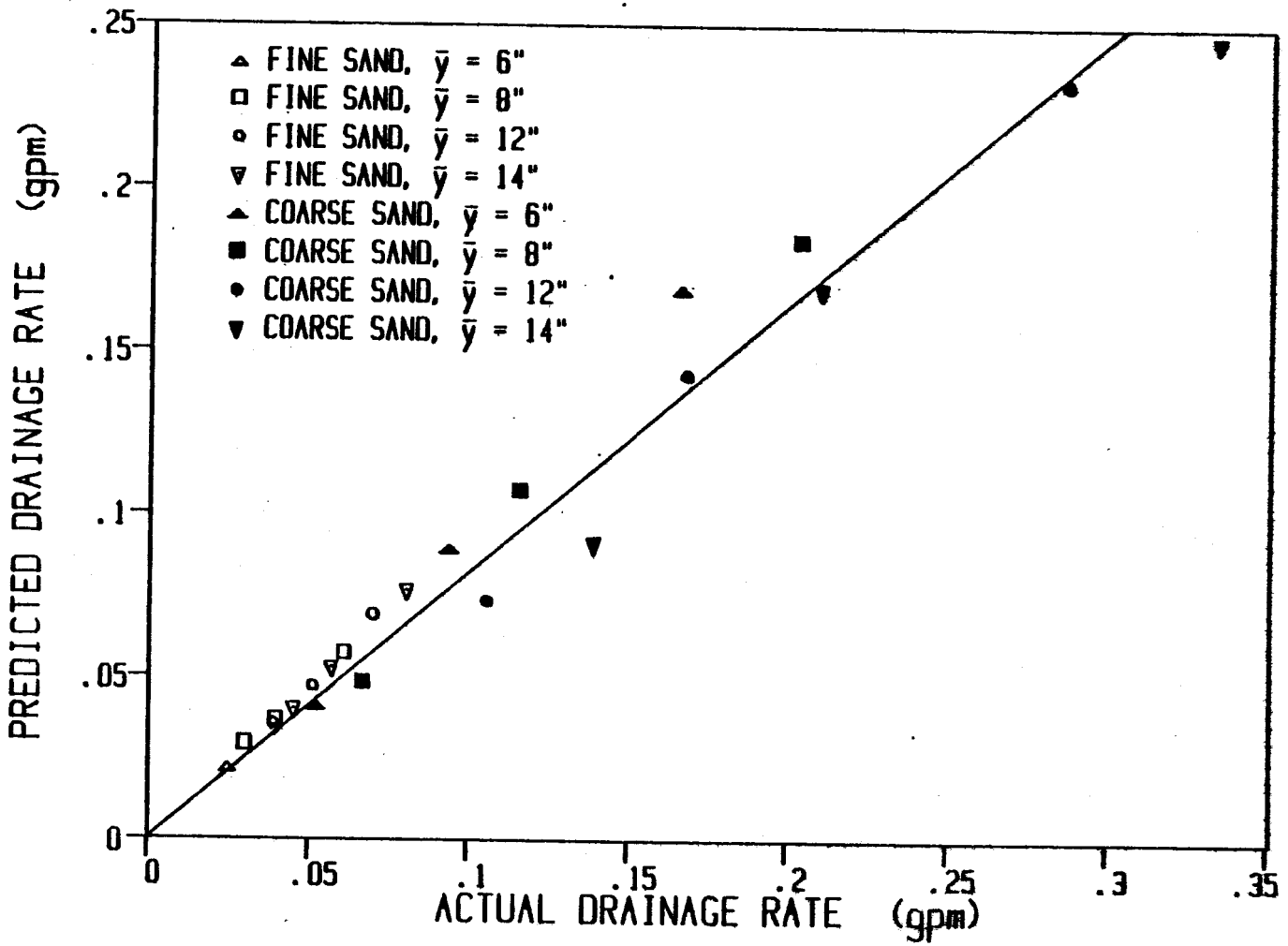

Figure 33. Predicted vs. actual drainage rate using measured drainage from short model to predict drainage from long model.

TABLE 11. REGRESSION ANALYSES SUMMARY FOR EVALUATION OF THE HELP LATERAL DRAINAGE EQUATION

Data Set	Q_P/Q_A*	95% Confidence Limits Q_P/Q_A	95% Confidence Limits Intercept	N**	r^2
Effect of length, constant α	0.819	0.749 to 0.890	-0.0070 to 0.0125	22	0.987
Effect of slope	1.302	1.086 to 1.519	-0.0269 to 0.0511	15	0.979
Effect of $\bar{y}$	1.023	0.866 to 1.193	-0.0207 to 0.0279	10	0.989
Effect of αL, constant L	1.196	1.115 to 1.276	-0.0099 to 0.0130	15	0.996

* Q_P = Drainage rate predicted by HELP equation.
Q_A = Drainage rate measured in drainage test.
** N = Number of values in data set.

Therefore, the effect of αL was similarly isolated by using Equation 1 to compute the ratio of drainage rate for an αL value of about 30.5 in. ($Q_{30.5"}$) to drainage rate for an αL value of about 15.3 in. ($Q_{15.3"}$), given the same sand and constant values of L and $\bar{y}$. This ratio was multiplied by the measured $Q_{15.3"}$ to predict $Q_{30.5"}$. Table 14 summarizes these comparisons and Figure 36 plots the predicted $Q_{30.5"}$ versus measured $Q_{30.5"}$. A regression analysis was conducted using the data in Table 14 and Figure 36 to find the slope of the best-fit line which also passed through the origin. The resulting slope was 1.20 with $r^2 = 0.996$. The 95-percent confidence interval for the slope did not include the value of 1.00. Therefore, $Q_{30.5"}$ as measured in the laboratory and as predicted by the HELP equation based on a measured $Q_{15.3"}$ are statistically different. The HELP lateral drainage equation overestimates the increase in drainage rate resulting from an increase in slope.

Earlier, the effect of length was isolated from the effects of slope, type of slope, type of sand, and $\bar{y}$, but it was not isolated from the effect of αL. To isolate the effects of length from the effect of αL, the ratio of drainage rate for the long model (Q_L) to the drainage rate for the short model (Q_s) given the same sand and constant values of $\bar{y}$ and αL was computed using Equation 1. This ratio was multiplied by the measured Q_s to predict Q_L. Table 15 summarizes these comparisons and Figure 37 plots the predicted Q_L versus measured Q_s. A regression analysis was conducted using the data in Table 15 and Figure 37 to find the slope of the best-fit line which also passed through the origin. The resulting slope was 0.71 with $r^2 = 0.99$. The 95-percent confidence interval for the slope did not include the value of 1.00. Therefore, Q_L as measured in the laboratory and as predicted by the HELP equation based on a measured Q_s are statistically different. The HELP lateral drainage equation overestimates the decrease in drainage rate resulting from an increase in length given the same sand, αL, and $\bar{y}$.

TABLE 12. EFFECT OF SLOPE IN THE HELP DRAINAGE EQUATION*

Type of Sand	L (in.)	$\bar{y}$ (in.)	$Q_{10\%}/Q_{2\%}$ from HELP Equation	Measured $Q_{2\%}$ (gpm)	Measured $Q_{10\%}$ (gpm)	Predicted** $Q_{10\%}$ (gpm)
Fine	305.4	6	3.187	0.030	0.050	0.096
		8	2.804	0.044	0.058	0.123
		12	2.300	0.056	0.072	0.129
		14	2.128	0.067	0.082	0.143
	629.4	8	4.090	0.030	0.061	0.123
		12	3.512	0.039	0.070	0.137
		14	3.287	0.045	0.081	0.148
Coarse	305.4	6	3.187	0.056	0.164	0.178
		8	2.804	0.070	0.183	0.196
		12	2.300	0.119	0.244	0.274
		14	2.128	0.151	0.264	0.321
	629.4	6	4.464	0.052	0.166	0.232
		8	4.090	0.067	0.204	0.274
		12	3.512	0.106	0.287	0.372
		14	3.287	0.139	0.334	0.457

* $Q_{2\%}$ = Drainage rate from 2-percent slope.
$Q_{10\%}$ = Drainage rate from 10-percent slope.

** Predicted $Q_{10\%}$ = ($Q_{10\%}/Q_{2\%}$ from HELP Equation) x (Measured $Q_{2\%}$).

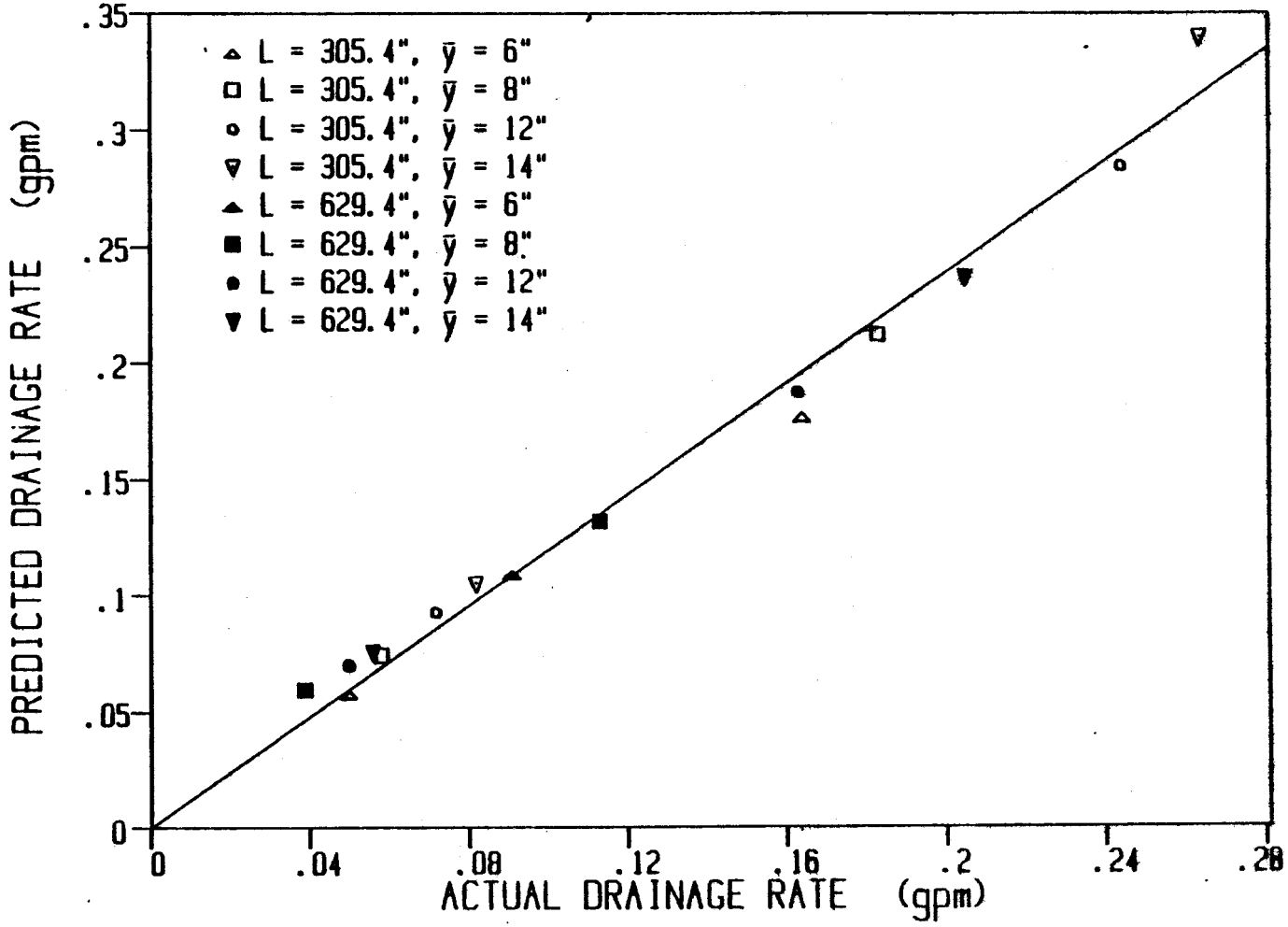

Figure 34. Predicted vs. actual drainage rate using measured drainage at 2-percent slope to predict drainage at 10-percent slope.

TABLE 13. EFFECT OF AVERAGE DEPTH OF SATURATION IN THE HELP DRAINAGE EQUATION*

Type of Sand	L (in.)	Slope (%)	$Q_{12"}/Q_{6"}$ from HELP Equation	Measured $Q_{6"}$ (gpm)	Measured $Q_{12"}$ (gpm)	Predicted** $Q_{12"}$ (gpm)
Fine	305.4	2	2.357	0.030	0.056	0.071
		5	1.918	0.032	0.058	0.062
		10	1.698	0.050	0.072	0.085
	629.4	2	1.998	0.025	0.039	0.050
Coarse	305.4	2	2.357	0.056	0.119	0.132
		5	1.918	0.098	0.177	0.188
		10	1.698	0.164	0.244	0.279
	629.4	2	1.998	0.052	0.106	0.104
		5	1.695	0.094	0.168	0.160
		10	1.574	0.166	0.287	0.261

* $Q_{6"}$ = Drainage rate from $\bar{y}$ = 6 in.
$Q_{12"}$ = Drainage rate from $\bar{y}$ = 12 in.

** Predicted $Q_{12"}$ = ($Q_{12"}/Q_{6"}$ from HELP equation) x (Measured $Q_{6"}$).

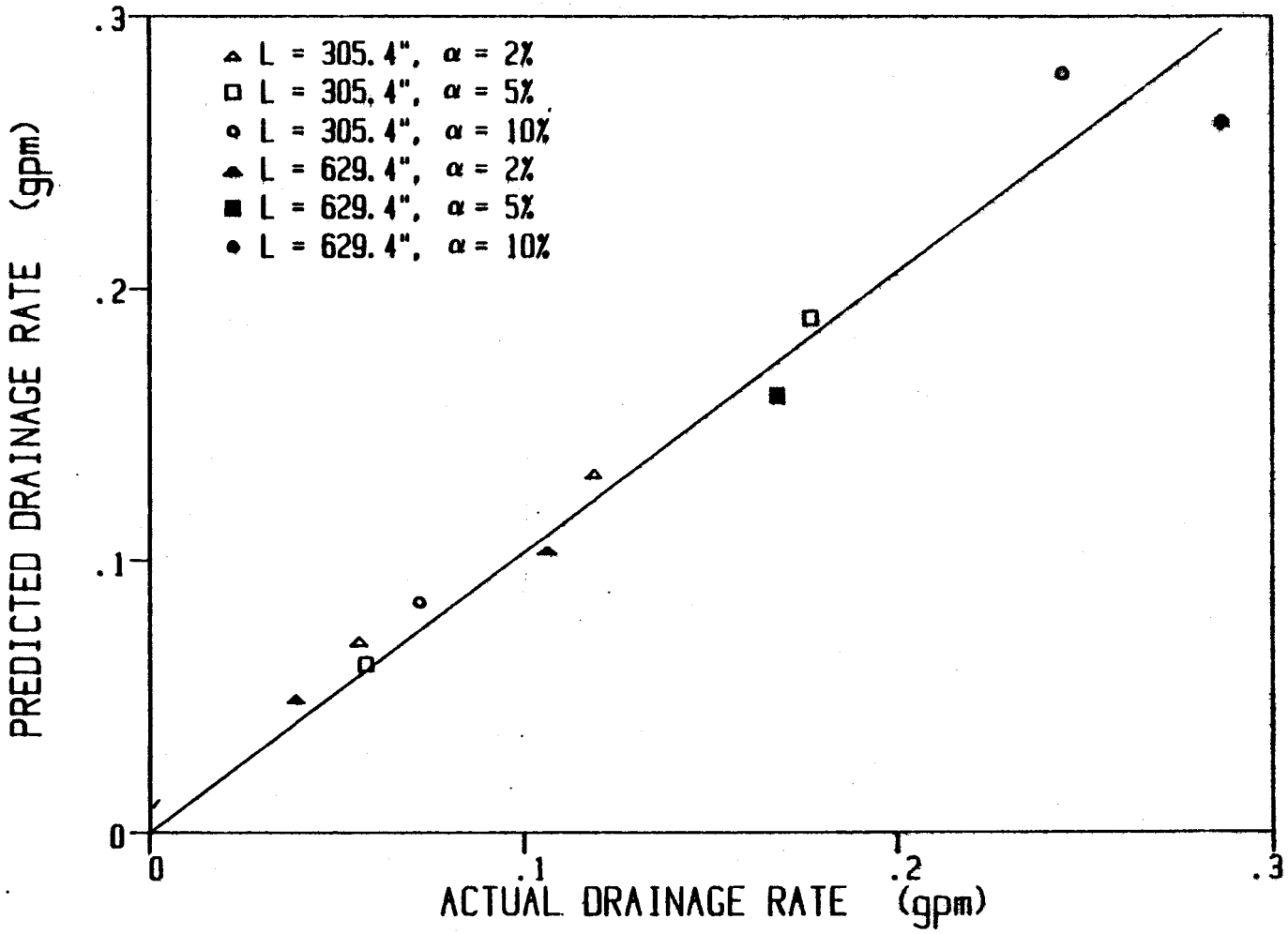

Figure 35. Predicted vs. actual drainage rate using measured drainage at $\bar{y}$ = 6 in. to predict drainage at $\bar{y}$ = 12 in.

TABLE 14. EFFECT OF αL IN THE HELP DRAINAGE EQUATION*

Type of Sand	L (in.)	$\bar{y}$ (in.)	$Q_{30.5"}/Q_{15.3"}$ from HELP Equation	Measured $Q_{15.3"}$ (gpm)	Measured $Q_{30.5"}$ (gpm)	Predicted** $Q_{30.5"}$ (gpm)
Fine	305.4	6	1.815	0.032	0.050	0.058
		8	1.736	0.043	0.058	0.075
		12	1.609	0.058	0.072	0.093
		14	1.557	0.068	0.082	0.106
	629.4	8	1.736	0.034	0.039	0.059
		12	1.609	0.043	0.050	0.069
		14	1.557	0.049	0.056	0.076
Coarse	305.4	6	1.815	0.098	0.164	0.178
		8	1.736	0.123	0.183	0.213
		12	1.609	0.177	0.244	0.284
		14	1.557	0.218	0.264	0.339
	629.4	6	1.815	0.060	0.091	0.109
		8	1.736	0.076	0.113	0.132
		12	1.609	0.117	0.163	0.188
		14	1.557	0.152	0.205	0.237

* $Q_{30.5"}$ = Drainage rate for αL = 30.5 in.
$Q_{15.3"}$ = Drainage rate for αL = 15.3 in.

** Predicted $Q_{30.5"}$ = ($Q_{30.5"}/Q_{15.3"}$ from HELP Equation) x (Measured $Q_{15.3"}$).

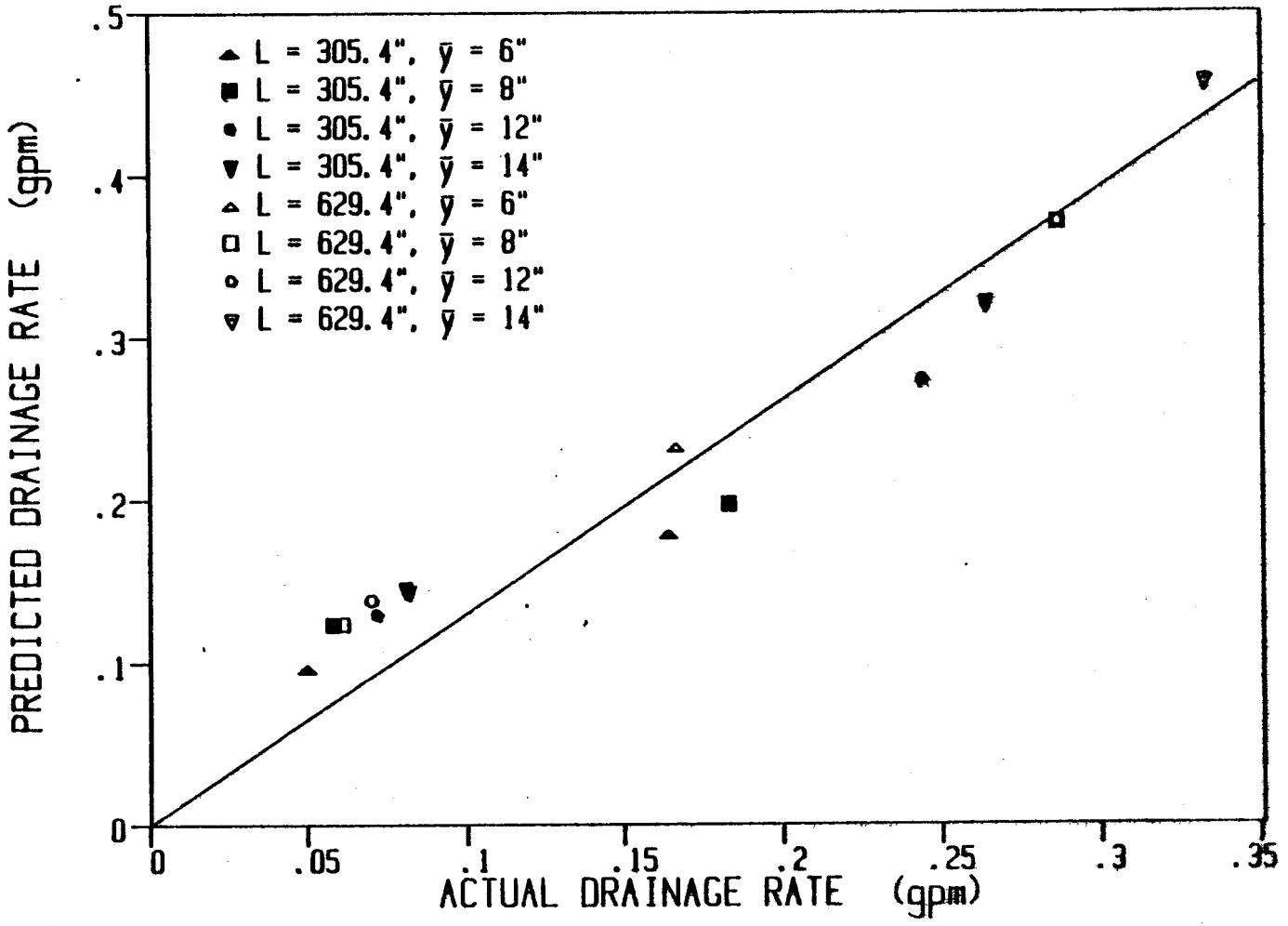

Figure 36. Predicted vs. actual drainage rate using measured drainage at αL = 15.3 in. to predict drainage at αL = 30.5 in.

TABLE 15. EFFECT OF LENGTH IN THE HELP DRAINAGE EQUATION GIVEN CONSTANT αL*

Type of Sand	αL (in.)	$\bar{y}$ (in.)	Q_L/Q_s From HELP Equation	Measured Q_s (gpm)	Measured Q_L (gpm)	Predicted** Q_L (gpm)
Fine	15.3	6	0.485	0.032	0.029	0.016
Fine	15.3	8	0.485	0.043	0.034	0.021
Fine	15.3	12	0.485	0.058	0.043	0.028
Fine	15.3	14	0.485	0.068	0.049	0.033
Fine	30.5	8	0.485	0.058	0.039	0.028
Fine	30.5	12	0.485	0.072	0.050	0.035
Fine	30.5	14	0.485	0.082	0.056	0.040
Coarse	15.3	6	0.485	0.098	0.060	0.048
Coarse	15.3	8	0.485	0.123	0.076	0.060
Coarse	15.3	12	0.485	0.177	0.117	0.086
Coarse	15.3	14	0.485	0.218	0.152	0.106
Coarse	30.5	6	0.485	0.164	0.091	0.080
Coarse	30.5	8	0.485	0.183	0.113	0.089
Coarse	30.5	12	0.485	0.244	0.163	0.118
Coarse	30.5	14	0.485	0.264	0.205	0.128

* Q_L = Drainage rate from long model.
Q_s = Drainage rate from short model.

** Predicted Q_L = (Q_L/Q_s from HELP equation) x (Measured Q_s).

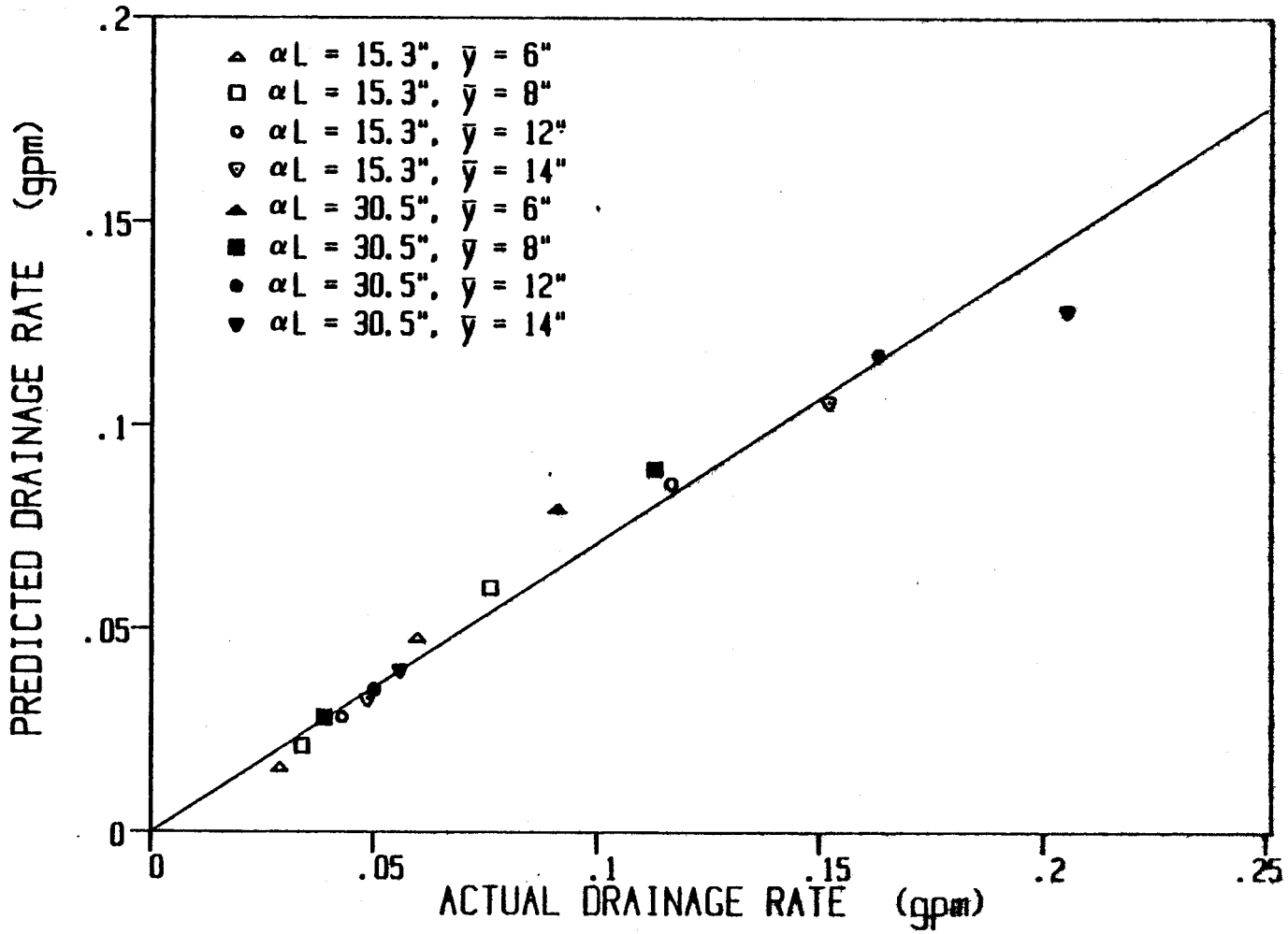

Figure 37. Predicted vs. actual drainage rate using measured drainage from short model to predict drainage from long model having the same value of αL.

SECTION 7

SUMMARY AND CONCLUSIONS

Drainage tests were performed on two large-scale physical models of landfill liner/drain systems to examine the effects that the length, slope and hydraulic conductivity of the drain layer and the depth of saturation above the liner have on the subsurface lateral drainage rate. The models have different lengths, 25.4 ft and 52.4 ft, and adjustable slope ranging from 2 to 10 percent. The models were filled with a 3-ft sand drain layer overlying a 1-ft clay liner. A 2-in. layer of gravel was placed under the liner to collect seepage from the clay liner. Drainage from two different sands was examined in both models.

Several drainage tests were run on each configuration of the models by applying water as rainfall to the surface of the sand layer and then measuring the water table along the length of the models and the lateral drainage volume as a function of time. Lateral drainage and water table profiles were measured during periods of increasing, decreasing, and steady-state drainage rates. In total, more than 60 tests were performed.

The hydraulic conductivity of the sand was measured in the laboratory permeameters, but its value was apparently quite different and varied in the drainage tests. The hydraulic conductivity of the sand at various depths of saturation was estimated for each test using the Boussinesq solution of Darcy's law for unsteady, unconfined flow through porous media and the HELP lateral drainage equation. These hydraulic conductivity values were compared to determine the agreement between the HELP model and the Boussinesq solution. For steady-state drainage the HELP model estimates of the hydraulic conductivity were 44 percent greater than the Boussinesq solution estimates. This result means that the HELP model underestimated the steady-state lateral drainage rate predicted by the Boussinesq solution by 30 percent. The HELP estimates were 31 percent greater than the laboratory measurements for the fine sand and 90 percent less than the laboratory measurements for the coarse sand. For unsteady drainage the HELP model estimates were only 13 percent greater than the Boussinesq solution estimates, which would underpredict the lateral drainage rate by 11 percent. The underprediction of the cumulative lateral drainage volume would be expected to be very small since the removal rate of water from the drain layer by all other means is much smaller than the lateral drainage rate. Consequently, the effect of differences in the predicted and actual drainage times is small.

The differences between the laboratory measurement of the hydraulic conductivity and either of the two estimates were much larger than the differences between the estimates. In addition, the hydraulic conductivity varied

as a function of the depth of saturation, apparently due to entrapment of air in the sand. Similarly, the drainable porosity varied as a function of depth of saturation due to the air. These phenomena make it very difficult to model the lateral drainage process and produce good agreement between the predicted and actual results for drainage rate and depth of saturation as a function of time.

An analysis was performed to determine how well the lateral drainage equation in the HELP model accounts for the effects of drainage length, slope of the liner, average depth of saturation and head above the drain contributed by the liner (αL) in the estimation of the drainage rate. The drainage equation overestimates the decrease in drainage rate by an increase in length given the same sand, slope, depth of saturation and head above the drain. Similarly, the equation overestimated the increase in drainage rate resulting from an increase in slope and head above the drain. The effects of depth of saturation predicted by the equation agreed very well with the actual results.

The following conclusions and recommendations are made. Lateral drainage in landfill liner/drain systems is quite variable, probably due to air entrapment. The hydraulic conductivity measurement made in the laboratory is quite different than the in-place value. Consequently, the estimation of the lateral drainage rate is prone to considerable error despite having a good equation or solution method for the estimation. Nevertheless, the prediction of the cumulative volume of lateral drainage is likely to be quite good since the depth of saturation will be overpredicted if the drainage rate is underpredicted and vice versa, thereby adjusting the drainage rate. However, the predicted depth of saturation will be quite different from the measured value.

The lateral drainage equation in the HELP model performs very well for tests on models at 2-percent slope but overpredicted drainage and depths at 10-percent slope. The model overestimates the effect of drainage length in reducing the drainage rate and also overestimates the effects of slope and head above the drain in increasing the drainage rate. Therefore, additional refinement in the equation should be performed to make the equation valid over a wider range of slopes and drainage lengths. Nevertheless, the HELP equation does provide a good estimation of the lateral drainage volume.

Evaluation of the effects of drainage length, slope of the liner, depth of saturation and head above the drain on the drainage rate predicted by the Boussinesq solution should be performed to determine whether the effects observed with the HELP drainage equation are unique. Similarly, an additional data set of drainage results should be collected to determine whether the effects are unique to this data set. Additional data should be collected for longer drainage lengths and greater slopes and from actual landfill/liner systems.

REFERENCES

1. Schroeder, P. R., Gibson, A. C., and Smolen, M. D. The Hydrologic Evaluation of Landfill Performance (HELP) Model. Volume II. Documentation for Version I. EPA/530-SW-84-010, U.S. Environmental Protection Agency, Office of Solid Waste and Emergency Response, Washington, D.C. 1984, 256 pp.

2. Schroeder, P. R., Morgan, J. M., Walski, T. M., and Gibson, A. C. The Hydrologic Evaluation of Landfill Performance (HELP) Model. Volume I. User's Guide for Version I. EPA/530-SW-84-009, U.S. Environmental Protection Agency, Office of Solid Waste and Emergency Response, Washington, D.C., 1984. 120 pp.

3. U.S. Environmental Protection Agency. RCRA Guidance Document for Landfill Design. Federal Register, General Services Administration, Washington, D.C., July 26, 1982.

4. Headquarters, Department of the Army, Office, Chief of Engineers. Laboratory Soils Testing. Engineer Manual 1110-2-1906, Washington, D.C., 1970.

5. Skaggs, R. W. Modification to DRAINMOD to Consider Drainage from and Seepage Through a Landfill. Appendix A. Numerical Solution to the Boussinesq Equation for Transient Water Movement over an Inclined Restrictive Layer, Draft Report. U.S. Environmental Protection Agency, Cincinnati, OH, 1982. 15 pp.

6. Penton Software, Inc. Statpro User's Manual. New York, 1985.

BIBLIOGRAPHY

Baver, L. D., Walter H. Gardner, and Wilford R. Gardner. 1972. Soil Physics. John Wiley and Sons, New York. 484 pp.

Carlson, K. J. 1971. Drainage from Level and Sloping Land. REC-ERC-71-44, Engineering and Research Center, Bureau of Reclamation, Denver, CO. 43 pp.

Dake, J. M. K. 1972. Essentials of Engineering Hydraulics. John Wiley and Sons, Inc., New York. 392 pp.

Freize, R. Allan, and John A. Cherry. 1979. Groundwater. Prentice-Hall, Inc., Englewood Cliffs, NJ. 553 pp.

Hillel, Daniel. 1971. Soil and Water: Physical Principles and Processes. Academic Press, New York. 288 pp.

Hillel, Daniel. 1982. Introduction to Soil Physics. Academic Press, New York. 364 pp.

List, E. John. 1965. Steady Flow to Tile Drains Above an Impervious Layer - A Theoretical Study. KH-R-9, California Institute of Technology, Pasadena, CA. 60 pp.

Luthin, James N. 1966. Drainage Engineering. John Wiley and Sons, Inc., New York. 250 pp.

APPENDIX A

HYDRAULIC CONDUCTIVITY ESTIMATES

The analysis performed in Section 6 of this report required estimates of the hydraulic conductivity of the drainage media. These estimates were generated using the numerical Boussinesq solution and the HELP model lateral drainage equation. Estimates were generated for most of the drainage tests including steady-state drainage, unsteady drainage following rainfall, and unsteady drainage from presaturated sand. The hydraulic conductivity values were estimated at several depths for the unsteady drainage tests. Values for steady-state drainage, unsteady drainage following rainfall, and unsteady drainage from presaturated sand are given, respectively, in Tables A-1, A-2, and A-3.

TABLE A-1. HYDRAULIC CONDUCTIVITY ESTIMATES FOR STEADY-STATE DRAINAGE

Type of Sand	Model Length (in.)	Slope (%)	Average Depth (in.)	Drain Rate (in./hr)	Hydraulic Conductivity (in./hr)	
					Boussinesq	HELP
Fine	305.4	1.8	12.6	0.0336	0.0061	0.0084
Fine	305.4	10.4	13.2	0.0543	0.0037	0.0055
Fine	629.4	10.3	12.7	0.0249	0.0041	0.0058
Coarse	305.4	1.9	11.4	0.0708	0.015	0.021
Coarse	305.4	10.0	11.3	0.1688	0.015	0.025
Coarse	629.4	2.3	11.3	0.0330	0.021	0.030
Coarse	629.4	9.9	11.8	0.1050	0.021	0.027

TABLE A-2. HYDRAULIC CONDUCTIVITY ESTIMATES FOR UNSTEADY DRAINAGE FOLLOWING RAINFALL

Type of Sand	Model Length (in.)	Slope (%)	Rainfall Duration (hr)	Depth (in.)	Hydraulic Conductivity (in./hr)	
					Boussinesq	HELP
Fine	305.4	1.8	1	9	0.0138	0.0147
Fine	305.4	1.8	1	8	0.0151	0.0158
Fine	305.4	1.8	1	7	0.0173	0.0180
Fine	305.4	1.8	2	19	0.0048	0.0063
Fine	305.4	1.8	2	17	0.0111	0.0107
Fine	305.4	1.8	2	10	0.0200	0.0211
Fine	305.4	1.8	2	10	0.0172	0.0180
Fine	305.4	1.8	6	17	0.0116	0.0117
Fine	305.4	1.8	6	9	0.0182	0.0188
Fine	305.4	1.8	24	19	0.0064	0.0063
Fine	305.4	1.8	24	15	0.0078	0.0080
Fine	305.4	1.8	24	5	0.0212	0.0218
Fine	305.4	1.8	24	4	0.0251	0.0262
Fine	305.4	4.9	6	17	0.0061	0.0069
Fine	305.4	4.9	6	7	0.0106	0.0122
Fine	305.4	10.4	1	6	0.0083	0.0096
Fine	305.4	10.4	1	5	0.0092	0.0109
Fine	305.4	10.4	2	17	0.0061	0.0059
Fine	305.4	10.4	2	11	0.0067	0.0066
Fine	305.4	10.4	6	16	0.0060	0.0058
Fine	305.4	10.4	6	8	0.0079	0.0082
Fine	305.4	10.4	24	15	0.0039	0.0038
Fine	305.4	10.4	24	12	0.0044	0.0043
Fine	629.4	2.1	1	8	0.0164	0.0165
Fine	629.4	2.1	1	7	0.0179	0.0184
Fine	629.4	2.1	2	20	0.0070	0.0108
Fine	629.4	2.1	2	16	0.0086	0.0104
Fine	629.4	2.1	2	10	0.0132	0.0135
Fine	629.4	2.1	6	20	0.0084	0.0099
Fine	629.4	2.1	6	10	0.0134	0.0136

(Continued)

TABLE A-2. (CONTINUED)

Type of Sand	Model Length (in.)	Slope (%)	Rainfall Duration (hr)	Depth (in.)	Hydraulic Conductivity (in./hr) Boussinesq	HELP
Fine	629.4	2.1	24	19	0.0081	0.0092
Fine	629.4	2.1	24	9	0.0128	0.0132
Fine	629.4	5.0	6	18	0.0050	0.0075
Fine	629.4	5.0	6	9	0.0073	0.0107
Fine	629.4	10.3	1	13	0.0054	0.0062
Fine	629.4	10.3	1	11	0.0062	0.0069
Fine	629.4	10.3	2	17	0.0061	0.0058
Fine	629.4	10.3	2	14	0.0057	0.0055
Fine	629.4	10.3	6	16	0.0068	0.0061
Fine	629.4	10.3	6	11	0.0064	0.0063
Fine	629.4	10.3	24	17	0.0065	0.0058
Fine	629.4	10.3	24	13	0.0062	0.0058
Coarse	305.4	1.9	2	15	0.0228	0.0228
Coarse	305.4	1.9	2	10	0.0276	0.0274
Coarse	305.4	1.9	2	4	0.0720	0.0748
Coarse	305.4	1.9	6	15	0.0225	0.0227
Coarse	305.4	1.9	6	11	0.0279	0.0274
Coarse	305.4	1.9	6	6	0.0418	0.0431
Coarse	305.4	1.9	24	8	0.0317	0.0319
Coarse	305.4	1.9	24	8	0.0316	0.0315
Coarse	305.4	1.9	24	5	0.0508	0.0527
Coarse	305.4	1.9	24	4	0.0734	0.0745
Coarse	305.4	5.4	2	9	0.0309	0.0306
Coarse	305.4	5.4	2	5	0.0383	0.0409
Coarse	305.4	5.4	6	9	0.0253	0.0251
Coarse	305.4	5.4	6	4	0.0394	0.0418
Coarse	305.4	10.0	2	6	0.0348	0.0370
Coarse	305.4	10.0	2	2	0.0472	0.0790
Coarse	305.4	10.0	6	7	0.0300	0.0334
Coarse	305.4	10.0	6	2	0.0456	0.0747

(Continued)

TABLE A-2. (CONCLUDED)

Type of Sand	Model Length (in.)	Slope (%)	Rainfall Duration (hr)	Depth (in.)	Hydraulic Conductivity (in./hr) Boussinesq	HELP
Coarse	305.4	10.0	24	3	0.0301	0.0424
Coarse	305.4	10.0	24	1	0.0431	0.0814
Coarse	629.4	2.3	2	16	0.0292	0.0288
Coarse	629.4	2.3	2	11	0.0301	0.0294
Coarse	629.4	2.3	2	5	0.0500	0.0508
Coarse	629.4	2.3	6	11	0.0277	0.0276
Coarse	629.4	2.3	6	3	0.0692	0.0761
Coarse	629.4	2.3	24	8	0.0354	0.0350
Coarse	629.4	2.3	24	4	0.0553	0.0582
Coarse	629.4	5.2	2	11	0.0213	0.0294
Coarse	629.4	5.2	2	4	0.0281	0.0463
Coarse	629.4	5.2	6	10	0.0159	0.0284
Coarse	629.4	5.2	6	5	0.0164	0.0349
Coarse	629.4	9.9	2	9	0.0278	0.0290
Coarse	629.4	9.9	2	7	0.0267	0.0309
Coarse	629.4	9.9	6	9	0.0282	0.0300
Coarse	629.4	9.9	6	4	0.0362	0.0449
Coarse	629.4	9.9	24	6	0.0248	0.0325
Coarse	629.4	9.9	24	3	0.0313	0.0527

TABLE A-3. HYDRAULIC CONDUCTIVITY ESTIMATES FOR UNSTEADY DRAINAGE FROM PRESATURATED SAND

Type of Sand	Model Length (in.)	Slope (%)	Depth (in.)	Hydraulic Conductivity (in./hr)	
				Boussinesq	HELP
Fine	305.4	1.8	14	0.0150	0.0156
Fine	305.4	1.8	12	0.0111	0.0110
Fine	305.4	1.8	10	0.0188	0.0191
Fine	305.4	1.8	9	0.0147	0.0148
Fine	629.4	2.1	24	0.0079	0.0116
Fine	629.4	2.1	10	0.0155	0.0161
Fine	629.4	2.1	6	0.0201	0.0201
Fine	629.4	2.1	4	0.0238	0.0245
Coarse	305.4	10.0	10	0.0243	0.0244
Coarse	305.4	10.0	5	0.0319	0.0434
Coarse	629.4	2.3	13	0.0260	0.0257
Coarse	629.4	2.3	7	0.0446	0.0454
Coarse	629.4	2.3	6	0.0456	0.0451
Coarse	629.4	2.3	3	0.0621	0.0647

APPENDIX B

COMPARISONS BETWEEN BOUSSINESQ SOLUTION AND HELP LATERAL DRAINAGE EQUATION

The HELP lateral drainage equation was developed from numerical solutions of the Boussinesq equation for saturated unconfined lateral flow through porous media under unsteady drainage conditions. Consequently, the two methods should predict the same drainage rate under the same unsteady drainage conditions when the same values are used for the design parameters. This appendix compares predictions by the two methods using actual test data to determine how well the HELP equation represents the Boussinesq solution.

In Section 6 hydraulic conductivities predicted by the two methods were briefly compared. Since the drainage rate computation is directly proportional to the hydraulic conductivity value in both methods, the estimates of hydraulic conductivity using measured values of drainage rate, depth of saturation, drainage length, slope and infiltration rate can be directly compared to determine the agreement between the methods. Comparisons are made in this appendix for steady-state drainage, unsteady drainage following rainfall and unsteady drainage from presaturated sand using the hydraulic conductivity values presented in Appendix A. Comparisons are also made to determine the effects of slope, drainage length, type of sand and depth of saturation on the agreement between the two equations.

Steady-state drainage differs from unsteady drainage since recharge alters the profile of the depth of saturation as a function of distance from the drain. Consequently, the drainage rate at a given average depth of saturation is greater for steady-state drainage than for unsteady drainage when the profile is falling, and is less than when the profile is rising. In actual drainage tests the amount of difference is confounded by the difference in air entrapment between the two modes of drainage. Comparisons between predicted hydraulic conductivity values for steady-state and unsteady drainage by the numerical solution of the Boussinesq equation and the HELP lateral drainage equation are summarized in Table B-1 where the ratio of hydraulic conductivity values is presented. The ratio of hydraulic conductivity estimates for steady-state drainage to those for unsteady drainage was 0.614 using the Boussinesq solution and 0.831 using the HELP equation. Therefore, using a constant hydraulic conductivity value for all types of drainage would produce greater error with the Boussinesq solution than with the HELP equation. These two regressions are presented in Figure B-1. A ratio of 1.000 and an intercept of 0.0000 indicate that the data are identical. In all of the regressions presented in this appendix, the intercept was not significantly different from zero. Therefore, the regressions were run using an intercept of 0.0000 to determine the ratios, K1/K2, presented in Tables B-1 and B-2.

TABLE B-1. HYDRAULIC CONDUCTIVITY REGRESSION ANALYSIS SUMMARY

Data Set	K1/K2	95% Confidence Limits K1/K2	95% Confidence Limits Intercept	N*	r^2
Steady-state drainage tests**	1.416	1.152 to 1.680	-0.0036 to 0.0039	7	0.992
All unsteady drainage tests**	1.134	1.052 to 1.217	-0.0023 to 0.0023	93	0.959
Unsteady drainage following rainfall**	1.152	1.059 to 1.246	-0.0026 to 0.0026	79	0.955
Unsteady drainage with presaturation**	1.049	0.927 to 1.171	-0.0035 to 0.0038	14	0.991
Estimates from Boussinesq solution†	0.614	0.285 to 0.942	-0.0076 to 0.0071	6	0.960
Estimates from HELP equation†	0.831	0.406 to 1.255	-0.0100 to 0.0093	6	0.964

* N = Number of values in data set.
** K1 = Hydraulic conductivity value using HELP equation.
K2 = Hydraulic conductivity value using Boussinesq solution.
† K1 = Hydraulic conductivity value for steady-state drainage.
K2 = Hydraulic conductivity value for unsteady drainage.

The 95-percent confidence limits for the ratio and the intercept are also presented in Tables B-1 and B-2 to show the significance of the results.

The ratio of the HELP estimate (KH) to the Boussinesq estimate (KB) for steady-state drainage is statistically different at 95-percent percent confidence from the ratio for unsteady drainage. The ratio for steady-state drainage was 1.416 while it was 1.134 for unsteady drainage. The regressions are shown in Figure B-2. The difference in the ratios for unsteady drainage following rainfall and from presaturated sands as shown in Figure B-3 was not significant at 95-percent confidence, but the ratio for presaturation was smaller and not significantly different from 1.000. The HELP hydraulic conductivity values are significantly greater than the values estimated by the Boussinesq solution. As presented in Section 6, this means that the lateral drainage rate is underestimated by the HELP model in comparison to the Boussinesq model by an average of 29 percent for steady-state drainage and 12 percent for unsteady drainage.

Six parameters were examined in the laboratory drainage tests: type of sand, slope, depth of saturation, drainage length, rainfall duration and

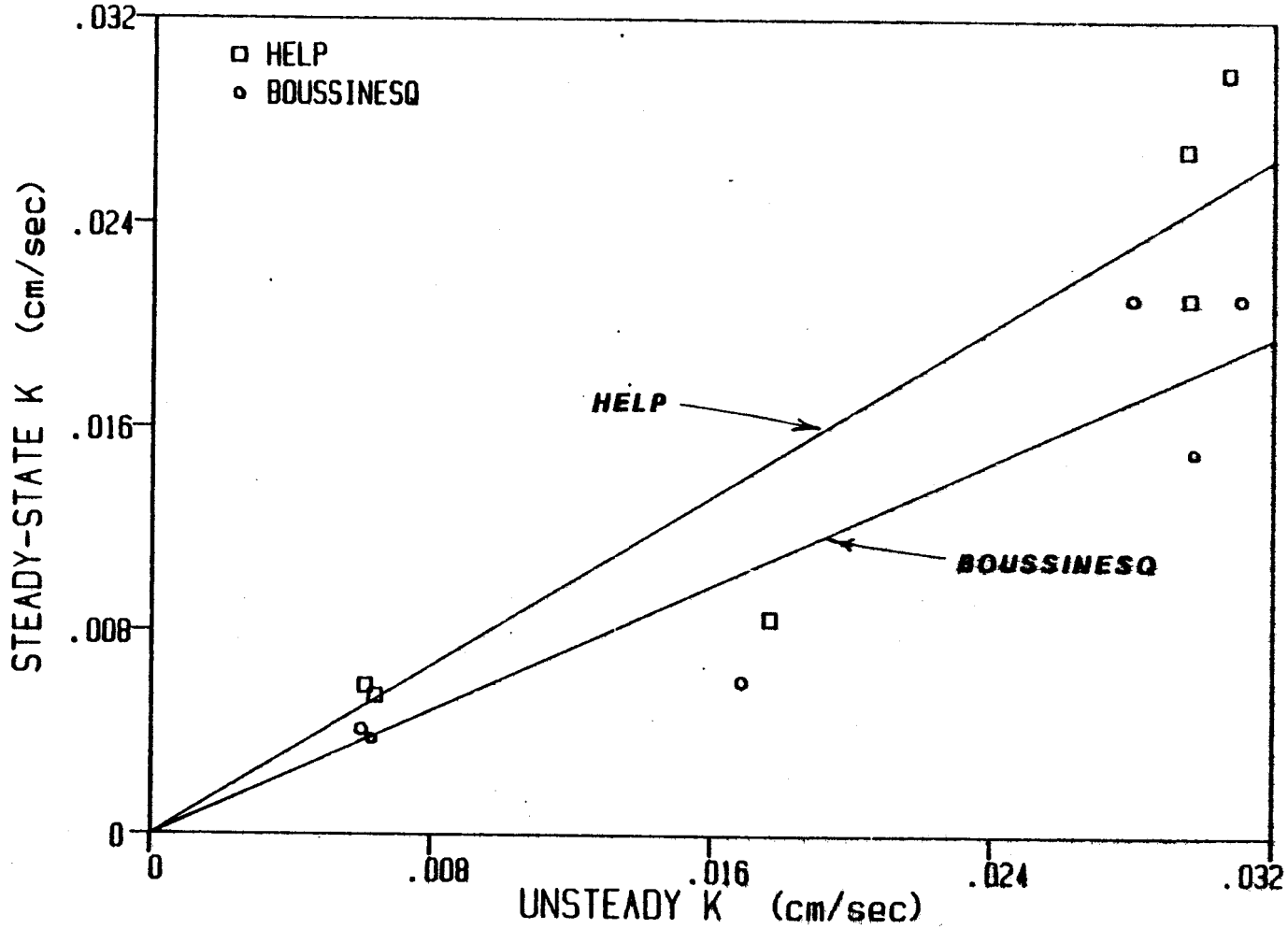

Figure B-1. Comparisons of hydraulic conductivity values for steady-state drainage to values for unsteady drainage as estimated by the HELP equation and the numerical Boussinesq solution.

TABLE B-2. HYDRAULIC CONDUCTIVITY REGRESSION ANALYSIS FOR UNSTEADY DRAINAGE FOLLOWING RAINFALL

Data Set	KH/KB*	95% Confidence Limits KH/KB	95% Confidence Limits Intercept	N**	r^2
Fine Sand	1.053	0.994 to 1.112	-0.0056 to 0.0079	42	0.993
Coarse Sand	1.162	0.930 to 1.395	-0.0082 to 0.0096	37	0.953
Short Model	1.157	1.018 to 1.295	-0.0045 to 0.0036	43	0.950
Long Model	1.145	1.023 to 1.266	-0.0025 to 0.0037	36	0.964
2% Slope	1.033	1.011 to 1.055	-0.0007 to 0.0007	39	0.999
5% Slope	1.216	0.800 to 1.632	-0.0083 to 0.0112	12	0.940
10% Slope	1.427	1.235 to 1.619	-0.0063 to 0.0026	28	0.957
Average Depth of 0" to 7"	1.195	0.946 to 1.443	-0.0087 to 0.0113	27	0.951
Average Depth of 8" to 14"	1.039	0.935 to 1.143	-0.0018 to 0.0024	31	0.984
Average Depth of 15" to 20"	1.022	0.937 to 1.106	-0.0007 to 0.0013	21	0.991
y = 0" to 7" 2% Slope	1.044	0.995 to 1.092	-0.0025 to 0.0023	11	0.999
y = 0" to 7" 10% Slope	1.503	1.016 to 1.989	-0.0164 to 0.0146	13	0.964
y = 8" to 14" 2% Slope	1.003	0.964 to 1.042	-0.0008 to 0.0010	16	0.999
y = 8" to 14" 10% Slope	1.136	0.855 to 1.416	-0.0039 to 0.0039	11	0.957
y = 15" to 20" 2% Slope	1.024	0.903 to 1.145	-0.0013 to 0.0022	12	0.992
y = 15" to 20" 10% Slope	0.935	0.664 to 1.206	-0.0016 to 0.0016	6	0.999

* KH = Hydraulic conductivity value using HELP equation.
KB = Hydraulic conductivity value using Boussinesq solution.
** N = Number of values in data set.

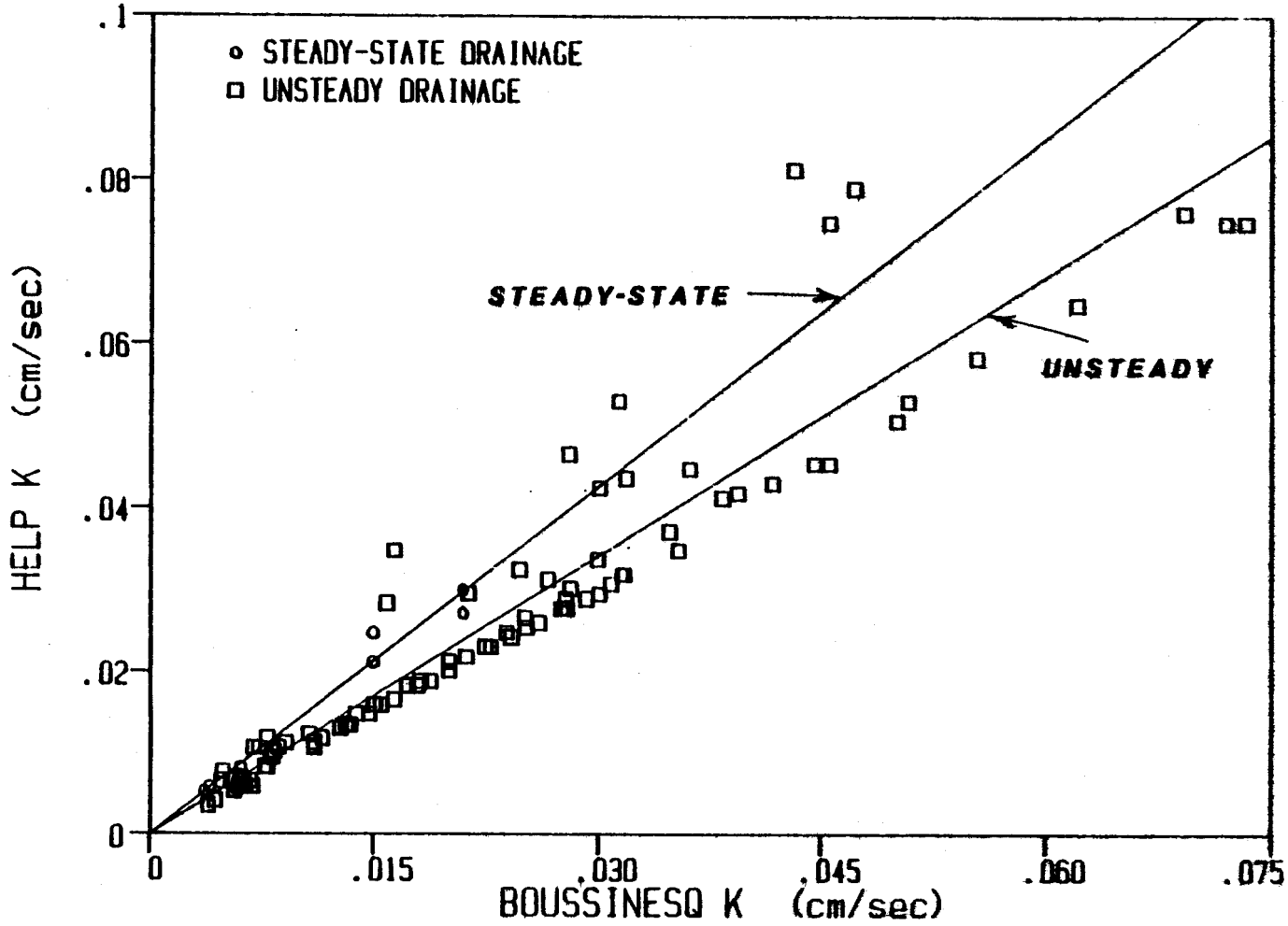

Figure B-2. Comparisons of hydraulic conductivity estimates by the HELP equation to estimates by the numerical Boussinesq solution for steady-state and unsteady drainage.

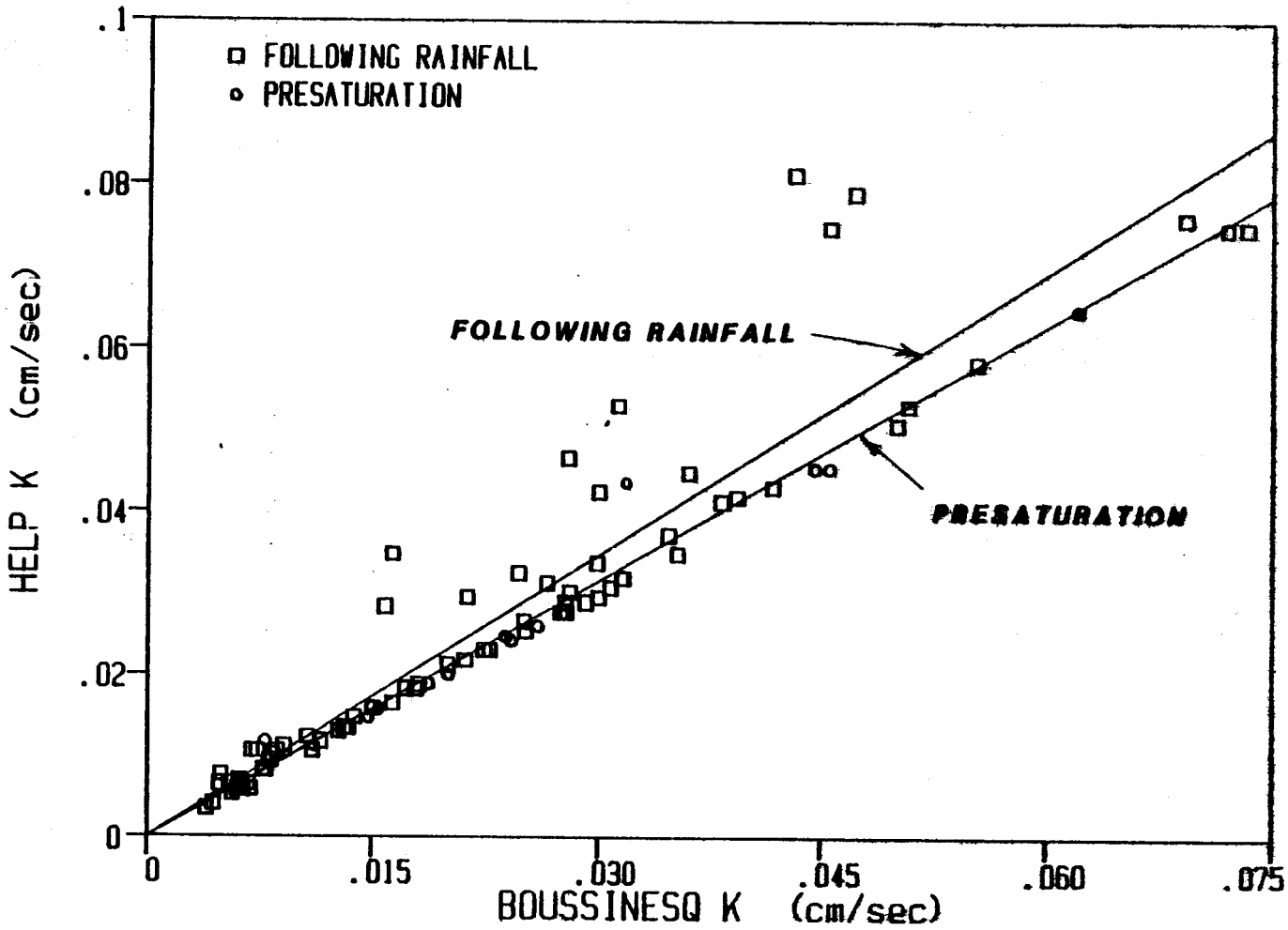

Figure B-3. Comparisons of hydraulic conductivity estimates by the HELP equation to estimates by the numerical Boussinesq solution for unsteady drainage following rainfall and from presaturated sands.

rainfall intensity. Inspection of the data indicated that rainfall duration and intensity had no effect on the drainage rate for a given sand, slope, length and saturated depth as depicted by the hydraulic conductivity estimates. This was verified by performing an unequal two-way analysis of variance (ANOVA) using slope as the blocks and either rainfall duration or intensity as the treatments. Blocks are the different levels of a variable that produced variance in the measured result. The levels of slope for the blocks were 2, 5 and 10 percent. Treatments are the different levels of the second variable that produce variance (6). Slope was selected for the blocks since it showed the greatest effects on the ratios of drainage rates presented in Section 6 and the ratios of hydraulic conductivity values as shown in Table B-2.

The effects of the remaining four parameters on the ratio of the hydraulic conductivity estimates were examined by two methods. The first method was linear regression of the HELP-generated and Boussinesq-generated estimates of hydraulic conductivity. This method does not examine interaction effects and can yield erroneous results due to interactions and cross-correlations. Therefore, unequal two- and three-way ANOVAs on the 79 ratios of the hydraulic conductivity estimates for unsteady drainage following rainfall were used as the second method because of their ability to account for interactions between variables.

The results of the linear regression analyses for type of sand, drainage length, slope, average depth of saturation and average depth of saturation at a given slope are presented in Table B-2. The ratio for estimates generated with data from drainage tests using fine sand was 1.053, while it was 1.162 for estimates for coarse sand. The regressions are shown in Figure B-4. However, the confidence interval for the coarse sand ratio was large and included the confidence limits for the fine sand ratio so the type of sand did not significantly affect the ratio. However, since the size of the confidence intervals differed by a factor of 3, the type of sand may have an interaction with at least one of the other variables. The ratios for short model estimates and long model estimates are very similar as shown in Figure B-5 and therefore the drainage length does not significantly affect the estimates. The ratio of KH/KB increased significantly with increasing slope as shown in Figure B-6, indicating that the HELP model underestimates the effects of slope in increasing the drainage rate as predicted by the Boussinesq solution. The effect of depth of saturation is shown in Figure B-7 where the hydraulic conductivity estimates were divided into three groups based on the depth of saturation for which the estimate was generated. These ratios were not significantly different because the confidence interval for the ratio at depths of saturation ranging from 0 to 7 inches was much larger than the others. As with the type of sand, an interaction may be occurring with another variable.

The interaction of slope and depth of saturation was examined by performing separate regressions for the effect of depth of saturation using estimates of hydraulic conductivity for drainage tests at 2-percent and 10-percent slopes. Figures B-8 and B-9 show the regressions for 2-percent and 10-percent slopes, respectively. At 2-percent slope the ratios did not differ at the three ranges of depth of saturation. At 10-percent slope KH/KB decreased significantly with increasing depth of saturation. Consequently, the HELP

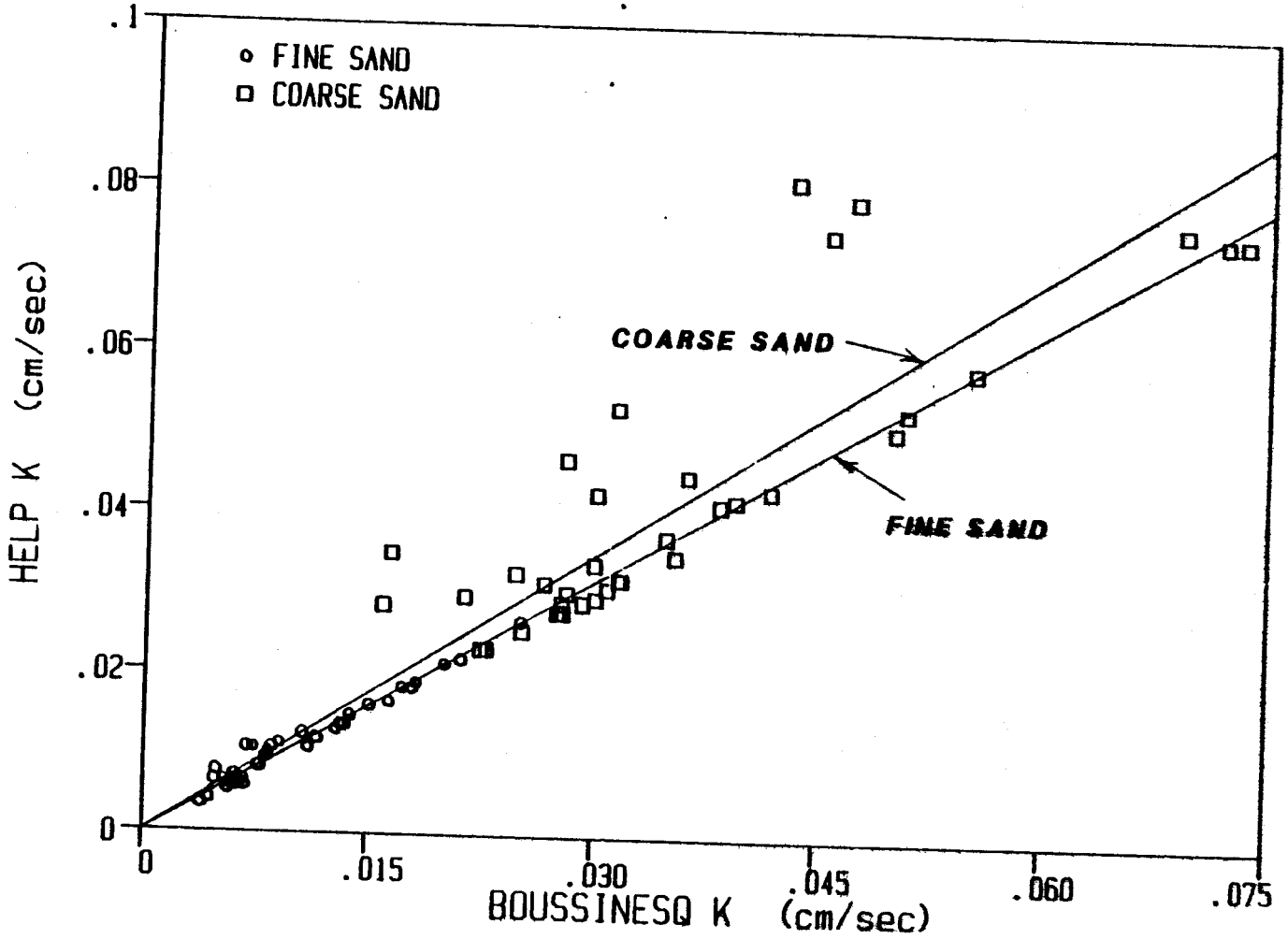

Figure B-4. Comparisons of hydraulic conductivity estimates by the HELP equation to estimates by the numerical Boussinesq solution for unsteady drainage from fine and coarse sands.

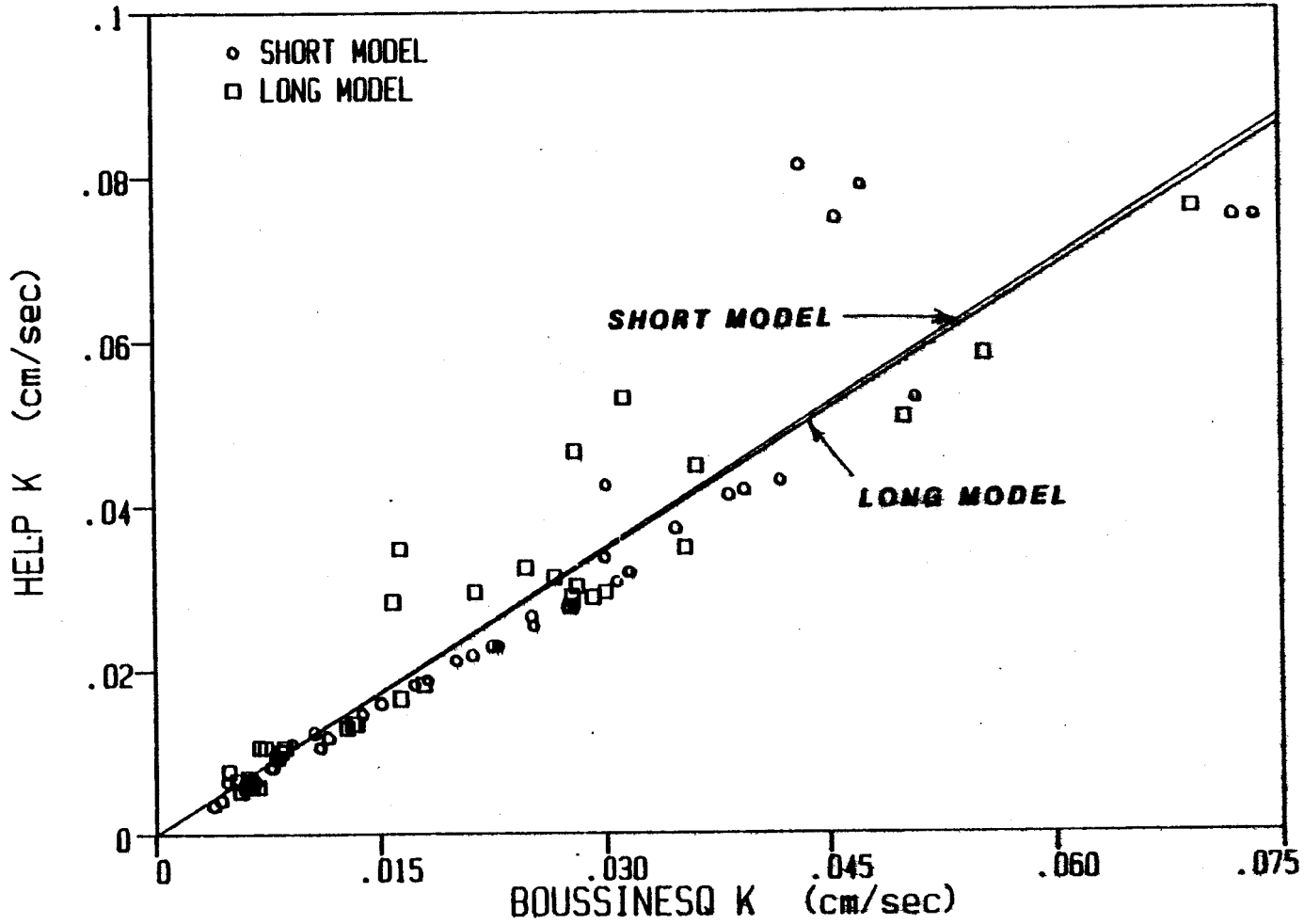

Figure B-5. Comparisons of hydraulic conductivity estimates by the HELP equation to estimates by the numerical Boussinesq solution for unsteady drainage from the short and long physical models.

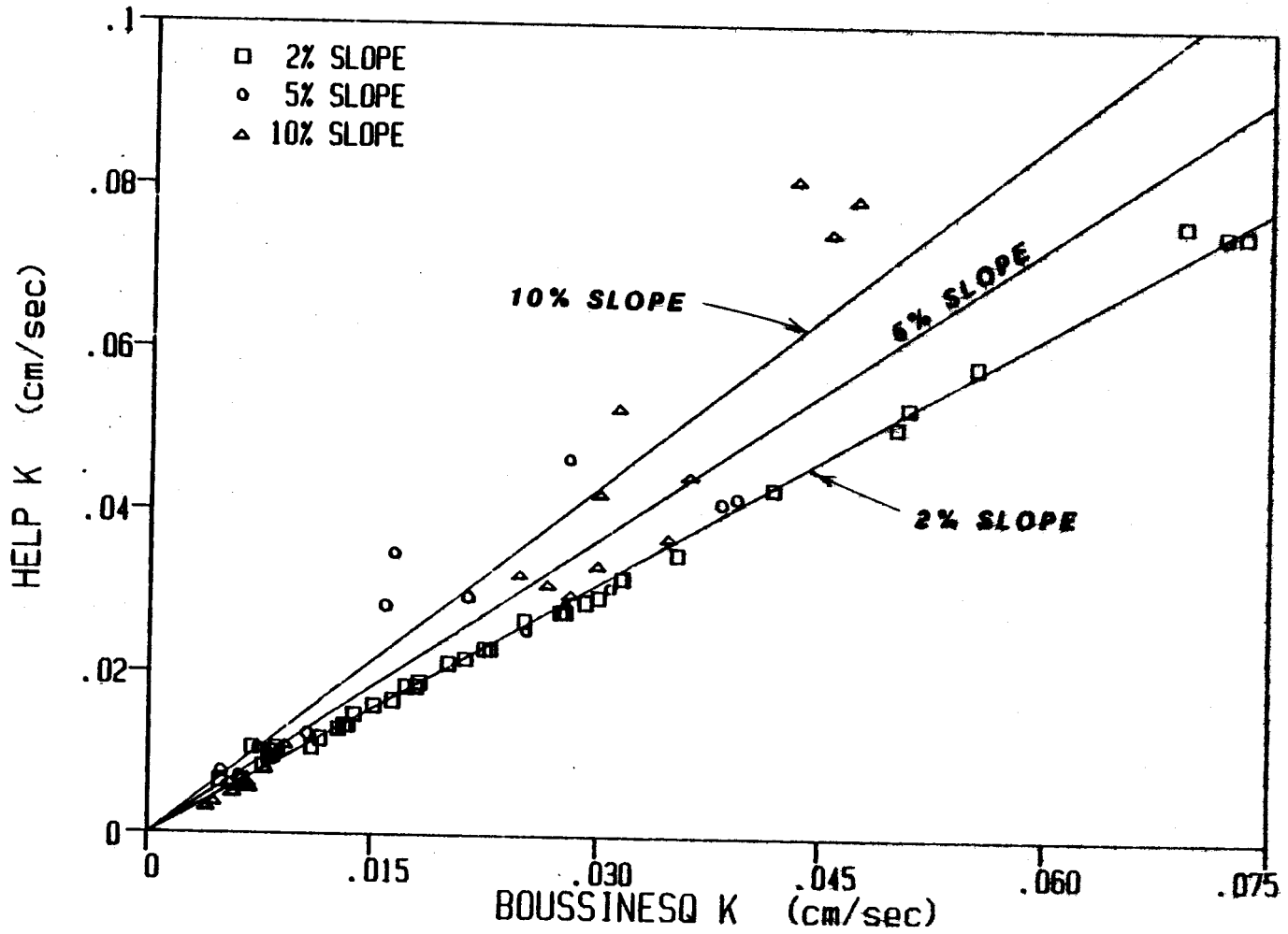

Figure B-6. Comparisons of hydraulic conductivity estimates by the HELP equation to estimates by the numerical Boussinesq solution for unsteady drainage from models at 2-, 5- and 10-percent slopes.

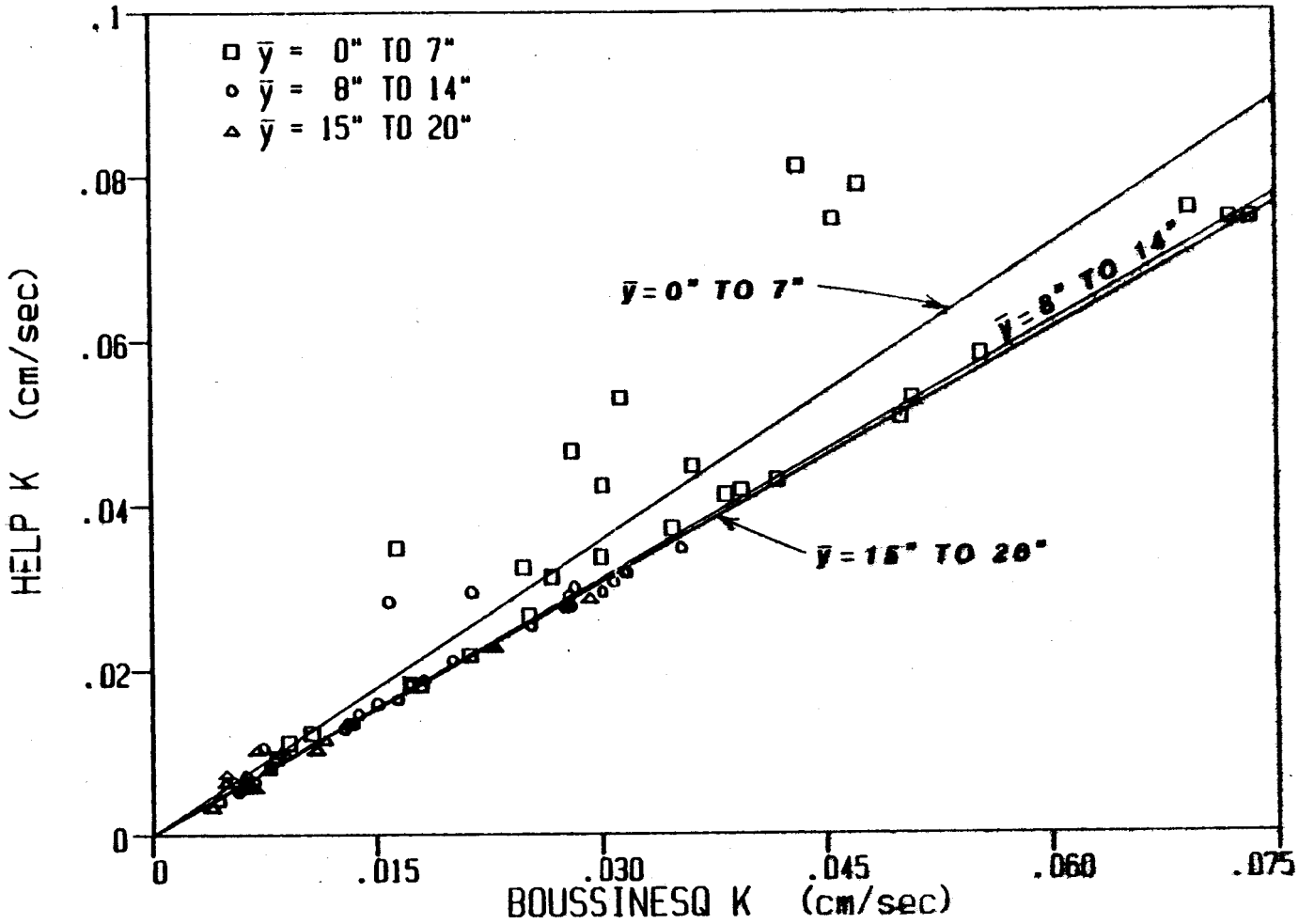

Figure B-7. Comparisons of hydraulic conductivity estimates by the HELP equation to estimates by the numerical Boussinesq solution for unsteady drainage at depths of saturation ranging from 0 to 7 in., 8 to 14 in., and 15 to 20 in.

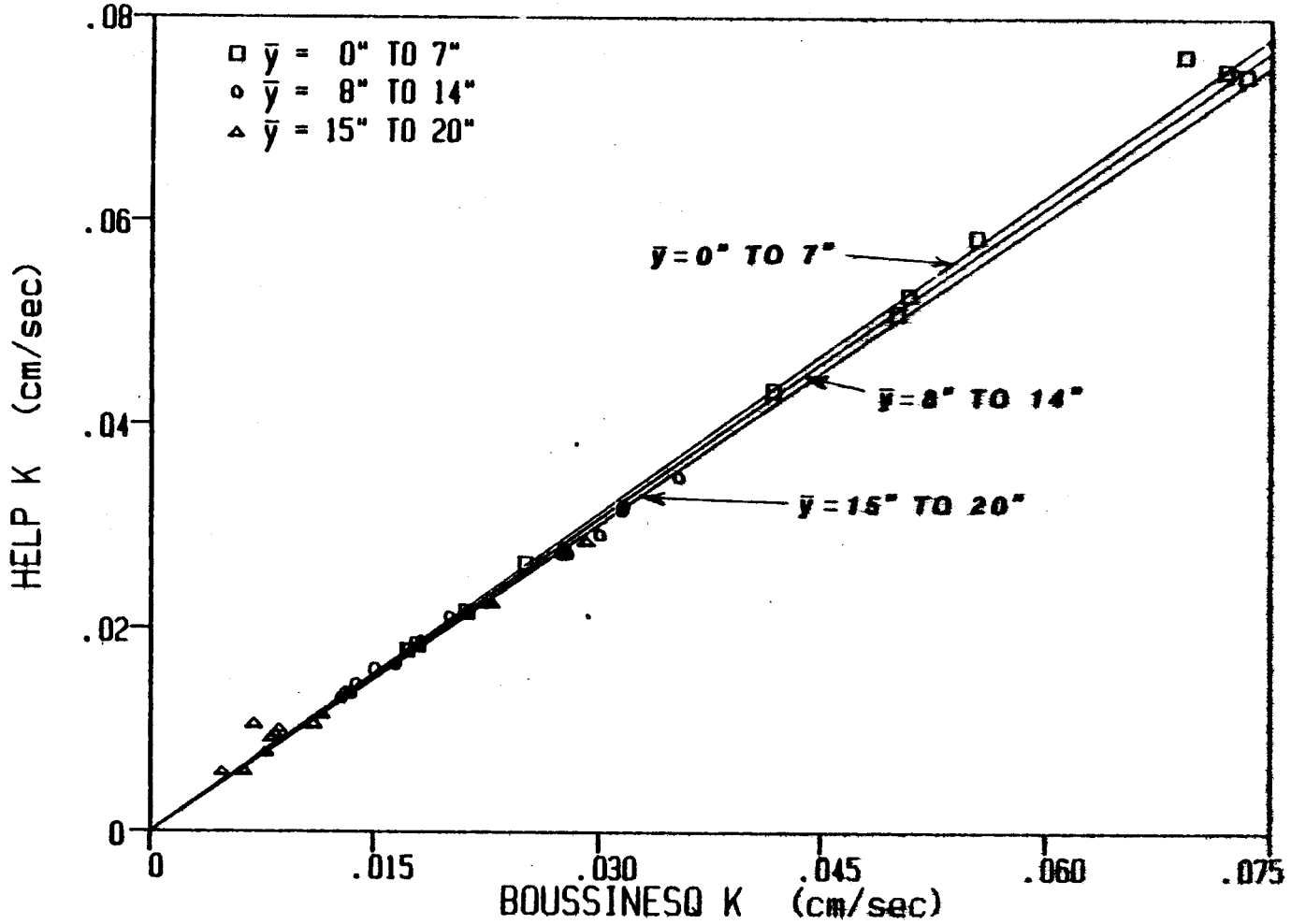

Figure B-8. Comparisons of hydraulic conductivity estimates by the HELP equation to estimates by the numerical Boussinesq solution for unsteady drainage from models at 2-percent slope with depths of saturation ranging from 0 to 7 in., 8 to 14 in., and 15 to 20 in.

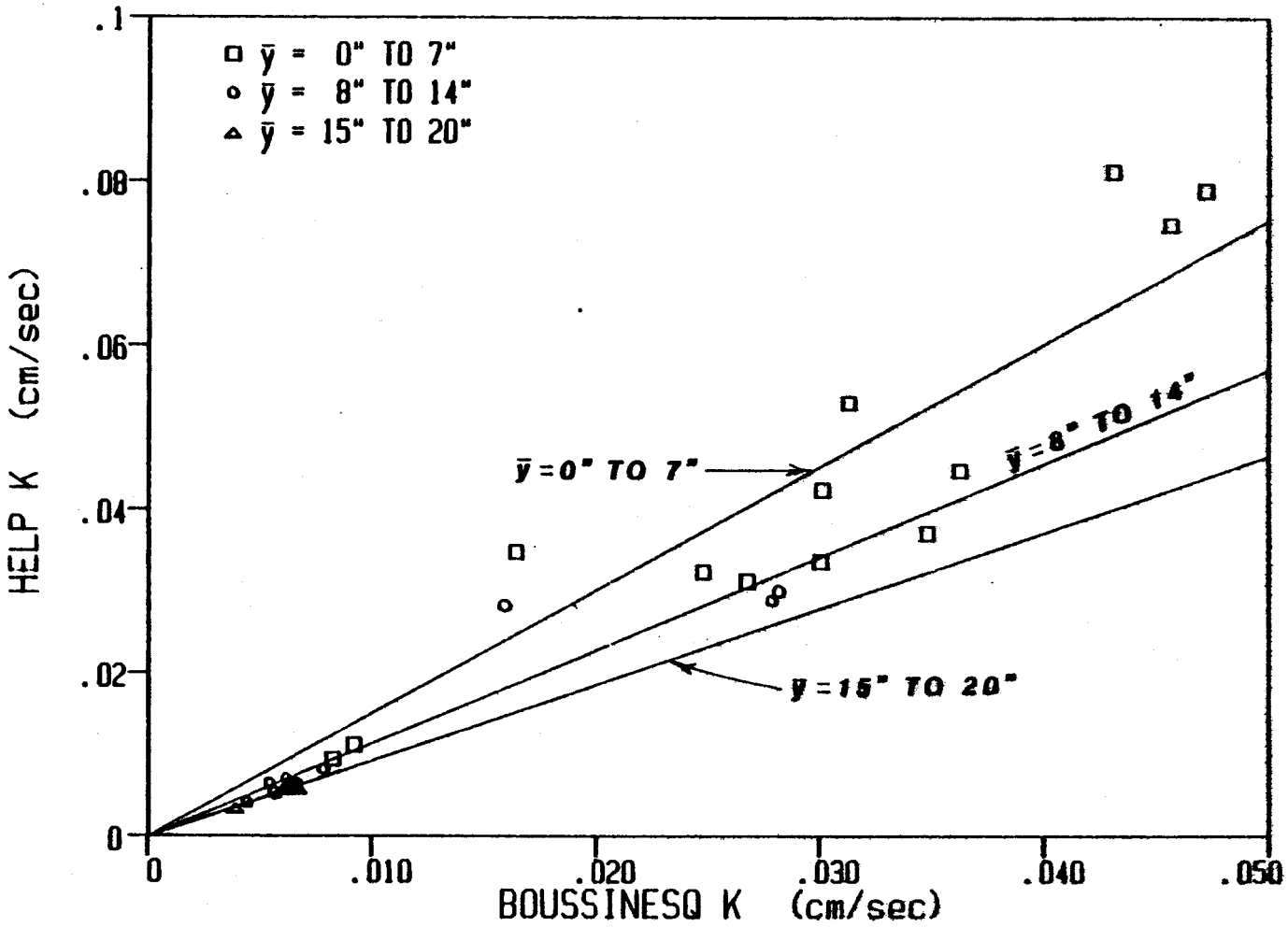

Figure B-9. Comparisons of hydraulic conductivity estimates by the HELP equation to estimates by the numerical Boussinesq solution for unsteady drainage from models at 10-percent slope with depths of saturation ranging from 0 to 7 in., 8 to 14 in., and 15 to 20 in.

equation underestimated lateral drainage at small depths and large slopes compared to the Boussinesq solution but agreed well at depths above 14 in.

Additional comparisons of the effects of design parameters and their interactions on KH/KB were made using unequal three-way ANOVA. Use of ANOVA on the 79 ratios for unsteady drainage following rainfall indicated that the main effects of slope, depth of saturation and drainage length and the interactive effects of slope with drainage length and slope with depth (listed in their order of importance) were all significant at 95-percent confidence. Using ANOVA on the 42 ratios from the tests on fine sand, only the effect of slope was significant at 95-percent confidence. For the 37 values from tests on coarse sand, the interactive effect of slope with drainage length and the main effect of slope were significant at 95-percent confidence.

Results of ANOVAs on the data sets divided by type of sand indicates that interaction occurred between the type of sand and the other effects such as depth of saturation, drainage length, and slope with depth, since these variables were not significant upon dividing the data sets. Therefore, an additional unequal three-way ANOVA was performed examining the effects of type of sand, slope and drainage length using all 79 ratios for unsteady drainage following rainfall. Depth of saturation was replaced by type of sand in the analysis since depth of saturation was not significant in either of the two ANOVAs performed on data for one type of sand. The results indicate that the interactive effect of slope with drainage length and the main effects of slope, type of sand and drainage length (listed in the order of importance) are significant at 95-percent confidence.

In conclusion, the HELP equation underpredicts the lateral drainage rate in comparison to the numerical solution of the Boussinesq equation by about 12 percent for unsteady drainage and by about 29 percent for steady-state drainage. The actual underprediction is a function of slope, product of the slope and drainage length, type of sand, and drainage length. The two models treat these effects in significantly different ways but, nevertheless, frequently produce similar drainage rates. Under the worst conditions, the drainage rate was underpredicted by 50 percent and overpredicted by 50 percent during unsteady drainage. Under steady-state conditions, drainage was underpredicted by a range of 13 to 40 percent.

APPENDIX C

COMPARISONS BETWEEN LABORATORY MEASUREMENTS AND NUMERICAL BOUSSINESQ SOLUTIONS

The HELP lateral drainage equation was developed to approximate numerical solutions of the one-dimensional Boussinesq equation for unsteady, unconfined, saturated flow through porous media. Appendix B and parts of Section 6 of this report present comparisons between the HELP equation and the Boussinesq solution to evaluate the validity of the HELP equation. Therefore, it is necessary to compare the Boussinesq solutions to the laboratory measurements. This forms a basis for judging the significance of the differences between the HELP equation predictions and the laboratory measurements, and between the HELP equation and the Boussinesq solution. This appendix presents the comparisons and discusses briefly how well the Boussinesq solution predicts the drainage results. In addition, the performance of the HELP equation is compared to the Boussinesq solution results to present the significance of the differences between the HELP predictions and the laboratory measurements.

Figures C-1 and C-2 show the range of measured drainage rates as a function of average head above the liner (average depth of saturation). Three predictions by the numerical Boussinesq solution using three hydraulic conductivity conditions are shown for each test condition. The first curve is based on the hydraulic conductivity measured in the laboratory permeameters. The second curve was obtained by using an average of the various hydraulic conductivity values estimated for the test condition by attempts to calibrate the Boussinesq solution. For the third curve, the hydraulic conductivity was entered as a power function of the average depth of saturation. This equation was developed by performing a curve fit of the hydraulic conductivity values obtained by calibration. These power functions are presented in Section 6. These figures are analogous to Figures 25 and 26 in Section 6, where the predictions were obtained using the HELP model instead of the Boussinesq solution.

The predictions using the laboratory-measured hydraulic conductivity value differ greatly from the actual results in all but one of the eight test conditions. Predictions based on the mean hydraulic conductivity values calibrated for the test conditions performed better and generally showed agreement over a narrow range of average depths. Better agreement was obtained using the function for hydraulic conductivity, but the relationship did not fall within the range of observations throughout the entire range of average saturated depth despite all of the attempts to calibrate the Boussinesq solution.

Comparing the results shown in Figures C-1 and C-2 with Figures 25 and 26 shows that the results obtained using the HELP equation with the same

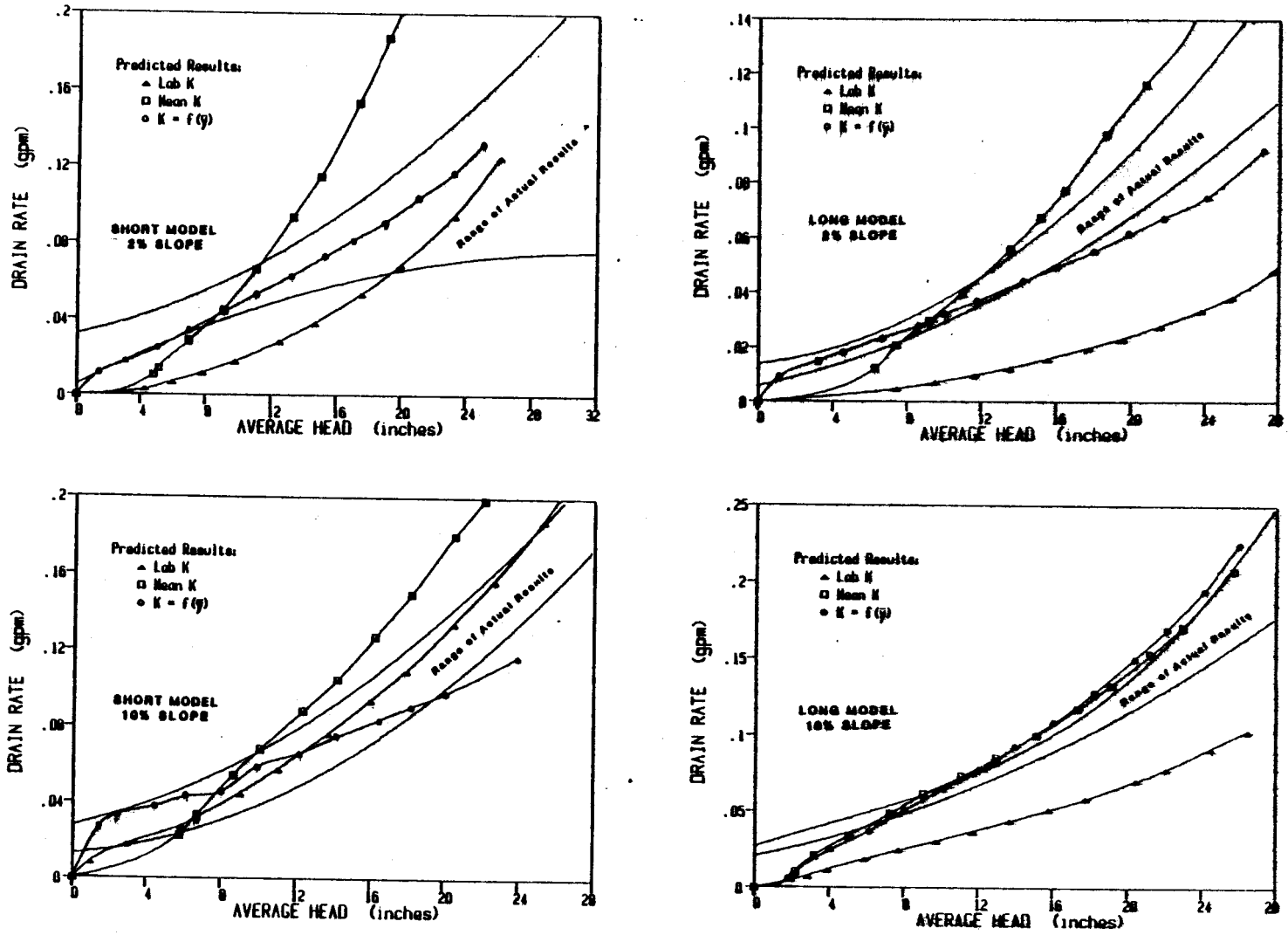

Figure C-1. Measured drainage rate vs. average head compared to numerical Boussinesq solutions for fine sand in both physical models at slopes of 2 and 10 percent.

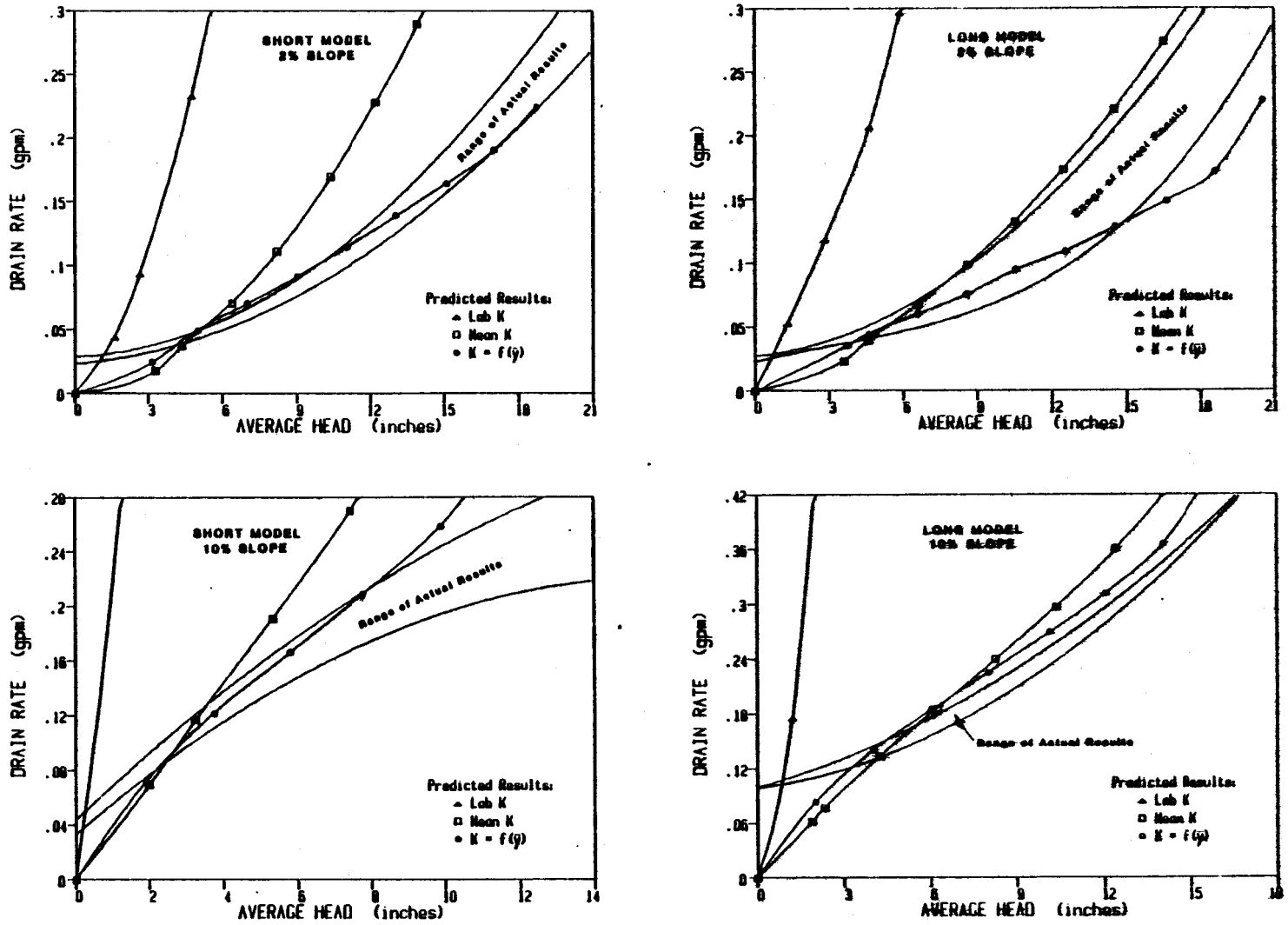

Figure C-2. Measured drainage rate vs. average head compared to numerical Boussinesq solutions for coarse sand in both physical models at slopes of 2 and 10 percent.

hydraulic conductivity values produced results that were slightly better, though perhaps not significantly, than the Boussinesq solution. This result is surprising since the hydraulic conductivity values were calibrated for the Boussinesq solution and not the HELP equation. Consequently, it is apparent that the HELP model performs as well as the Boussinesq solution. In addition, the differences between the two methods are much smaller than the differences between the predicted and actual results, and in some cases are smaller than the range in the actual results.

Figures C-3 through C-6 show the measured drainage rate and the predicted drainage rate as a function of time using the Boussinesq solution with the power function of depth of saturation used for the hydraulic conductivity value. Figures C-3 through C-6 also show the measured average depth of saturation and the predicted depth as a function of time. These figures are analogous to Figures 22 through 30 in Section 6 where the predicted values were obtained using the HELP equation. The results shown in these figures vary greatly; some show good agreement, some show poor agreement, and some show good agreement only after infiltration ceases. The same is true for both the drainage rate and the average depth of saturation. In general, the results were very comparable to the results obtained using the HELP model but were significantly better for test conditions having 10-percent slope. The HELP model yielded better results for test conditions having 2-percent slope. The HELP equation predicted smaller drainage rates for a given average depth of saturation.

Figures C-7 through C-10 show the measured and predicted head above the drain as a function of the distance from the drain under conditions when the average head is increasing and decreasing, respectively, labeled fill and drain. The figures also show the head contributed by the sloped liner. The predicted results were obtained from the numerical Boussinesq solution. Similar head profiles are not predicted by the HELP model and therefore no comparisons can be made for the HELP model. In general, the Boussinesq solution predicts a more level profile with a steeper gradient near the drain under conditions of decreasing heads. Under conditions of increasing heads the Boussinesq solution still tends to predict steeper gradients near the drain, but elsewhere the profile tends to be nearly parallel to the clay liner; the actual profiles varied greatly.

To summarize, the Boussinesq solution after calibration still produces results significantly different from those measured in the drainage tests. The results obtained with the HELP model were generally as good or better than the Boussinesq solution. The HELP equation performed better on tests conducted with 2-percent slope and the Boussinesq solution performed somewhat better on tests conducted at 10-percent slope. The differences between predictions by the two methods for a given set of conditions were small in comparison to the range of actual results. Similarly, the differences between the predictions and the actual results were much larger than the differences between the HELP equation and the Boussinesq equation.

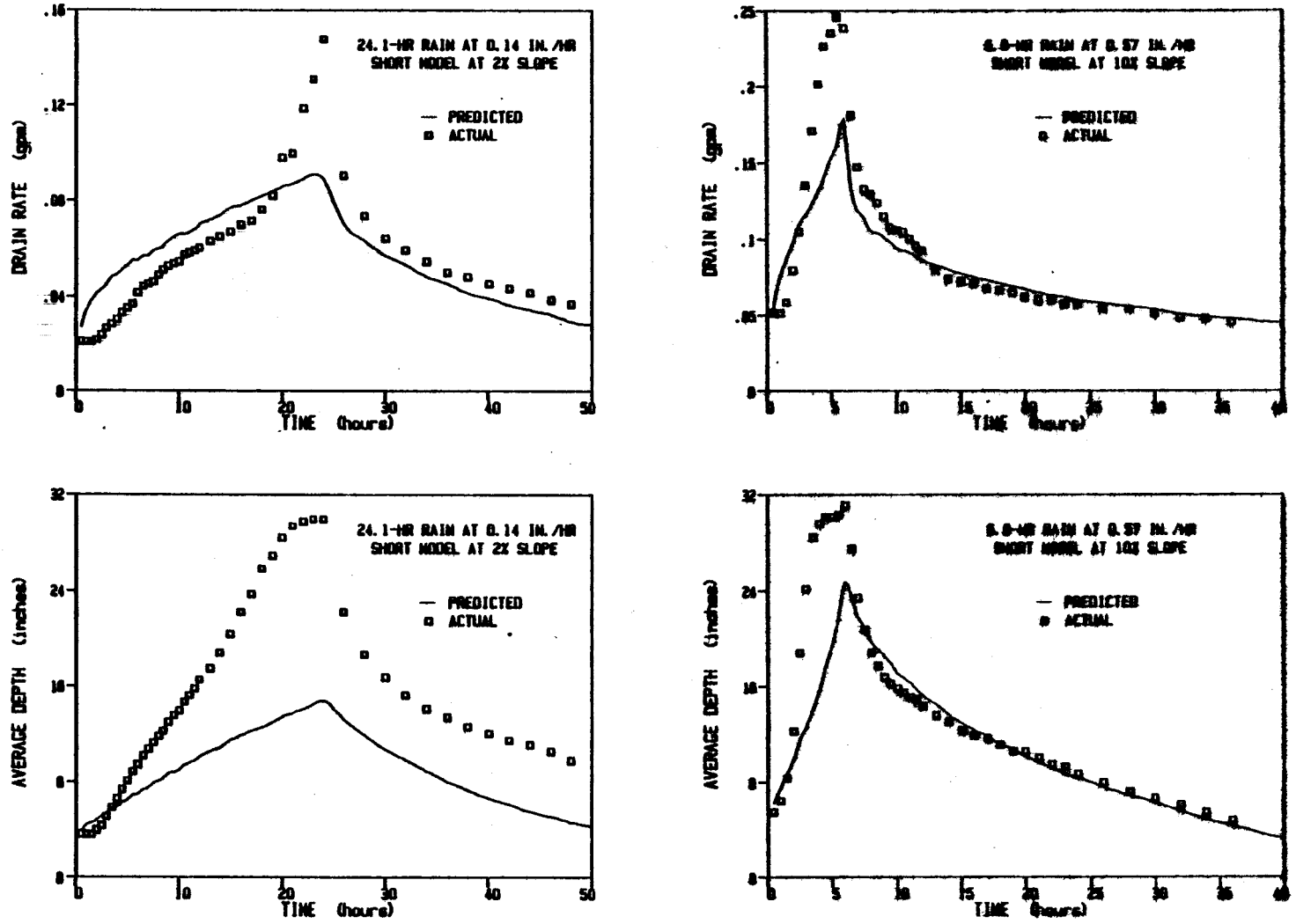

Figure C-3. Measured drainage rate and average saturated depth vs. time compared to numerical Boussinesq solutions for fine sand in short model at slopes of 2 and 10 percent.

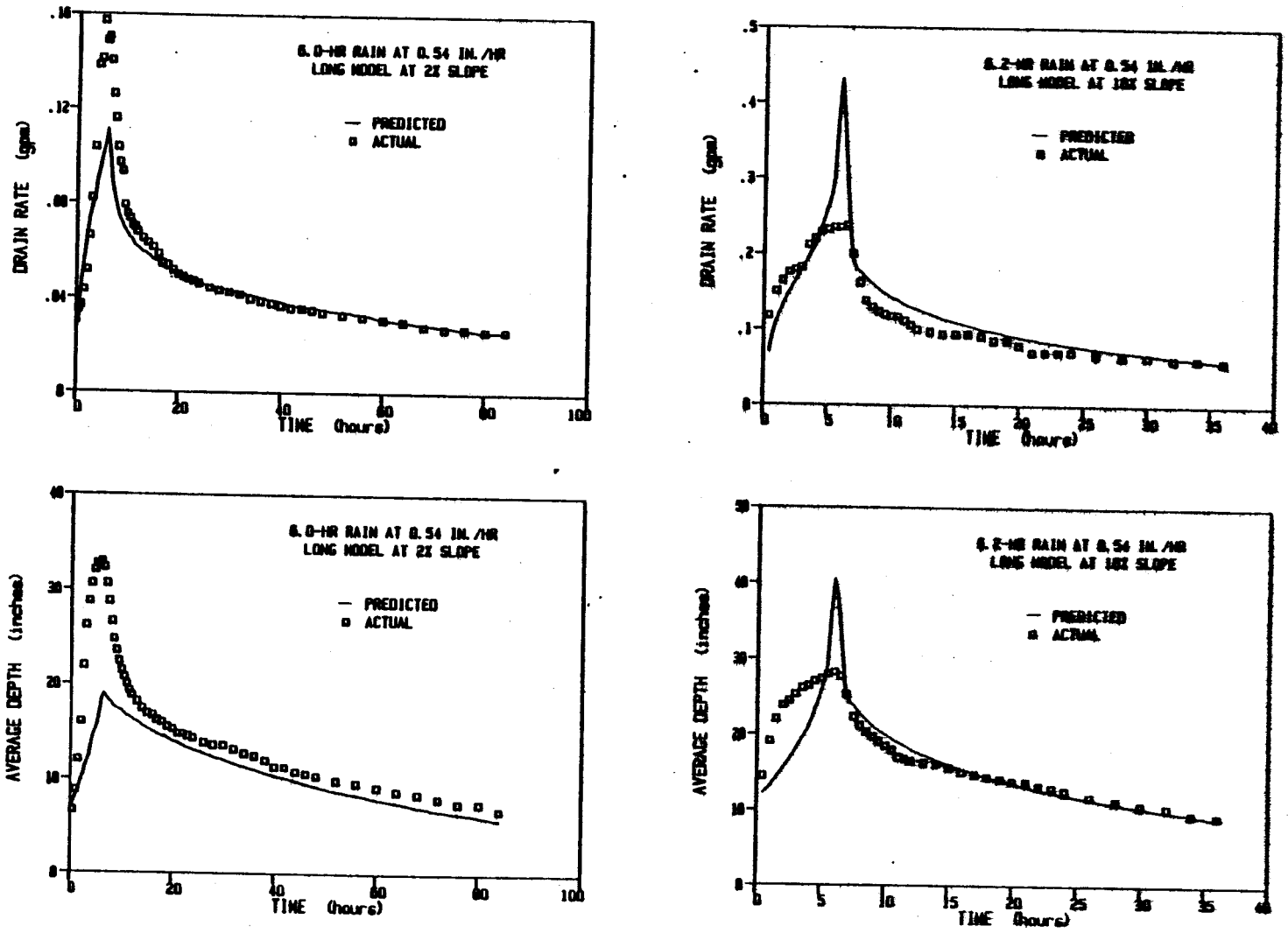

Figure C-4. Measured drainage rate and average saturated depth vs. time compared to numerical Boussinesq solutions for fine sand in long model at slopes of 2 and 10 percent.

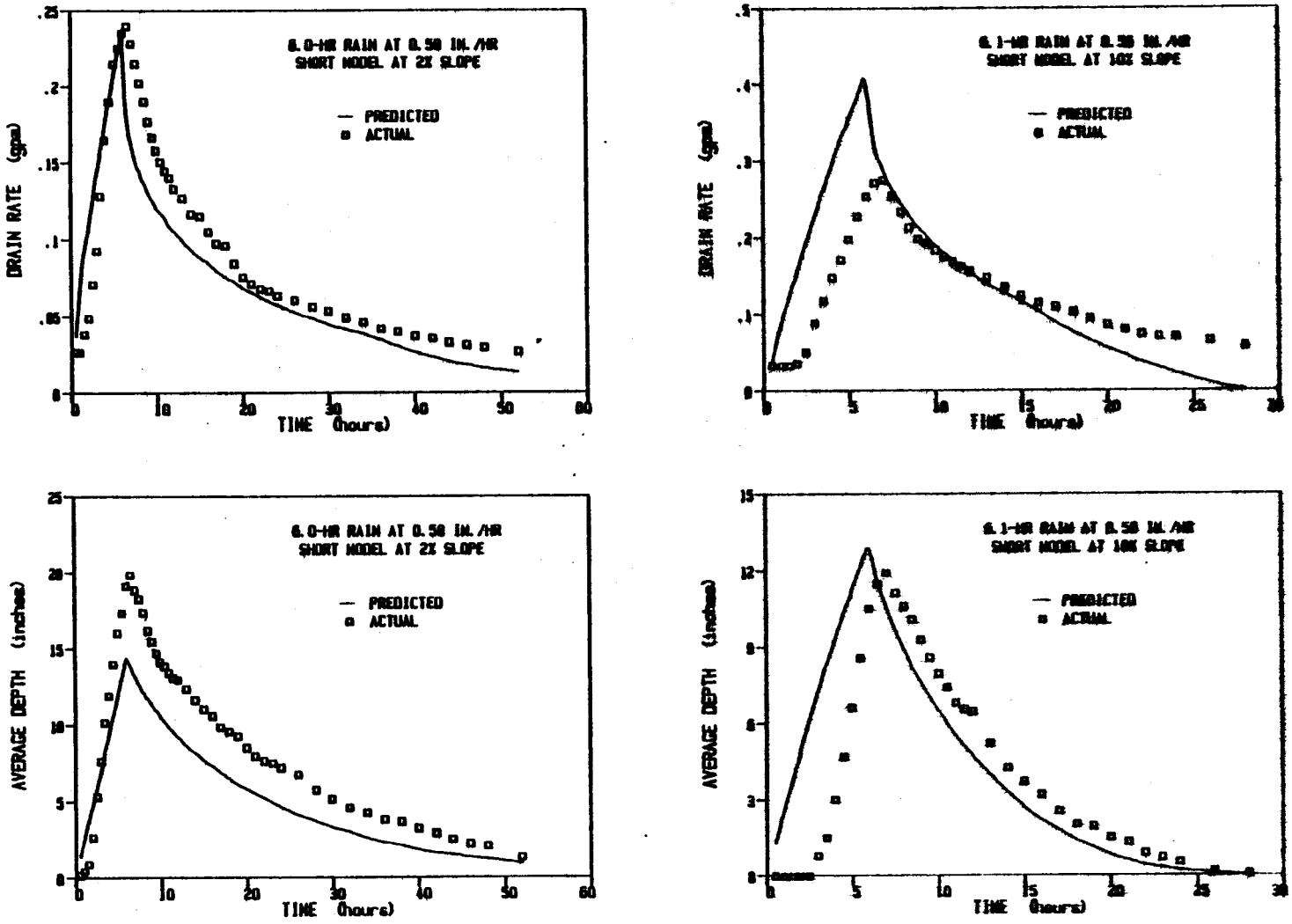

Figure C-5. Measured drainage rate and average saturated depth vs. time compared to numerical Boussinesq solutions for coarse sand in short model at slopes of 2 and 10 percent.

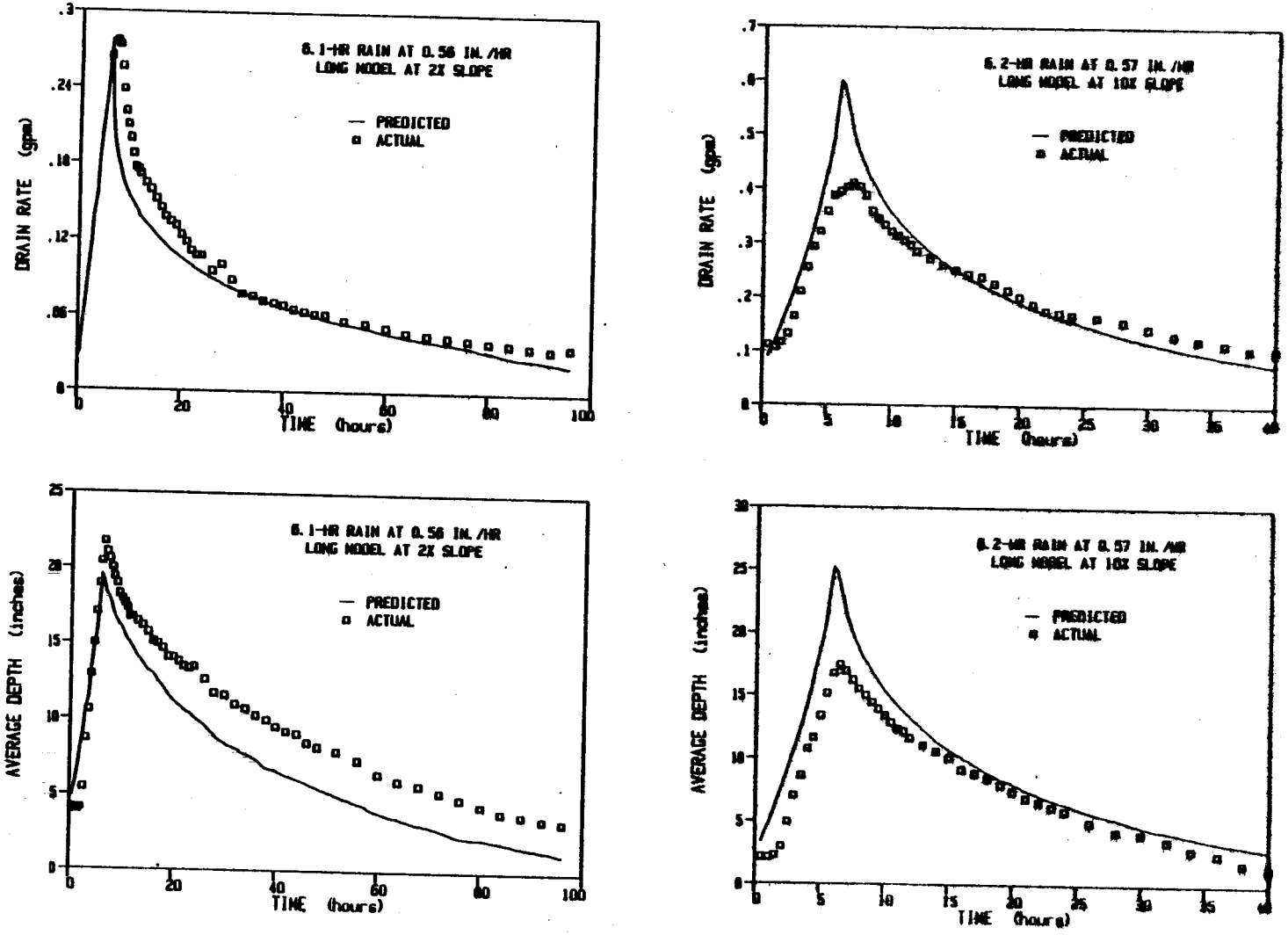

Figure C-6. Measured drainage rate and average saturated depth vs. time compared to numerical Boussinesq solutions for coarse sand in short model at slopes of 2 and 10 percent.

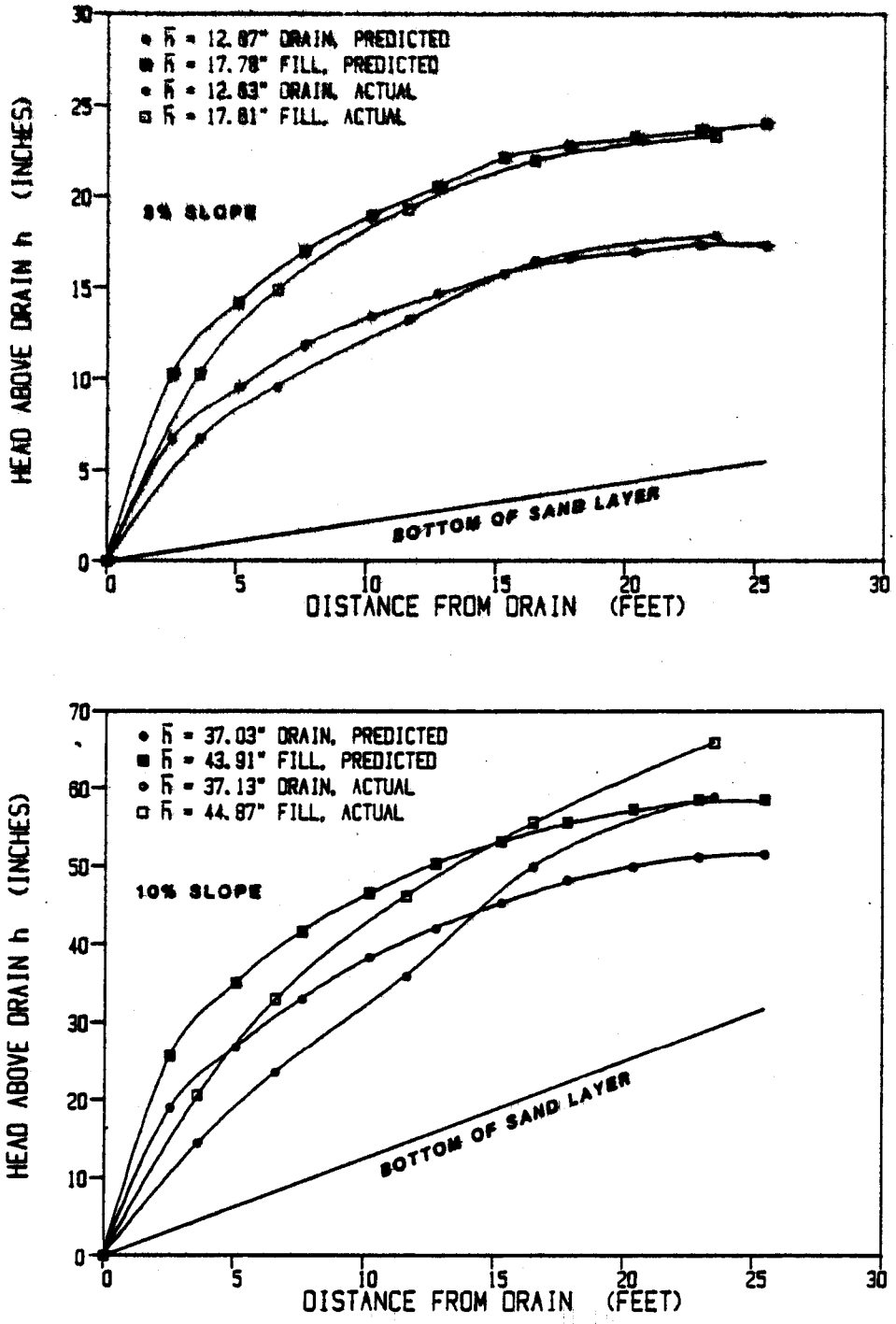

Figure C-7. Measured head profiles for unsteady drainage during 24-hr rainfall test at 2-percent slope and during 6-hr rainfall test at 10-percent slope compared to numerical Boussinesq solutions for fine sand in short model.

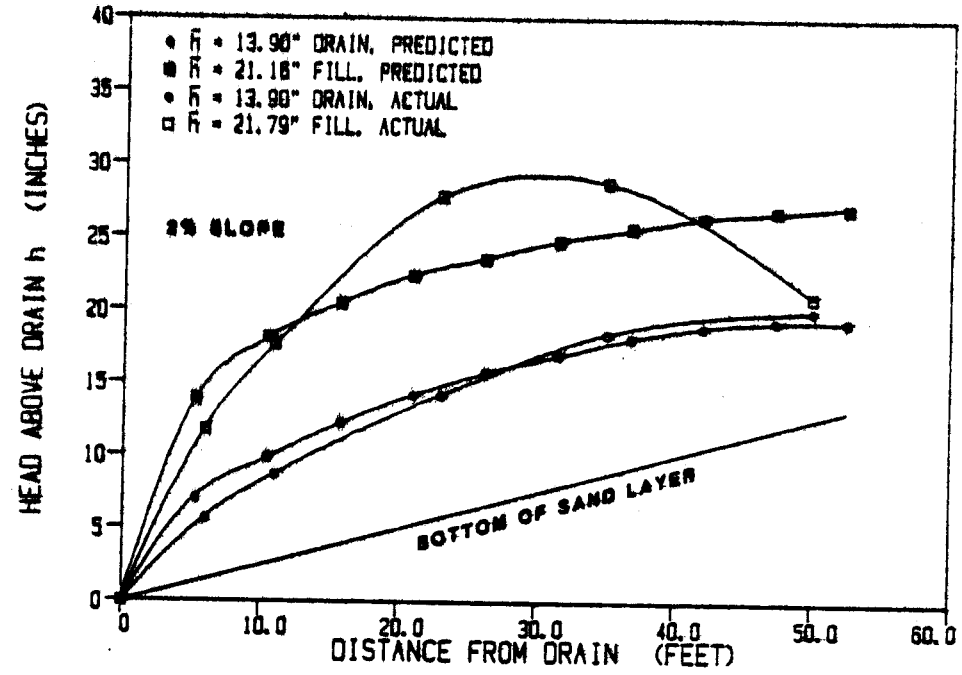

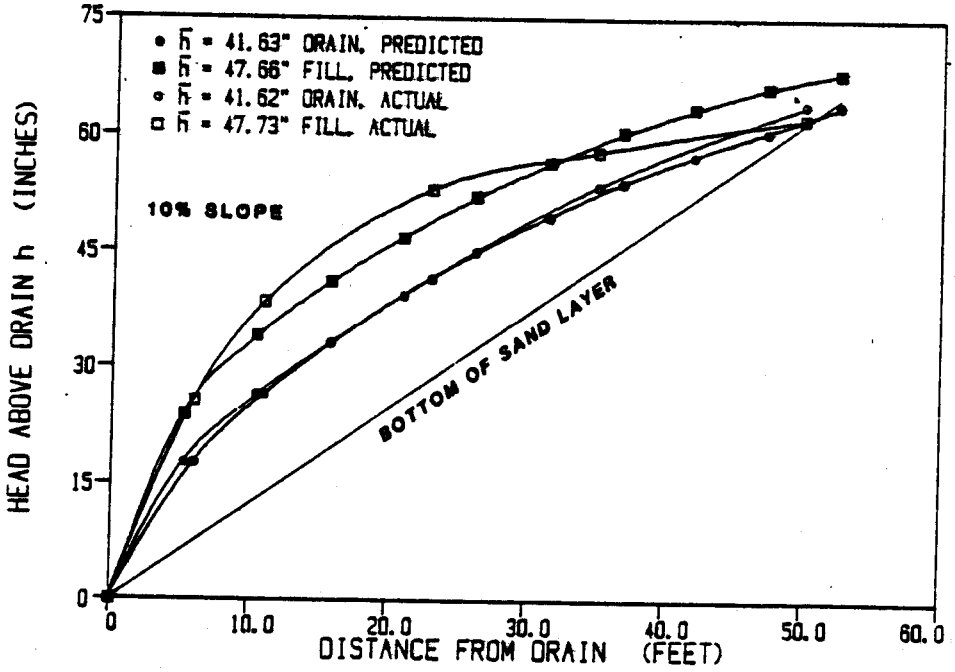

Figure C-8. Measured head profiles for unsteady drainage during 6-hr rainfall test compared to numerical Boussinesq solutions for fine sand in long model at slopes of 2 and 10 percent.

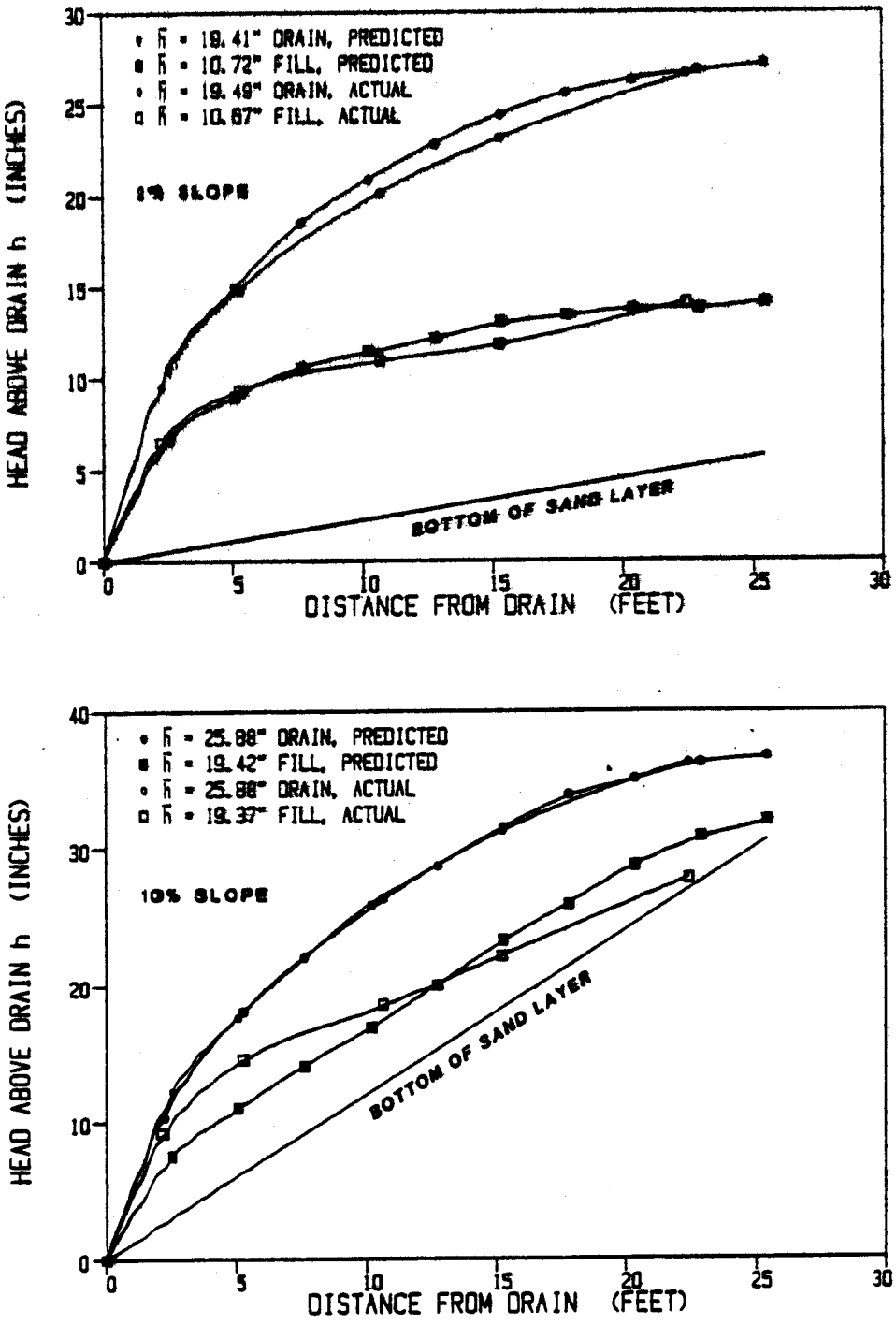

Figure C-9. Measured head profiles for unsteady drainage during 6-hr rainfall test compared to numerical Boussinesq solutions for coarse sand in short model at slopes of 2 and 10 percent.

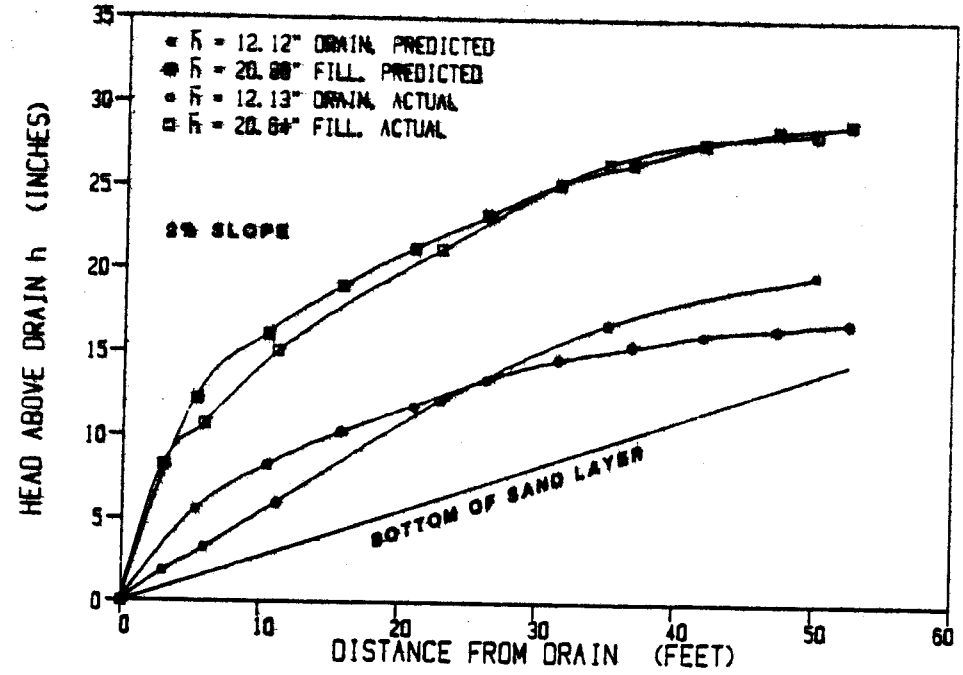

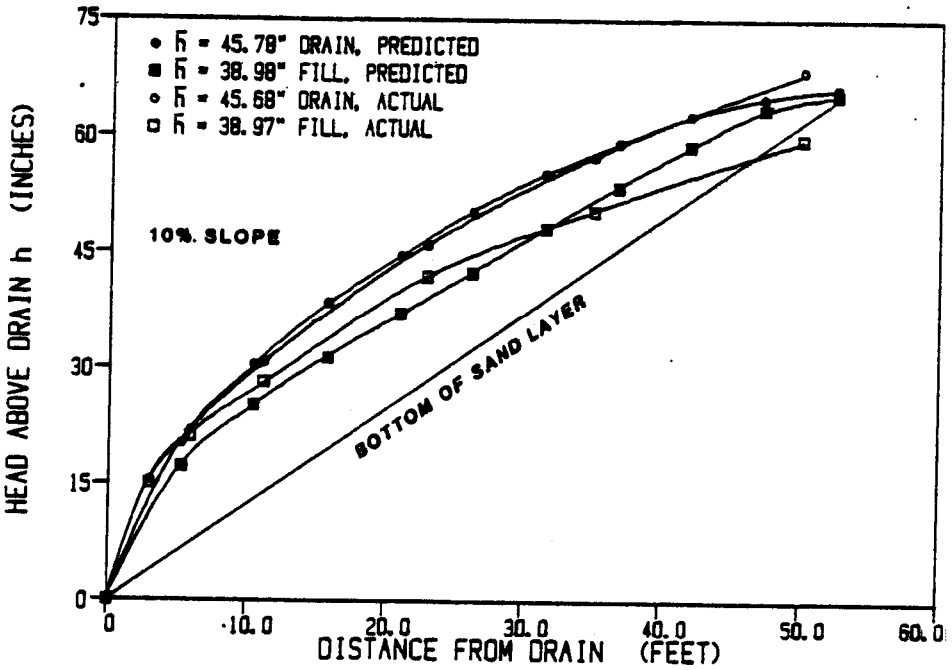

Figure C-10. Measured head profiles for unsteady drainage during 6-hr rainfall test compared to numerical Boussinesq solutions for coarse sand in long model at slopes of 2 and 10 percent.